Norwegian University
of Life Sciences

Master's Thesis 2021 60 ECTS
Faculty of Environmental Sciences and Natural Resource Management

Constraints for Carbon Degradation in Subarctic Thawing Peatland Permafrost in Northern Scandinavia

Sigrid Trier Kjær
Environment and Natural Resources

Abstract

Permafrost soils are globally under pressure and subject to climate change induced permafrost thawing. Peat plateaus are found in peatlands with discontinuous permafrost and store large quantities of carbon (C). They are particularly vulnerable to climate change which leads to thawing of permafrost, collapse of peat plateaus and thermokarst formation. The aim of this thesis was to investigate potential rates and controlling factors for C degradation in peat plateaus in Northern Norway. Ongoing thawing of peat plateaus is known to mobilise C, but the understanding of what controls the biogeochemical turnover of C in these subarctic environments is still limited. This study compared three peat plateaus (Iškoras, Áidejávri and Lakselv) in Finnmark, Norway which represent a well-documented chronosequence of permafrost formation.

Peat cores from each site were incubated either oxically or anoxically at 10°C after controlled thawing. The cores were divided in seven layers representing both active layer, transition zone and permafrost peat. Chemical properties of each layer were determined, including pH, water-extractable dissolved organic carbon (DOC), element composition and stable isotope ratios of C and nitrogen (N). Kinetics of oxygen (O_2) uptake as well as carbon dioxide (CO_2) and methane (CH_4) release were recorded at high temporal resolution during the first 19 days after thawing using an automated, temperature-controlled incubator coupled to a gas chromatograph. After 19 days, incubation was continued off-line with weekly or biweekly gas measurements until a total incubation time of 96 days. Release of DOC was measured in the slurry treatments after 0, 17 and 96 days. Two additional experiments were performed with permafrost peat from Iškoras, testing the effect of native DOC and nutrient addition (glucose, phosphate, ammonium, and sulphate) on organic matter (OM) decomposition.

Carbon degradation varied among the three peat plateaus, but all showed a similar trend over depth with highest CO_2 production in the top of the active layer and a second maximum in the permafrost layer. CO_2 production of thawed permafrost peat under oxic conditions was 42 - 104% of that of the active layer, demonstrating a substantial CO_2 production potential of thawed permafrost peat. Highest decomposition rates were obtained under oxic conditions, but the DOC release was larger under anoxic conditions and in general much larger than CO_2-C release. Leached DOC may lead to GHG emissions downstream of peat plateaus. CO_2 accumulation showed a positive relationship with the initial concentration of native DOC which was most pronounced when O_2 was present, indicating that some fraction of the DOC released from permafrost was instantly available for microbial

decomposition. Experiments with nutrient additions showed that C decomposition only increased if nutrients were added in combination with glucose, which exemplifies the pivotal role of C quality for microbial decomposition activity. Anoxic CH_4 formation and release were several orders of magnitude smaller than anoxic CO_2 production, making it unlikely that CH_4 formation is a significant pathway of C degradation upon permafrost thaw. Nitrous oxide (N_2O) production was small and only seen in few active layer samples incubated anoxically. Overall, peat quality seemed to be a strong controller of decomposition activity with C content, peat C/N ratio, pH and iron content being the most important predictors. The distribution of $\delta^{13}C$ and $\delta^{15}N$ along the peat profile proved to be a useful indicator for site-specific peat formation and perturbation history and hence peat quality.

Abstrakt

Permafrostjorde er globalt set under stort pres. Klimaforandringer og stigning i globale temperaturer forårsager optøning af permafrosten. Palsaer er tørvejord opløftet af permafrost, og de fungerer som lagre for store mængder karbon (C). De er særligt sårbare over for klimaforandringer, idet disse fører til optøning og kollaps af palsaerne og videre til dannelse af termokarstsøer. Det er velkendt, at den igangværende optøning af palsaer mobiliserer C, men forståelsen af, hvilke faktorer der begrænser nedbrydningen af C i disse subarktiske områder, er forsat begrænset. Dette speciale undersøgte tre palsaer (Iškoras, Áidejávri and Lakselv) i Finnmark i Norge, for at sammenligne potentielle nedbrydningsrater og kontrollerende faktorer. Tilsammen udgør de tre palsaer en veldokumenteret kronosekvens af permafrost.

Tørvekerner fra hver af de tre palsaer blev inkuberet enten aerobt eller anaerobt ved 10°C efter kontrolleret optøning. Kernerne blev opdelt i syv lag, hvoraf tre lag repræsenterede aktivlaget, et lag overgangszonen og tre lag permafrostlaget. For hvert lag blev de kemiske egenskaber bestemt, herunder pH, opløst organisk karbon (DOC), grundstofsammensætning og forhold mellem naturlig forekommende stabile isotoper af henholdsvis C og nitrogen (N). Gaskinetik for optag af oxygen (O_2) samt udslip af kuldioxid (CO_2) og metan (CH_4) blev målt med høj tidslig opløsning i de første 19 dage med en automatisk, temperaturkontrolleret inkubator koblet til en gaskromatograf. Inkubationen blev efter 19 dage fortsat med manuelle gasmålinger hver eller hver anden uge indtil 96 dage efter start af inkubationen. Frigørelse af DOC blev målt efter dag 0, 17 og 96. To tillægsforsøg blev udført med permafrosttørv fra Iškoras for at teste effekten af allerede tilstedeværende DOC og effekten af tilsætning af en række næringsstoffer (glukose, fosfat, ammonium og sulfat) på nedbrydning af tørv.

Nedbrydningen af C varierede mellem de tre palsaer, men de viste alle den samme tendens på tværs af dybde, hvor højeste produktion af CO_2 blev målt i toppen af aktivlaget og i permafrostlaget. Produktionen af CO_2 fra optøet permafrosttørv under aerobe forhold var 42 til 104 % af produktionen i toppen af aktivlaget, hvilket viser at optøet permafrosttørv kan opnå et betydeligt produktionspotentiale af CO_2. De højeste udslip af CO_2 blev målt under aerobe forhold, mens frigørelsen af DOC var højere under anaerobe forhold. Frigørelsen af DOC var betydelig højere end udslippet af CO_2-C, hvilket kan øge drivhusgasudslippet fra økosystemer nedstrøms, når DOC udvaskes fra palsaerne. Produktionen af CO_2 korrelerede positivt med den initiale mængde af allerede tilstedeværende DOC. Dette var mest udtalt, når O_2 var til stede, hvilket tyder på, at DOC frigivet ved optøning af permafrost er tilgængelig for mikrobiel respiration med det samme. Tilsætning af nærringstoffer øgede kun nedbrydningen af C, hvis næringsstofferne blev tilsat sammen med glukose. Anaerob dannelse og frigørelse af CH_4 var adskillige størrelsesordener mindre end anaerob produktion af CO_2, hvilket tyder på, at CH_4 dannelse under anaerobe forhold ikke står for nogen signifikant nedbrydning af C. Lattergas (N_2O) produktion var lav og sås kun i få anaerobe prøver fra aktivlaget. Samlet set tyder resultaterne på, at kvaliteten af tørv har stor indvirkning på nedbrydningsaktivitet, samt at C-indhold, C/N-forhold, pH og jern-indhold er vigtige indikatorer for nedbrydningshastighed og -omfang. Fordelingen af $\delta^{13}C$ og $\delta^{15}N$ var brugbare indikatorer for bestemmelse af tørvkvalitet.

Acknowledgements

First and foremost, I want to thank my main-supervisor Peter Dörsch (NMBU) for the enormous support he has provided through the entire process; for helping me pursue an interesting project, for joining the fieldwork, for teaching me many new things in the laboratory and for all the hours spent in the (home) office to improve my thesis. I am grateful for all the work you put into this project and our collaboration has meant a great deal to me.

I would also like to thank my co-supervisor Sebastian Westermann (UiO) for his help in creating this project and for sharing his extensive knowledge of the Norwegian peat plateaus. This has helped me build a strong understanding of these systems.

I would also like to thank Hanna Lee and my co-supervisor Inge Althuizen (NORCE) for teaching me more about permafrost ecosystems and for putting my thesis in a bigger perspective. Our paper discussions have been interesting, and I have learned a lot.

I also want to thank the laboratory staff at the Faculty of Environmental Sciences and Natural Resource Management, NMBU. I especially want to give a big thanks to Trygve Fredriksen, Pia Frostad and Solfrid Lohne for all the help and support you provided me in the laboratory.

I want to thank Nora Nedkvitne for our great collaboration. She has been a huge help and support for me, and I really appreciate our teamwork and friendship throughout the whole process.

And finally, I give thanks to my family, who apart from cheering me on also helped with proofreading.

Oslo, 2021.

Table of Contents

List of figures and tables

List of Appendices

1 Introduction

Between 15 and 22 % of the terrestrial surface of the Northern hemisphere is underlain by permafrost (Obu et al., 2019). Permafrost is defined as soil or sediment which is continuously frozen (≤ 0°C) for at least two consecutive years (Turetsky et al., 2007). In the northern hemisphere, permafrost-affected peatlands are estimated to cover ~1.7 million km^2 which equals between 8 and 12 % of the total permafrost area (Hugelius et al., 2020; Obu et al., 2019). The C deposits in permafrost peatlands have been estimated to amount to ~185 Pg C (Hugelius et al., 2020), which equals about one third of all C stored in permafrost affected soils (Lindgren et al., 2018). Permafrost peatlands are especially vulnerable to climate change since temperature raise is most pronounced in the Northern regions of the world. This phenomenon is known as Arctic amplification (Voigt et al., 2017a). It has been estimated that only half of the preindustrial extent of peat permafrost will remain if the global temperature stabilises at +2°C warming, while all peat permafrost will disappear if it stabilises at +6°C (Hugelius et al., 2020).

The future extent of peat permafrost and its climate feedbacks are difficult to estimate. Permafrost peatlands store large quantities of C but the understanding of C dynamics and organic matter (OM) decomposition for this type of landscape is limited by a lack of observational data (Hugelius et al., 2020). Only few studies have measured the C degradation potential in thawed permafrost peat (Panneer Selvam et al., 2017; Treat et al., 2014; Waldrop et al., 2021). Therefore, estimates of how thawing permafrost peatlands in Scandinavia will contribute to climate induced greenhouse gas (GHG) release are very limited and inaccurate (Chaudhary et al., 2020).

C dynamics in thawing peatland permafrost are difficult to model and are per date not included in Earth System Models (ESM) commonly used to study climate feed backs (Lawrence et al., 2018). Peatland permafrost models could be based on either existing peatland models or existing permafrost models (Chaudhary et al., 2020; Martin et al., 2019), but would have to combine modelling of both peatland C and permafrost thermal dynamics. Peatlands are difficult to model even without permafrost and therefore permafrost models do not include peatlands. Vice versa, permafrost models including C dynamics are at their infancy (Chadburn et al., 2017) as comprehensive model schemes including physical and biogeochemical processes are lacking.

The present study uses peat plateaus in Northern Norway to improve the understanding of biogeochemical processes in thawing peat permafrost in Northern Scandinavia. Peat plateaus are morphological features created in areas with sporadic permafrost and can therefore be found in proximity (scale of meters) to permafrost-free soil (Martin et al., 2019). Peat plateaus, also known as palsas, are peatland mounds with a frozen core lifted above the water table through ice expansion (Alewell et al., 2011). This process is self-reinforcing since the uplift decreases winter snow cover which would otherwise insulate the peat. Warming during summer thaws the top layer of the permafrost and the layer that thaws is referred to as the active layer. The depth of the active layer is controlled by summer temperatures and winter conditions that affect the freezing of the active layer. A transition zone (≤ 0.1m) is found between the active layer and the permafrost, which will occasionally thaw (Quinton & Baltzer, 2012). A conceptual model of a permafrost peat plateau is shown in Figure 1.

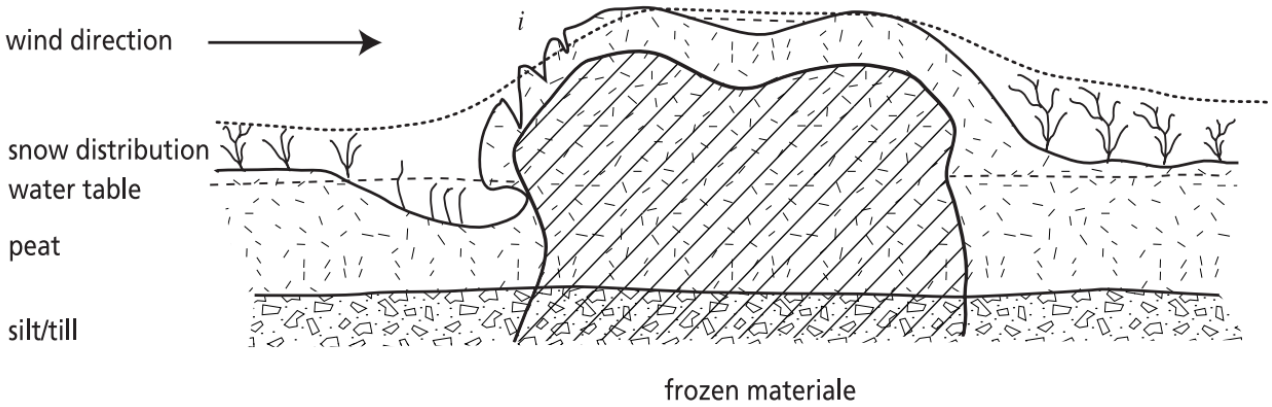

Figure 1: Conceptual model of a peat plateau (cross section). The hatched area indicates frozen peat and soil. The mid-winter snow distribution and water table position are shown with stippled lines. The snow distribution during winter is an important factor controlling permafrost since it acts as an insulation layer. Due to the elevated position, the snow cover will be shallower on the peat plateau than the surrounding mire, which keeps the permafrost cold. The wind-ward side of the peat plateau has started to collapse giving rise to a thermokarst lake. From Hofgaard (2003)

Peat plateaus in northern Norway have decreased in lateral extent by 33-71% from the 1950s to the 2010s, with the largest change recorded in the last decade (Borge et al., 2017). An example of well-documented lateral decrease in peat plateaus extent in Northern Norway is the Lakselv site (Fig. 2), which was also part of the present study. Historically, northern peatlands have acted as a long-term sink for C since the Holocene (Panneer Selvam et al., 2017), but this may change since the thawing of permafrost will alter the C cycle in these landscapes.

Permafrost thawing happens either gradual or abrupt. A Swedish study found that the active layer depth in peat permafrost has increased by ~1 cm year^{-1} since 1978 in northern Sweden (Åkerman &

Johansson, 2008). Increase in snow precipitation and higher temperatures following climate change will increase permafrost thaw (Payette et al., 2004). In recent years, abrupt thawing of permafrost has been documented in large permafrost areas (Treat et al., 2021; Turetsky et al., 2020). Abrupt thawing is considered a much faster process and affects larger areas over shorter time compared to gradual thawing. Most importantly, it results in collapse of parts of the permafrost at the plateau fringes, exposing thawing permafrost to O_2 or to anoxia in case the permafrost peat brakes directly into a thermokarst pond. Thermokarst lakes are small, water-logged basins in which thawed peat becomes inundated (Fig. 1). As permafrost in peat plateaus thaws, thermokarst lakes are formed. An example of thermokarst formation can be seen in Figure 2; thermokarst lakes emerged in 2008 at places which were peat plateaus in 1959.

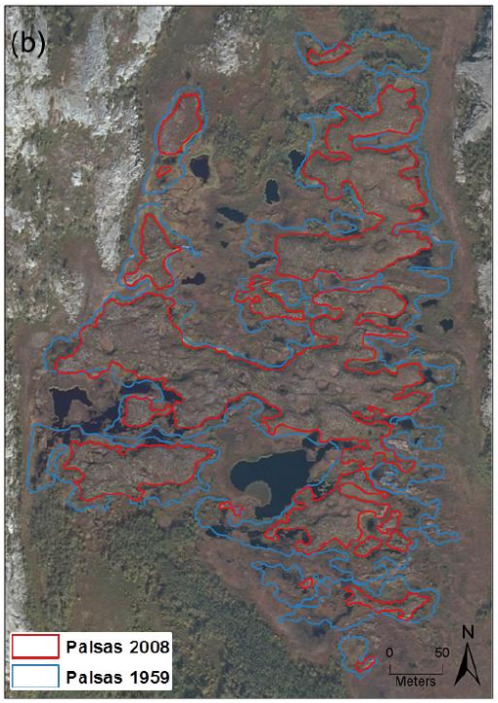

Figure 2: Aerial images documenting peat plateau recession at Lakselv, Northern Norway. Blue lines show extent of peat plateaus in 1959 and red lines in 2008. From Borge et al. (2017). See also Fig. 3

It is unclear whether the climate change driven transformation from peat plateaus to thermokarst and non-permafrost peatlands results in an overall increase of C storage or whether the system is turned into a net C source (Treat et al., 2015; Turetsky et al., 2007). Newly released OM is susceptible to microbial decomposition resulting in CO_2 and CH_4 emission to the atmosphere or runoff of DOC. Depending on the degradability of the released DOC, permafrost thawing contributes to further browning of water ways (de Wit et al., 2016) and/or downstream GHG emissions (Spencer et al., 2015). CH_4 has a global warming potential 28 times higher than that of CO_2 over 100 years (IPCC, 2014), and it is therefore important to understand how climate change affects the dynamics of C turnover and partitioning to CO_2, CH_4 and DOC in permafrost peat plateaus and thermokarst lakes.

Permafrost thawing can lead to both negative and positive climate feedbacks based on the radiative forcing of CO_2, CH_4 and N_2O as well as changes in albedo (Turetsky et al., 2007). Thermokarst formation can increase CH_4 emissions as previously frozen peat becomes inundated while accumulation of new peat in the thermokarst driven by vegetation change binds CO_2 (Estop-Aragones et al., 2018; Turetsky et al., 2007). Warmer temperatures and longer growing seasons in the (Sub)Arctic might simulate plant growth (greening), thus increasing the net primary productivity (NPP) and storing new C in the soil. The quality of accreted C may also change as vegetation changes leading to a new steady state in C storage. It has been estimated, however, that the increase in

microbial degradation of C will exceed increased C uptake by plants, thus turning permafrost regions into a net source for C emissions to the atmosphere (Treat et al., 2015). A model study found that peat plateaus lose ~30% of their initial C stock during the first decade after thawing, while the recovery of the C as peat can take anywhere from centuries to millennia (Jones et al., 2017). Recent studies also state that increased plant growth accelerates C decomposition of old organic matter by stimulating microbial decomposers in the rhizosphere, a process called rhizosphere priming (Keuper et al., 2020). This could potentially limit C accumulation by peat formation after peat plateau thawing/collapse.

Thawing permafrost peat can also enhance nitrogen (N) mineralisation, and this might result in release of N_2O, which has a global warming potential 265 higher than that of CO_2 over 100 years (IPCC, 2014). Peatlands are environments poor in N, and the presence of vegetation is known to limit N_2O release in (sub)arctic areas since N mineralised after permafrost thaw is reabsorbed by plants. Yet, microbial and chemical N-transformations associated with N mineralisation (nitrification, denitrification, chemo-denitrification) might emit some of the released N as N_2O to the atmosphere especially where vegetation is sparse. This has been observed in western Siberia and Finland among other places (Marushchak et al., 2011; Voigt et al., 2017b). The magnitude of N_2O emission from peat plateaus is difficult to assess, but it is estimated that N_2O will contribute little to the total radiative forcing from thawing peatland permafrost (Hugelius et al., 2020).

Little is known about the magnitude and controlling factors of C degradation in peat plateaus. A widespread method to evaluate potential C degradation is to incubate peat in the laboratory, which in the present study was employed for different depths including thawed permafrost peat. Even though this method may overestimate C degradation, it is a useful tool for exploring controlling factors of post-thaw C degradation. Improved knowledge of potential rates and regulating factors may also help to constrain mathematical models that aim to predict climate feedbacks from thawing permafrost.

This MSc project was performed in collaboration with Nora Nedkvitne, and the experiments were designed and conducted together to study both C degradation (this thesis) and mercury mobilisation (Nora Nedkvitne's thesis). The goal of this thesis was to quantify post-thaw C degradability of active layer and newly thawed permafrost OM and to explore factors constraining decomposition such as availability of O_2, C quantity and quality and nutrients. The following questions were addressed:

1. Does post-thaw C degradability differ among Norwegian permafrost peat plateaus depending on geomorphology, age and climate?
2. Can OM degradability be predicted by the chemical properties of the frozen peat?

3. Does degradability follow peat age and stratigraphy in the order active layer (AL) > transition zone between (TZ) > permafrost (PF)?
4. Are decomposition rates significant under anoxic conditions and will this trigger CH_4 emissions? Do initially oxic conditions make the material more available for subsequent anoxic degradation?
5. How is C degradation influenced by physical disintegration (bio/cryoturbation)?
6. Is degradation associated with apparent microbial growth, and if yes, which conditions are conducive to growth?
7. Is microbial degradation of permafrost material limited by other nutrients than C?

2 Materials and Methods

2.1 Site Description

Sampling was conducted at three permafrost peat plateaus in Finnmark, Norway (Fig. 3). The peat plateaus were selected to represent a well-documented chronosequence of permafrost from coastal Lakselv with warmer and wetter maritime climate to colder and dryer continental climate in Áidejávri (Borge et al., 2017). The three peat plateaus are characterised by cryic histosols (WRB (2014). Peat plateaus cover approximately 110 km^2 of the area in the Finnmark county (Borge et al., 2017).

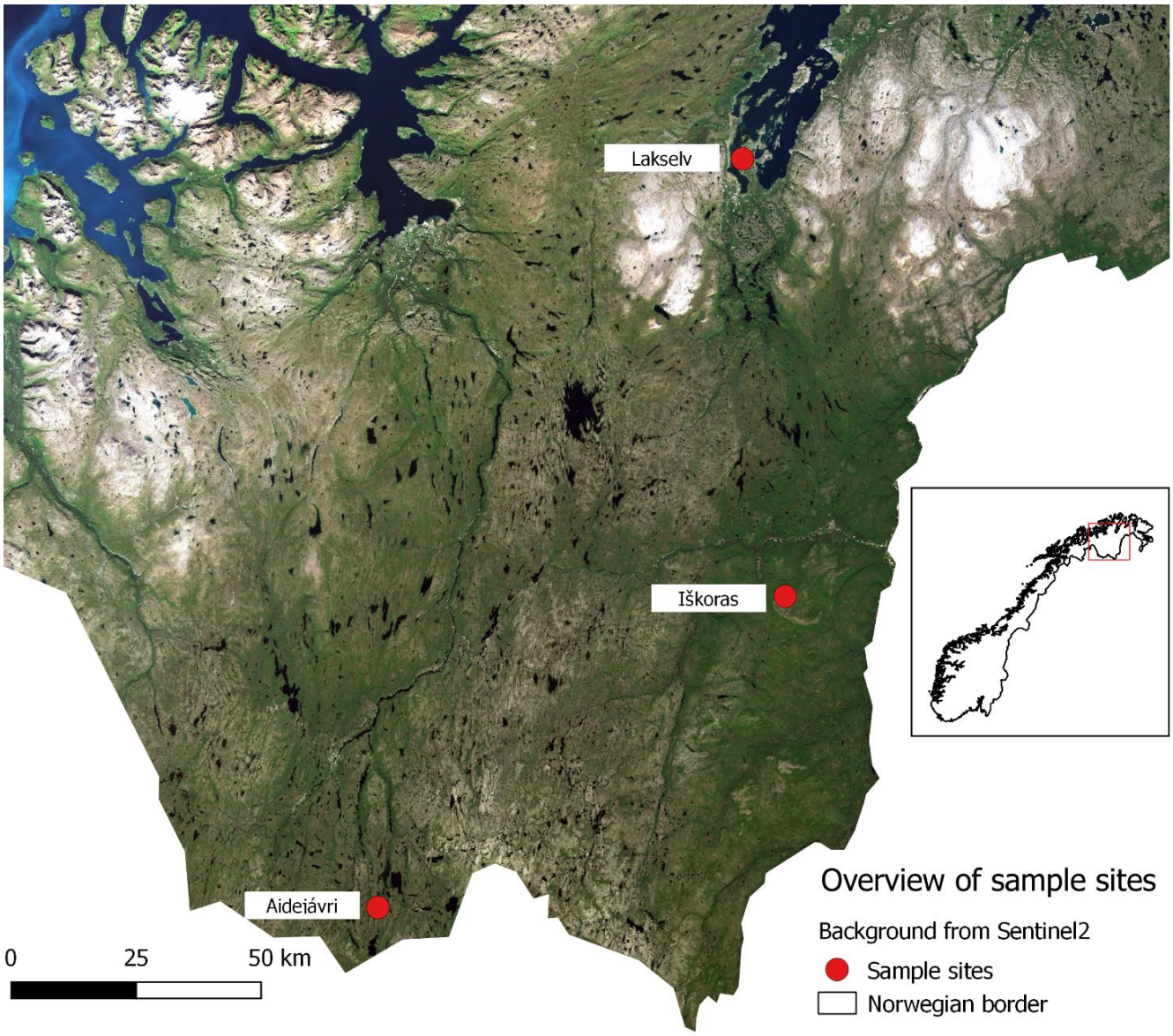

Figure 3: Satellite (Sentinel2) image of the sampling area in Northern Norway between 68° to 70° N. The red dots denote the sampling sites. From Kartverket (2019; 2020)

2.1.1 Iškoras

Iškoras (Fig. 4) is located on Finnmarksvidda (69º20’27” N, 25º17’44” E; 381 m a.s.l.) about 90 km from the nearest fjord. The mean annual air temperature was -1.9°C and the mean annual precipitation 478 mm for the period 1991-2020 (Klimaservicesenter). Peat development at Iškoras started around 9200 cal. yr. BP, and permafrost formation around 800 cal. yr. BP (Kjellman et al., 2018). In general, peatlands on Finnmarksvidda have developed over depressions with fine-grained glacio-fluvial and glacio-lacustrine deposits surrounded by rock outcrops and basal till (Kjellman et al., 2018). The geological bedrock at the Iškoras site is primarily mica slate and quartz-feldspar slate (NGU, 2021a).

Figure 4: Photograph of the Iškoras site with the sampled peat plateau in the foreground and a wet fen in the background

2.1.2 Áidejávri

Áidejávri (Fig. 5) is situated further inland on the Finnmarksvidda (68°44’59” N, 23°19’06” E; 398 m a.s.l.). This site had a mean annual air temperature of -1.3°C and a mean annual precipitation of 433 mm for the period 1991-2020 (Klimaservicesenter). The peatlands at Áidejávri have formed over similar quaternary deposits as those at Iškoras but nothing is known about when peat and permafrost formed. The geological bedrock is dominated by amphibolite (NGU, 2021a).

Figure 5: Photograph of the Áidejávri site with the sampled peat plateau in the foreground and another peat plateau in the background. The lower areas in the middle were wet fen

Figure 6 shows near-surface ground temperature at a peat plateau in Áidejávri from November 2018 to September 2020 when sampling was conducted. The active layer at the sampling point was 0.45 m. The temperature profile exemplifies the typical seasonal variation in peat plateau surface

temperatures with minima at -7.8°C in winter, fluctuations during winter due to changes in snow cover and summer temperatures up to +17.5°C (Martin et al., 2019).

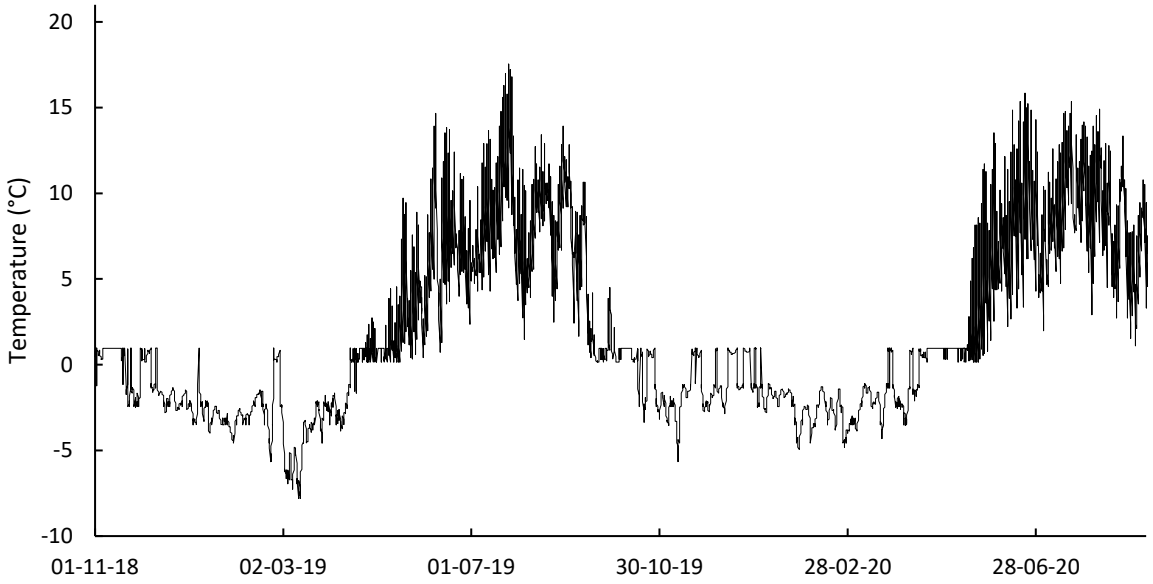

Figure 6: Near-surface ground temperature in a peat plateau close to the sampling site at Áidejávri (pers. com., S. Westermann, UiO)

2.1.3 Lakselv

Lakselv (Fig. 7) is situated close to the sea appr. 0.5 km from the shore of the Porsangerfjorden (70º7'14" N, 24º59'47" E; 50 m a.s.l.). Lakselv has a maritime climate with a mean annual temperature of +1.7 °C and a mean annual precipitation of 392 mm for the period 1991-2020 (Klimaservicesenter). The peatland started developing around 6150 cal. yr. BP which makes it the youngest of the three investigated sites. This is because of delayed deglaciation and isostatic uplift. The permafrost phase started around 150 cal. yr BP (Kjellman et al., 2018). The peatlands in Lakselv developed over fine-grained and silt-rich glacio-marine fillings (Kjellman et al., 2018; NGU, 2021b), and the bedrock consist primarily of quartzite sandstone (NGU, 2021a).

Figure 7: Photograph of the Lakselv site with the sampled peat plateau to the left. Behind the sampling equipment to the right there was a small thermokarst lake

2.2 Peat Sampling

The peat was sampled in the period 5th to 10th September 2020. At each site, a plot was selected based on former knowledge about the area as well as field inspection. Before sampling the cores, permafrost

depth was determined using a soil probe. The active layer (AL) was defined as the layer thawed when sampling was conducted, which concurred at the time of year when the AL reaches its maximum depth. At the time of sampling, the active layer was 0.6 m at Iškoras and Lakselv and 0.5 m at Áidejávri.

The AL was carefully removed in a U-shape using a saw and a small shovel (Fig. 8). The remaining portion was excavated, trimmed to remove adhering soil and divided into three equal layers which were placed in separate plastic boxes and kept cool until placed in a refrigerator at 3.8°C (SD=0.47) in the laboratory.

Figure 8: Photograph of sampling at Lakselv, showing how the AL was removed before taking the AL core

Figure 9: Photograph of the bottomn of the PF core sampled at Lakselv, showing the transition of organic to mineral soil

After removing the active layer, permafrost cores were taken using a metal pipe that was hammered vertically in ~5 cm increments into the permafrost. The depth of each sample was determined by measuring the hole before coring. The pipe had an outside diameter of 4 cm and an inside diameter of 3 cm. A metal block was placed on top the pipe and a sledgehammer was used to force the pipe down. Tailor-made metal jacks were used to pull up the pipe. A long, wooden stick was used to press the sample out. A tissue was placed at the end of the stick before inserting it to clean out the pipe and limit contamination of consecutive samples. Each sample was pressed out of the pipe onto a cutting bord (Fig. 9) and transferred in ~5 cm pieces to VWR 50 ml centrifuge tube, which were immediately placed into a cooling box kept just under 0°C by a mixture of crushed ice and salt until being transferred to a freezer kept at -20°C on the same day. The same setup with ice and salt was successfully used for transporting the samples frozen back to the laboratory at Ås, where the samples were kept in a -17.8°C (SD = 0.39) freezer until analysis.

Incremental coring was continued until the mineral soil below the peat was reached. The thickness of the organic layer varied at the three sites. At Iškoras, the mineral soil started at 1.67 m depth, at Áidejávri at 1.04 m and at Lakselv at 0.85 m. To facilitate comparison of different depths across sites, the permafrost samples were assigned to functional layers, i.e., transition zone (TZ) and permafrost (PF). For this, each core was divided into seven operational layers consisting of three active layers, one transition zone and three permafrost layers (Fig. 10). The layers do not share the same absolute depth across the three peat plateaus and hence must be considered as operational layers (Table 1). The deepest layers (PF3) from Áidejávri and Lakselv were categorised as mineral soil based on visual inspection and will henceforth be called mineral soil. An example of the visual difference between organic and mineral soil can be seen in Figure 9.

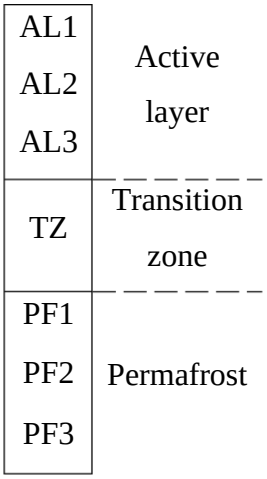

Figure 10: Conceptual model of one complete core divided in active layer (AL1, AL2 and AL3), transition zone (TZ) and permafrost (PF1, PF2 and PF3)

Table 1: Overview of operational layers and their depths

Layer	Iškoras		Áidejávri		Lakselv	
	Top (cm)	Bottom (cm)	Top (cm)	Bottom (cm)	Top (cm)	Bottom (cm)
AL1	0	15	0	15	2	12
AL2	25	35	20	35	20	35
AL3	45	55	40	50	40	60
TZ	60	73	50	60	60	70
PF1	80	86	69	80	70	80
PF2	106	118	89	100	80	85
PF3	150	162	104*	110*	85*	95*

* these layers were defined as mineral soil based on visual inspection

2.3 Sample Preparation and Incubations

2.3.1 Pre-incubation

Incubations were set up in different batches, studying one complete core (AL, TZ and PF) at a time (Fig. 10). All incubations were prepared and treated the same way, except for the experiment with nutrient addition (Ch. 2.3.4). To remove the frozen core from the tube, the bottom of the storage tube was sawn off and the frozen core was pressed onto a clean cutting board (Fig. 11A, B). The core was cut tangentially into 6 slices (Fig. 11C, D). One subsample was transferred to a scintillation vial for

determining water content and elemental composition after freeze-drying, another subsample was used to study Hg mobilisation (thesis Nora Nedkvitne). The remainder was distributed equally to four 120 ml serum bottles (Fig. 11E). Cores representative for TZ and PF layers were processed while being frozen to not release gases stored in the peat.

Samples from the active layer were processed analogously without being frozen. All serum bottles, i.e., each four replicates for each AL, TZ, and PF layer, were capped with Butyl septa and placed on ice while Helium (He) washing the headspace using an automated manifold and a vacuum pump for a total of 5 minutes using 7 cycles of alternating vacuum and He-filling (Fig. 11F). This was done to remove gases released during sample preparation and transfer, and to minimise exposure to O_2 during thawing. Helium overpressure was removed before placing the bottles into a temperature-controlled unit at 3.8°C for overnight thawing. AL samples were put into the same unit to ensure equal treatment.

Figure 11: Photographs detailing the handling of PF cores in the laboratory. A: The bottom of centrifuge tube is sawn off. B: Intact frozen core on cutting board. C: Slicing the core tangentially. D: Grouping portions from different cores belonging to the same layer in four represenative subsamples. E: Filling the subsamples into 120 ml serum bottles using a funnel and a glass stick. F: He washing the bottles after being capped

2.3.2 Gas Analyses

After at least 20 hours of thawing at 3.8°C, all bottles were placed in a temperature-controlled water bath at 10°C (Fig. 12) and gases released during thawing were analysed. The water bath can hold 44 serum bottles (120 ml) and is placed under the robotic arm of an autosampler (GC-Pal, CTC) which pierces the septum bottles with a hypodermic needle and pumps ~1ml via a peristaltic pump (Gilson 222XL) to a multi-column, multi-detector gas chromatograph (Agilent 7890A) equipped with automatic sample admission system. Afterwards, the pump is reversed to pump sample gas not injected onto the columns back to the bottle together with He. This keeps the pressure in the bottles at a constant ~1 atm. The GC had two PLOT columns: a poraplot Q column to separate CH_4, CO_2 and N_2O from bulk air and a molesieve column to separate O_2/Ar from N_2. The GC has three detectors: A thermal conductivity detector (TCD) to measure O_2, CO_2 and N_2, a flame ionisation detector (FID) to measure low concentrations of CH_4, and an electron capture detector (ECD) to measure low concentrations of N_2O. The setup is described in detail in Molstad et al. (2007) and Molstad et al. (2016) and shown in Figure 12.

Figure 12: Photograph of the automated incubator used in the study; The unit consists of a temperature-controlled water bath with submersible stirring boards, a freely programmable autosampler periodically piecing the septum bottles with a hypodermic needle and a peristaltic pump transferring ~1ml headspace to a multi-channel gas chromatograph with loop injection

2.3.3 Incubation Treatments

After measuring the initial release of gases in TZ and PF bottles after thawing (≥20 h), replicate bottles from each layer (including AL) were divided into four different treatments. Two treatments were kept as ‘loose’ peat material at natural moisture content without disturbance (Fig. 13A). The other two bottles were made into slurries by adding 52 ml of ultra-distilled water (3.8 °C) as shown in Figure 13B. One bottle of each set (loose and slurry) was washed with He as described above to

remove gases released during thawing and to adjust anoxic conditions, while the other was washed with He/O_2 (80/20) to create initially oxic conditions. To each of the slurry bottles a magnetic stirrer was added before capping for continuous stirring on a submersible stirring board in the 10°C water bath. Slurry bottles were stirred for one hour to fully disperse the peat, whereafter the peat material was allowed to settle, and 2 ml supernatant was sampled with a syringe through the septum for chemical analyses.

Figure 13: Photographs of loose and slurry treamtents. A: A depth profile from Iškoras in serum bottles. From left to right: AL1, AL2, AL3, TZ, PF1, PF2, and PF3. B: Creating the slurry by adding ultra-distilled water through the septum with a syringe,while releasing overpressure through a syringe without plunger but filled with water to prevent air from enering the bottle

pH was measured using HACH H170 after transferring 0.5 ml of the samples to an 1.5 ml Eppendorf tube (1.5 ml) as shown in Figure 14. The remainder of the sample was filled in an Eppendorf tube and centrifuged at 10,000 G for 10 minutes. The supernatant was siphoned off with a syringe and filtered through a 0.45 µm filter (Sterile Syringe Filter with polyethersulfone membrane, VWR International) into a new Eppendorf tube. This sample was used to determine water-extractable DOC by a Total Organic Carbon Analyser (TOC-V, Shimatzu, Japan) coupled to an autosampler (ASI-V) using combustion and near infrared detection of CO_2 after removing carbonates by HCl.

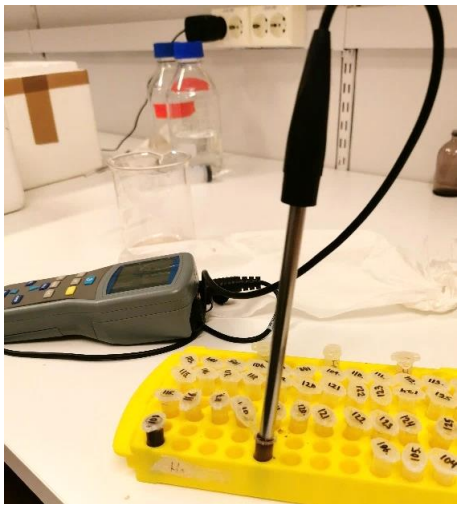

Figure 14: Photograph of how pH was measured in 0.5 ml slurry

After the slurries had been sampled, all bottles (both with loose peat and slurry) were subjected to He- or He/O_2 washing once again using an automated manifold and a vacuum pump (Fig. 15A). This was done to remove accumulated gases and to obtain zero background concentrations for CO_2 and CH_4. The final washing also denotes the start of the incubation at 10°C in the water bath (Fig. 15B). Before starting gas measurements, overpressure was removed. Dry bottles filled with standard

mixtures of known concentrations (AGA, Norway) were prepared and included into the measurement sequence for calibration and for evaluating the dilution resulting from back-pumping of He after each sampling. Gas concentrations in the headspace were measured automatically every 4.5 h until 413-450 h to capture initial gas kinetics after thawing at high temporal resolution.

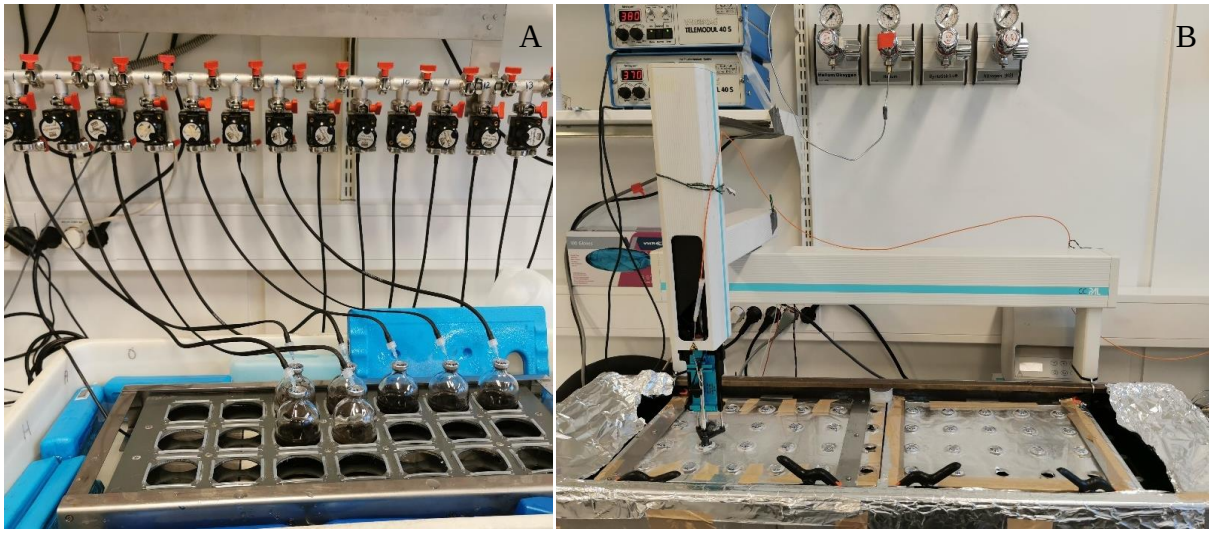

Figure 15: A: Photograph of the manifold used for washing the bottles with either He og He/O_2 in an ice bath while stirring the bottles on a submersible stirrer. B: The incubation robot taking a sample from a serum bottle incubated in the water bath at 10°C

2.3.4 Nutrient Treatments

Besides incubating samples from the depth profiles under four different incubation conditions as described above, two additional experiments were carried out. The first was a DOC manipulation experiment for testing whether decomposition rates would depend on the concentration of native DOC. For this experiment, only PF peat from Iškoras was used. Three treatments were applied (in triplicate): regular, low and high DOC. The idea was to transfer DOC from the low DOC treatment to the high DOC treatment. This was achieved by preparing slurries with Iškoras PF material as described above. After stirring for one hour, the slurries were transferred to 50 ml centrifuge tubes. After centrifugation at 4100 G for 10 minutes, the supernatant was extracted (Fig. 16A) and filtered through a 0.45 µm filter into a fresh 50 ml centrifugation tube (Fig. 16B). The filtrate was then transferred to bottles with thawed PF material, resulting in the treatment with artificially augmented native DOC. The same amount of water that was removed from the bottles was replaced with ultra-distilled water, resulting in the low DOC treatment. A third set of bottles with PF material received an equal amount of ultra-distilled water representing the regular DOC treatment. Other than the transfer of filtered extract between low and high

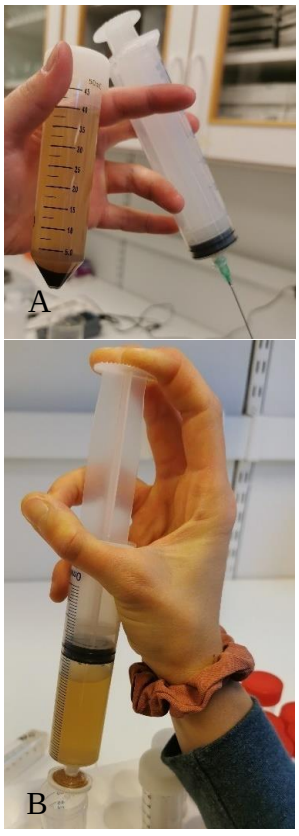

Figure 16: Extracting DOC for the DOC manipulation experiment A: Extract after centrifugation. B: Filtration of extract. The filtrate was added to a new PF sample thereby increasing the amount of DOC being initially present

DOC treatments, the bottles were handled equally and processed as described above, including pH and DOC analysis before incubation. The DOC experiment was run anoxically to begin with, but as very little activity was detected, the bottles were flushed with He/O_2 after ~10 days of incubation.

In a second manipulation experiment, different nutrients (glucose, ammonium, phosphate and sulphate) were added to homogenised PF material from Iškoras prior to incubation, to test whether decomposition was nutrient limited. The nutrient concentrations were chosen to ensure ample amounts and reasonable stoichiometric ratios between C and N, P and S, respectively (Table 2). The C-addition was around ten times higher than those of N, P and S. A treatment with Mercury (Hg) addition was added for Nora Nedkvitne's work in an attempt to promote Hg methylation without contaminating the peat to a degree that would limit biological C degradation. The mercury concentration was chosen based on Yang et al. (2016).

Table 2: Final concentrations of nutrient added to homogenised Iškoras PF material to test nutrient limitation of C decomposition. Bottles were prepared in triplicate and given are final concentrations of added nutrients

Treatment	Glucose ($C_6H_{12}O_6$)	Ammonium (NH_4Cl)	Phosphate (KH_2PO_4)	Sulphate (Na_2SO_4)	Mercury (Hg^{2+})
	mM bottle^{-1}	mM bottle^{-1}	mM bottle^{-1}	mM bottle^{-1}	nM bottle^{-1}
Control	-	-	-	-	-
Carbon	54.49	-	-	-	-
Nitrogen	-	4.39	-	-	-
Phosphorus	-	-	4.50	-	-
Nitrogen and phosphorus	-	4.32	4.43	-	-
Sulphur	-	-	-	4.51	-
Mercury	-	-	-	-	2.91
All	48.26	3.89	3.97	3.97	2.73

To obtain enough PF material for replicate incubations with different nutrients, PF tubes from several depths were thawed overnight and pooled. For this, the peat was transferred to a beaker and stirred manually (Fig. 17A, B), before distributing equal amounts to 24 serum bottles (Fig. 17C). The bottles were randomised before adding the nutrients to minimise the effect of inhomogeneities. Slurries were prepared with ultra-distilled water and nutrients were added from stock solutions to their final concentrations. Also, this experiment was started anoxically but was switched to oxic conditions (by He/O_2 washing) after 8 days.

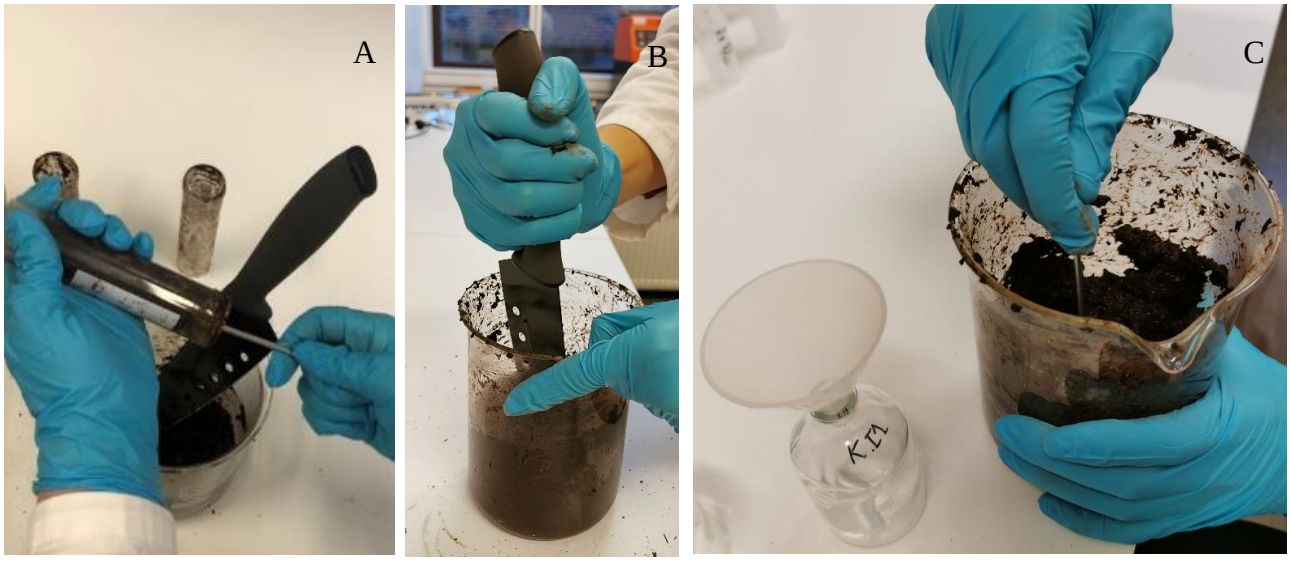

Figure 17: Preparation of the experiment with nutrient additons. A: Pooling of PF cores that had thawed over-night in the tubes . B: Mixing PF material with a knife. C: Distributing the PF material to serum bottles

2.3.5 Long Term Incubation

After 19 days of incubation with high-resolution gas monitoring, bottles were transferred to a temperature-controlled unit adjusted to 9.7°C (SD=0.04), where the incubations were continued without continuous stirring. The slurries were shaken at least once a week, after which headspace samples were retrieved for offline gas chromatography. After about one month, the measurement frequency was decreased to biweekly. Long term gas monitoring was done in two ways. For the first 2-5 weeks, 1 ml of headspace gas was extracted with a gas-tight syringe with stop cock and transferred to a He-filled (1 atm) 10 ml bottle capped with a Butyl septum. The gas samples were analysed offline on a GC similar to the one described in Ch. 2.3.2. To maintain constant pressure in the serum bottles, 1 ml He was injected into the bottles after sampling, which was corrected for when processing the data. Due to the dilution in the He-filled bottles and background contamination, reproducibility for O_2 was poor, and it was therefore decided to move the bottles intermittently to the automated incubator (Ch. 2.3.2) which measures headspace concentrations directly.

2.3.6 Gas Kinetics

The GC determines peak areas (PA) for CO_2, CH_4, O_2, N_2 and N_2O, which were converted to ppm using a one-point calibration based on the PAs of standard gases of known concentrations (CO_2, N_2O CH_4) or air (O_2, N_2) analysed in the same batch. Dilution of headspace gas by back-pumping of He (Ch. 2.3.2) was corrected for. In addition, O_2 and N_2 concentrations were corrected for contamination from the atmosphere. Sampling loss and dilution were determined from concentration changes of standard gases in dry bottles. All rate calculations were based on corrected concentrations. To account for dissolution of gases, equilibrium between gaseous and dissolved phases was assumed (Molstad et

al., 2007; Wilhelm et al., 1977) and rates were calculated per bottle including both gaseous and dissolved gases (mol h^{-1} $bottle^{-1}$), before normalising them to g dry weight peat.

To estimate rates, corrected gas concentrations were plotted over time (Fig. 18). In brief, every gas curve was inspected visually, and linear portions chosen to estimate instantaneous, steepest, stable, and long-term rates of concentration change. Figure 18A shows how instantaneous, steepest, and stable rates were determined for CO_2 and O_2. The intervals chosen for estimating production and consumption rates for CO_2 and O_2, were always the same since uptake of O_2 is linked to CO_2 production. Figure 18B shows the corresponding CH_4 values. Here, the instantaneous rate was the steepest one. Gas kinetics differed strongly between samples, ranging from almost linear accumulation (e.g. CO_2 in Fig. 19) to strongly dynamic ones with apparent lag, growth and stationary phases during product accumulation (Fig. 18). All estimated rates were normalised to g dry weight peat and tabulated in excel for further processing. Long-term production rates were calculated as the linear slope of gas accumulation during long-term incubation (Fig. 20).

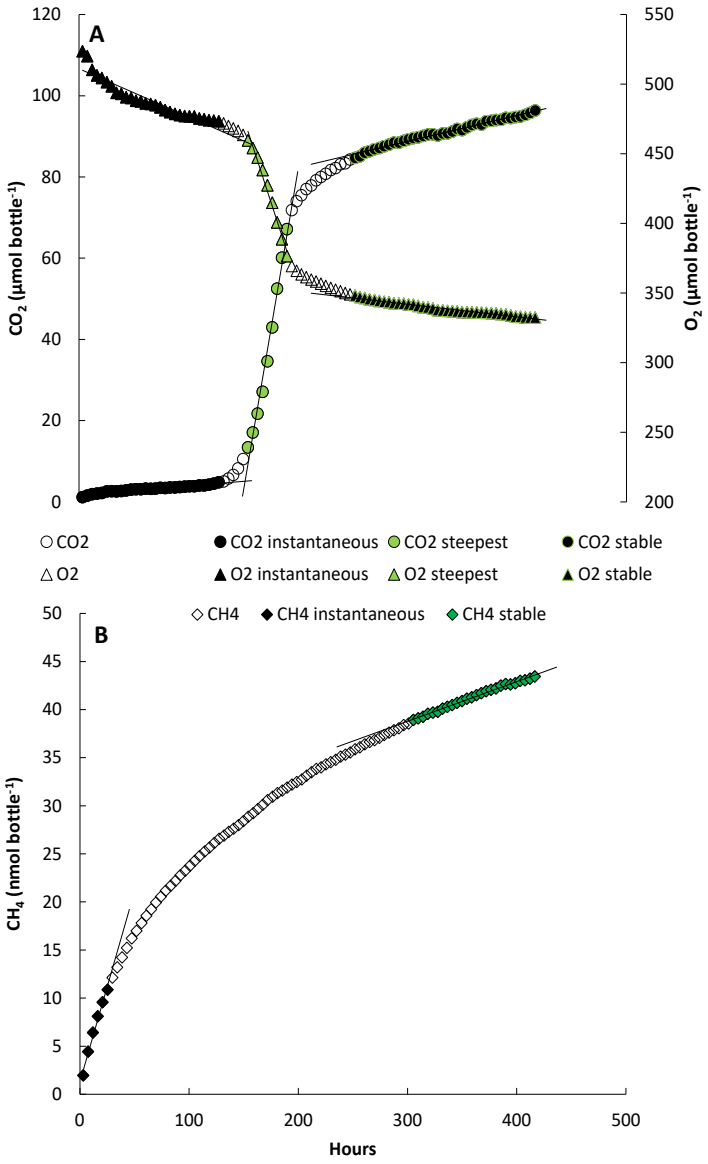

Figure 18: Examples for how rates were estimated for different phases during incubation using corrected concentrations. Shown are concentration data form the oxic slurry incubation of Iškoras TZ. A: CO_2 and O_2. B: CH_4

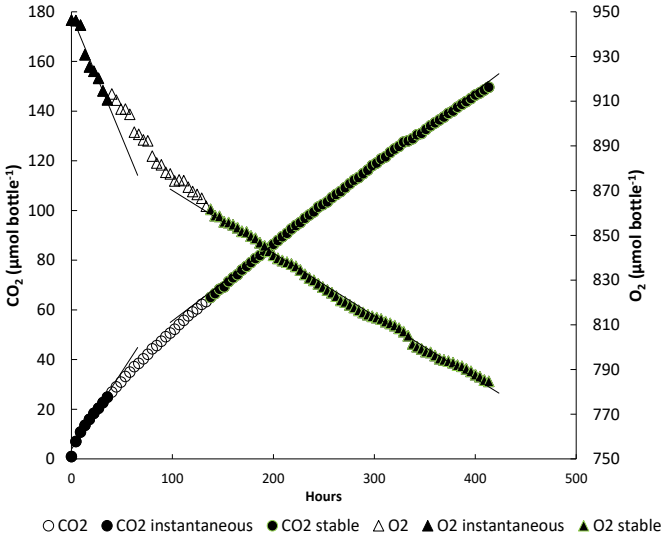

Figure 19: Example of quasi-linear, zero-order kinetics. Shown are data from the loose oxic incubation of top active layer (AL1) at Iškoras

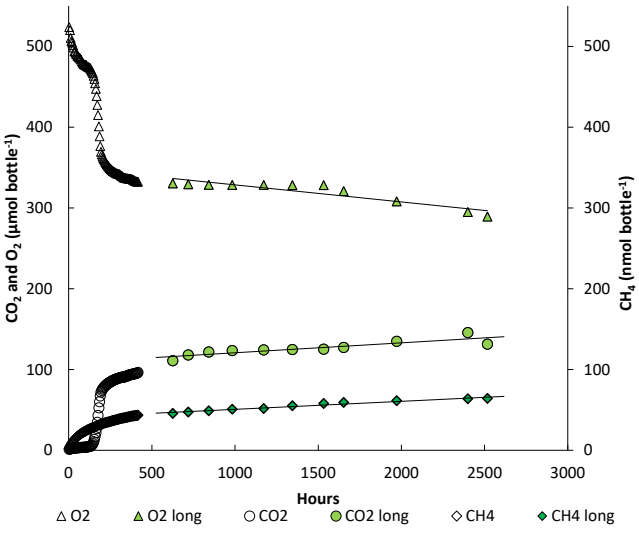

Figure 20: Example of long term gas dynamics. Shown are data from the oxic slurry incubation of Iškoras TZ with determination of long rates for O_2, CO_2 and CH_4

2.4 Peat Properties

All samples were analysed for their elemental composition using a combination of inductively coupled plasma mass spectrometry (ICP-MS), inductively coupled plasma optical emission spectrometry (ICP-OES) and elemental analyser-isotope ratio mass spectrometry (EA-IRMS). To prepare samples for analysis, between 2 and 19 g of fresh sample were placed in a scintillation vial and freeze-dried (SP Scientific VirTis BenchTop Pro with Omnitronics™) for 48-96 hours, depending on the amount of sample. The samples were weighed before and after drying to determine their water content. Freeze-dried samples were homogenised in an agate mortar (Retsch RM 200). The samples were not sieved and spoons and funnels out of plastic were used to minimise metal contamination. The Agate mortar was cleaned between each sample, and extra cleaning was performed between cores. For some depths, two samples had to be pooled to obtain enough material for analyses.

2.4.1 Elemental Analysis

Prior to elemental analysis using IPC-MS (Agilent Technologies 8800 ICP-MS Triple Quad) and ICP-OES (PerkinElmer FIMS), samples were decomposed in an ultraclave (ultraCLAVE, Milestone). First, 0.20-0.25 g of the homogenised, freeze-dried material was weighed in acid-washed Teflon tubes. Each tube was filled with 2 ml ultrapure dH_2O and 5 ml ultrapure concentrated HNO_3. Samples were incubated overnight to ensure moisturisation, before decomposition. The decomposed sample was then added to a fresh 50 ml centrifugation vial, amended with 20 ml ultrapure dH_2O and 1 ml concentrated HCl before filling up the tube to 50 ml with ultrapure dH_2O. The tubes were shaken 10 times to ensure mixing. Each batch included standards of known elemental composition; Spinage

NCS ZC73013 was used in all analyses since it has a standard value for Hg. The four other standards were Bush Branches and Leaves (NCS DC 73349), Peach Leaves (1547), Pine Needles (1575) and River Sediment (LGC6187). In total 27 elements were analysed, 21 by ICP-MS (Mn, Ni, Cu, Zn, As, Se, Cd, La, Ce, Pr, Nd, Sm, Eu, Gd, Dy, Ho, Er, Tm, Yb, Hg, and Pb) and six by ICP-OES (P, S, Fe, Al, Ca, and Mg).

2.4.2 Elemental Analyser - Isotope Ratio Mass Spectrometry

Amounts and natural abundance stable isotope ratios of C and N were measured using a flush combustion elemental analyser coupled to an isotope ratio mass spectrometer (continuous-flow EA-IRMS; Thermo-Finnigan Delta Plus XP). First, the EA was tested for leaks and the IRMS magnet calibrated for finding m/z 30 (N_2) and m/z 44 (CO_2) in the same run. Linearity was tested by running zero-enrichment test with different reference pressures. Certified standards were included in every measurement batch to directly calibrate $\delta^{13}C$ and $\delta^{15}N$. For this, three replicates each of IAEA-N-1 (~1 mg) and IAEA-CO-8 (~2 mg) were weighted and analysed together with the peat samples. Ethylenediaminetetraacetic acid (EDTA) samples (0.8-1.2 mg) were used as running standards to check for drift.

Preliminary tests were performed to determine the right sample amount. A sample amount of 6-12 mg was weighted in tin capsules. For each batch, two to three blanks (empty capsules) were included to check for contamination by background gases. Certified standards, running standards, samples and blanks were all prepared the same way. Material was inserted into a tin capsule using a small spatula. The weight of the material was noted, and the tin capsule was carefully folded using tweezers.

The samples were placed in autosampler rack of the EA, which drops them one by one into the heated oxidation reactor. The tin capsule and all non-C and non-N elements were trapped in an ash crucible. The gases produced in the oxidation reactor are transported to the reduction reactor where NO_x gases were reduced to N_2. For further details see Carter and Barwick (2011).

Peak areas of the abundant isotopomers (m/z 28 for N_2 and m/z 44 for CO_2) were used to calculate C and N content, based on a calibration curve prepared from a range of EDTA amounts (Eq. 1).

Equation 1:

$$mass\ (mg) = \frac{a*pa+b}{soil\ (mg)}$$

where *a* is the slope and *b* is the intercept, *pa* is the measured peak area and *mass* the weight of either C or N.

Isotopic abundances were obtained in delta (δ) notation relative to the N_2 and CO_2 reference tanks. For correcting $\delta^{13}C$ and $\delta^{15}N$ values, the deviation in delta values from the certified reference standards was determined (+ 0.4‰ for IAEA-N1 and -5.764 ‰ for IAEA-CO8) and added or subtracted from the measured values. For $\delta^{13}C$ values, a drift was seen in the running standards, which could be described by a second order polynomial regression (Fig. 21). This was used to further correct the values for drift.

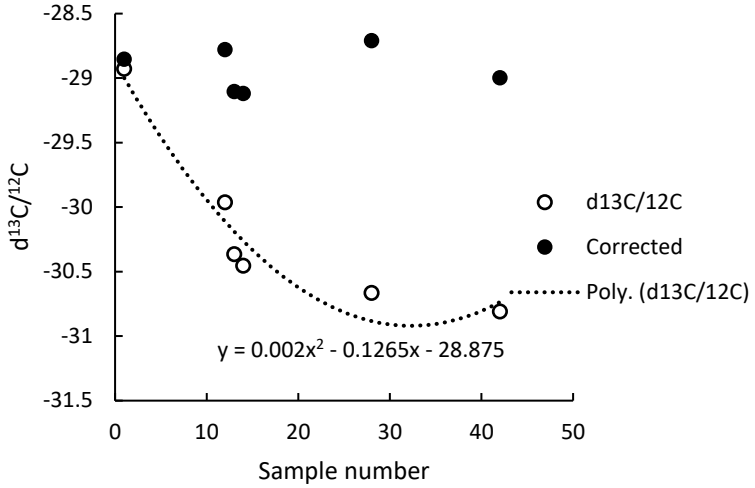

Figure 21: Drift of $\delta^{13}C$ values in running standards (EDTA) interspersed between samples (hollow markers) fitted to a second order polynomial (line). The corrected values for the running standards are shown as markers with solid fill

2.5 Data Analysis

2.5.1 ANOVA

All depths were treated as individual samples without replication. To compare differences across peat plateaus, depths and treatments, samples from different depths of AL, TZ and PF or different incubation treatments were pooled ('pseudo-replication') and subjected to one-way ANOVA. For the experiments with DOC manipulation or nutrient addition, triplicates were available. ANOVA was performed with Minitab 19. Statistical significance was assumed at $P<0.05$.

2.5.2 Principal Component Analysis

Principal component analysis (PCA) was used to explore the relationship between CO_2 and CH_4 production rates and peat properties. PCA reduces the dimensionality of multivariate data sets while maintaining the variation within the dataset (Ringner, 2008). PCA was performed using Minitab 19. All variables were standardised and scaled by division through their mean value. An outlier plot using Mahalanobis' distance was produced for each analysis. The Mahalanobis distance determines the distance between a sample and the mean distribution of samples in a multi-dimensional space. No outliers were detected. Score and loading plots were produced based on the first two components (explaining most of the variation) and evaluated for grouping and factor loading.

3 Results

In the following sections, selected results from Iškoras, Áidejávri, and Lakselv are presented. First, the peat chemistry is presented, and differences and similarities among the three peat plateaus are highlighted. The subsequent sections focus on results from the incubations experiments. CO_2 production in peat samples from all three peat plateaus was on average by ~4 orders of magnitude higher than CH_4 production. Therefore, the main focus will be on CO_2 production followed by a short section on CH_4 and N_2O production.

3.1 Peat Characteristics

Among the measured elements, only selected results are presented to highlight differences among peat plateaus and across different layers. The depths presented here are the same as used in the incubation experiments (Table 1). Note that the profiles cannot be compared directly as the absolute positions of AL, TZ and PF differed between the sites (Table 2). The complete data of measured elements can be found in the Appendix (Table 1).

3.1.1 Carbon and pH

All three peat plateaus had a C content of roughly 50% (by weight) in the top layer, which decreased towards PF1 at Lakselv, while Iškoras and Áidejávri had remarkably stable C contents throughout the active layer (Fig. 22A). At Áidejávri, C content declined steeply from PF1 to PF3, the latter being defined as mineral soil. Also, at Lakselv PF3 was visually identified as a mineral soil, but here the C concentration was much higher (324 mg C g dw^{-1}). At Lakselv, the lowest C concentration was not found in the mineral soil (PF3) but in in the top permafrost (PF1). Hence, the visually defined mineral soil in Lakselv (Fig. 9) must have been a mixture of peat and mineral soil, thus explaining the relatively high C-content. Given the low pH in the peat, inorganic C can be considered negligible and total C content should therefore equal organic C content.

Extractable DOC and pH were measured after ≥20 h of thawing under anoxic conditions and stirring of one hour. For all three peat plateaus, pH increased with depth except for PF2 at Lakselv which was somewhat lower than PF1 and PF3 (Fig. 22C). Peat samples from Áidejávri and Lakselv had higher pH than those from Iškoras. Iškoras, on the other hand, had the highest DOC concentrations, especially in TZ and PF layers (Fig. 22B). For Iškoras and Áidejávri, the highest DOC concentrations were found in PF1. In PF1, DOC concentrations were 2.2 and 4.4 times higher for Iškoras than for Áidejávri and Lakselv, respectively. At Lakselv the highest DOC concentration was observed in AL1.

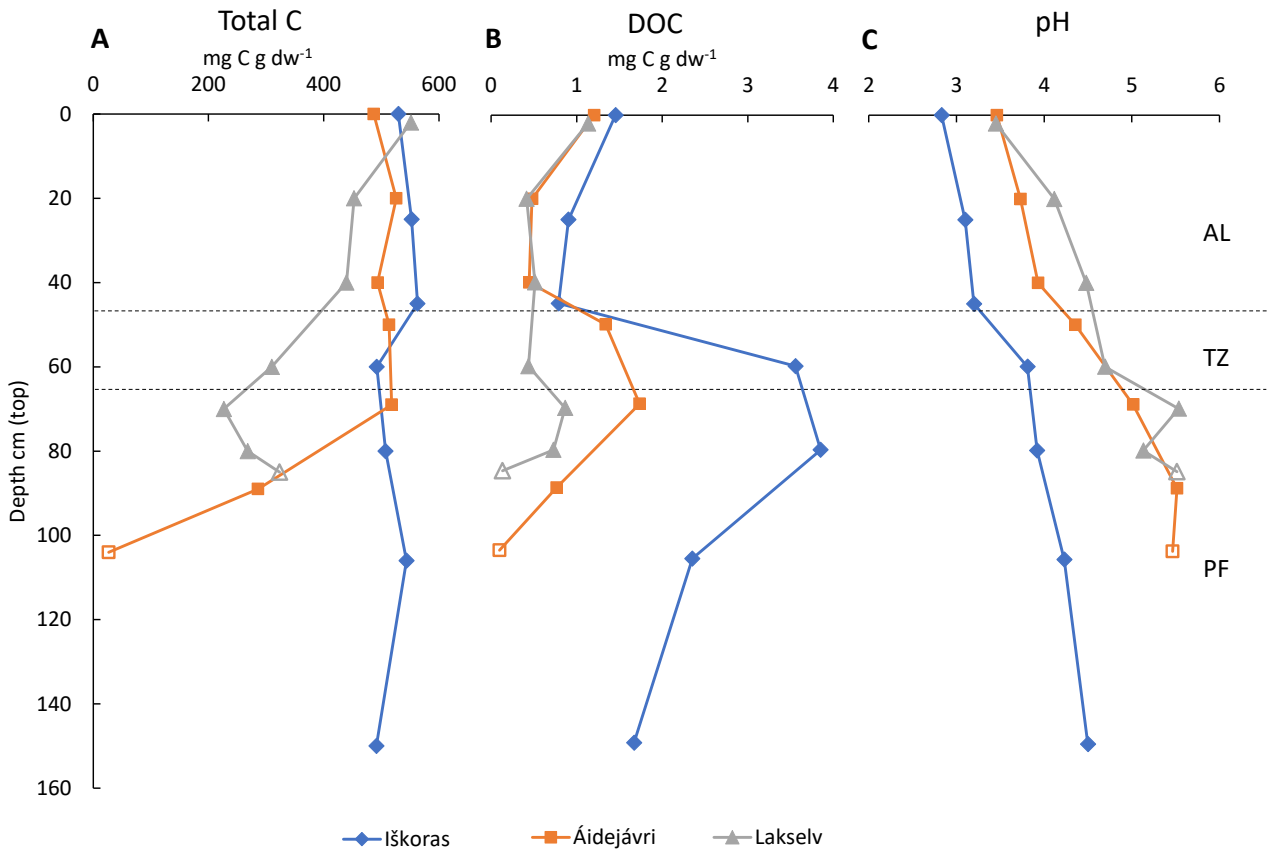

Figure 22: Depth profiles of A: total C, B: Extractable DOC and C: pH in water. pH was measured in oxic slurries for Iškoras and in oxic and anoxic slurries for Áidejávri and Lakselv (average). Hollow symbols denote mineral soil

3.1.2 ^{13}C and ^{15}N Natural Abundance

Figure 23 shows the depth profiles of bulk $\delta\ ^{13}C$ and $\delta^{15}N$ values at the three peat plateaus. Total C was slightly enriched in $\delta\ ^{13}C$ in AL1 and decreased markedly towards AL2 at all three sites. Permafrost material from Lakselv had a relatively stable, depleted $\delta\ ^{13}C$ value, whereas PF material at Iškoras and Áidejávri showed more variable $\delta\ ^{13}C$ values with depth. As with $\delta\ ^{13}C$, the $\delta^{15}N$ values were highest in the top layer (AL1) at all three sites and decreased throughout the active layer, most so at Iškoras, and least at Lakselv. For Iškoras the lowest $\delta^{15}N$ value was measured in AL3, which was the lowest value measured for all three sites. From AL3 to TZ, the $\delta^{15}N$ value increased again and remained stable with depth. Both Áidejávri and Lakselv showed less variability with depth.

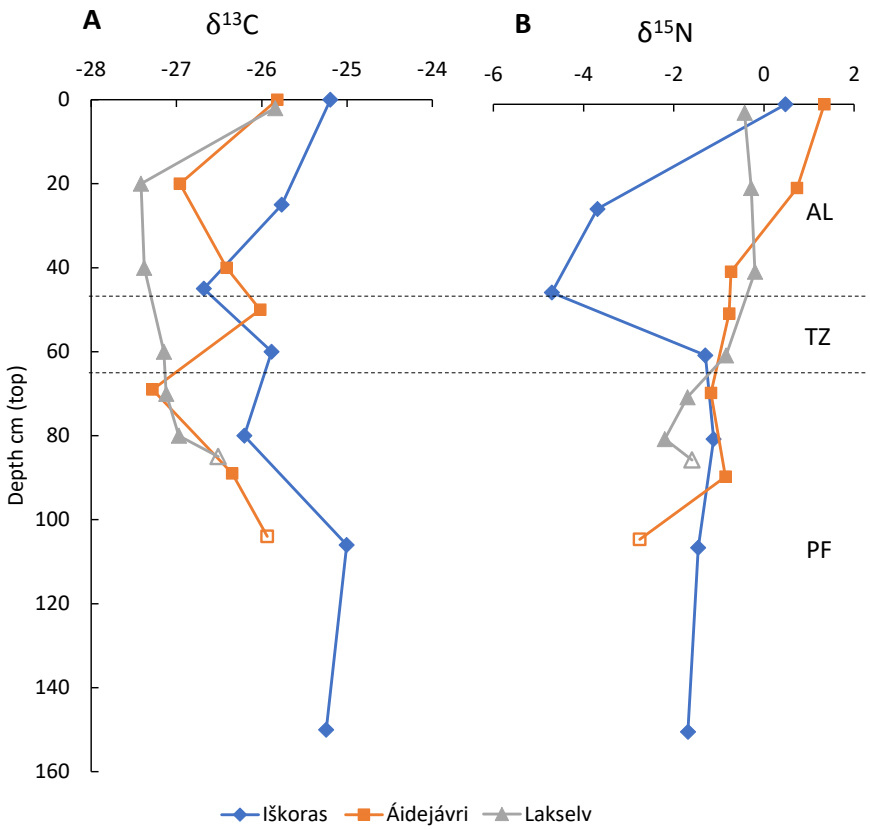

Figure 23: Depth profiles of stable isotopes ratios ($\delta^{13}C$ and $\delta^{15}N$) at the three sites. A: $^{13}C/^{12}C$ ratio. B: $^{15}N/^{14}N$ ratio. Hollow markers are mineral soil

3.1.3 Macro- and Microelements

To compare total C content with N and P contents, C/N and C/P ratios were calculated (Fig. 24). In all three peat plateaus, the C/N ratio was highest in the top layer (AL1), reflecting input of fresh plant material. At Iškoras the C/N ratio gradually decreased from AL2 to PF1, before increasing again in deeper PF layers. Áidejávri and Lakselv showed a more drastic decline in C/N from AL1 to AL2 below which C/N did not change much. The C/P ratio was overall highest at Iškoras and lowest at Lakselv. In Áidejávri, the lowest C/P ratio of all samples was found in the mineral soil PF3. Where Iškoras had the lowest C/P ratio in AL1 and PF3, Lakselv had the highest.

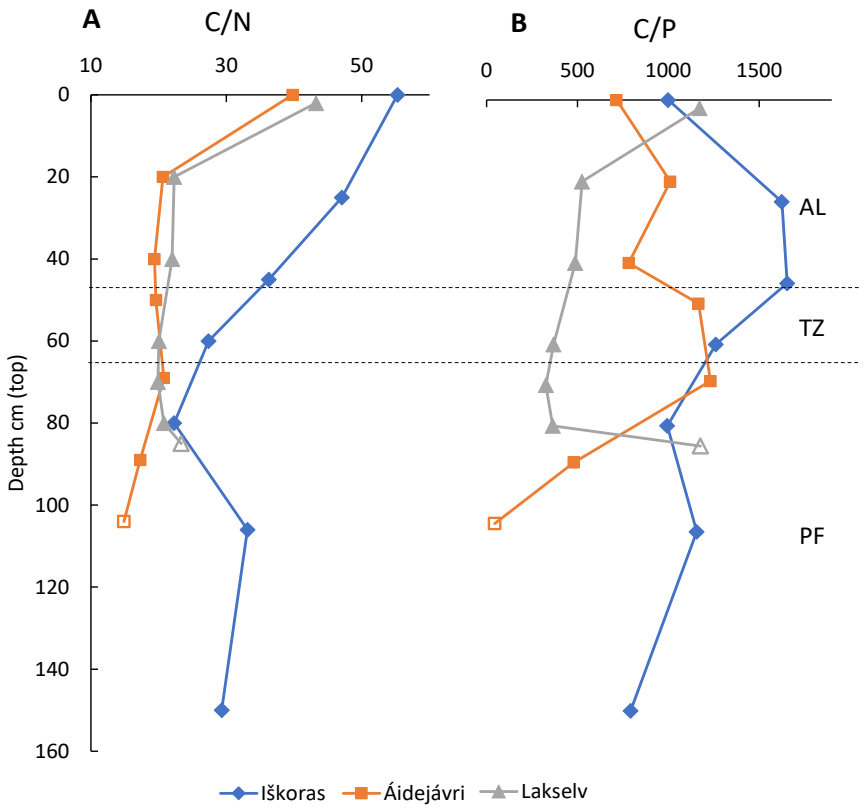

Figure 24: A: C/N and B: C/P ratios for all depths at the three sites. Hollow markers are mineral soil

In total 28 non-C elements were measured. A PCA including all measured elements (Fig. 25) resulted in a clear grouping of sites except for AL1 samples, which grouped together. Samples from Lakselv differed from the other two sites in that they correlated positively with element concentrations except for N, S and Ca in the loading plot (compare Fig. 25 and 26). Lakselv had higher concentrations of most non-C elements than Áidejávri and Iškoras (Table A 1). Áidejávri samples, in turn, were positively correlated with N, S and Ca.

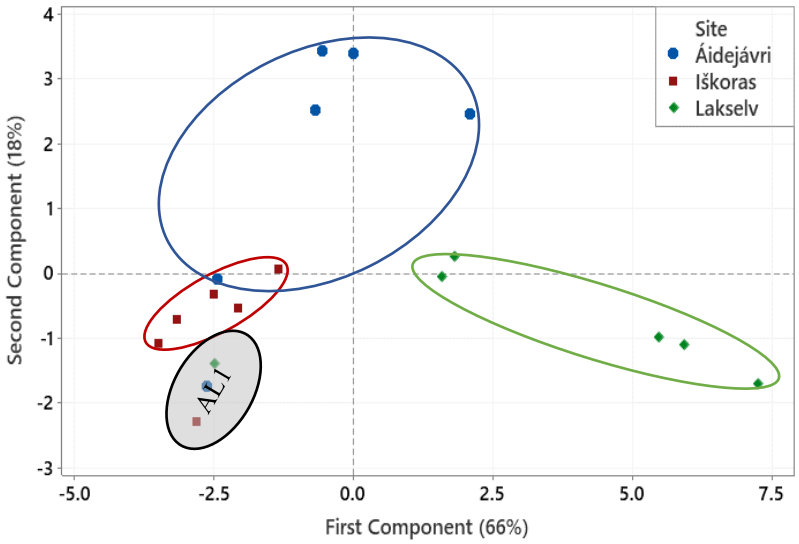

Figure 25: Score plot of a PCA with peat chemistry (28 non-C elements across three sites and 6 layers). Points of same colour represent the different peat layers at each site (excluding FF3). Groupings are highlighted with circles

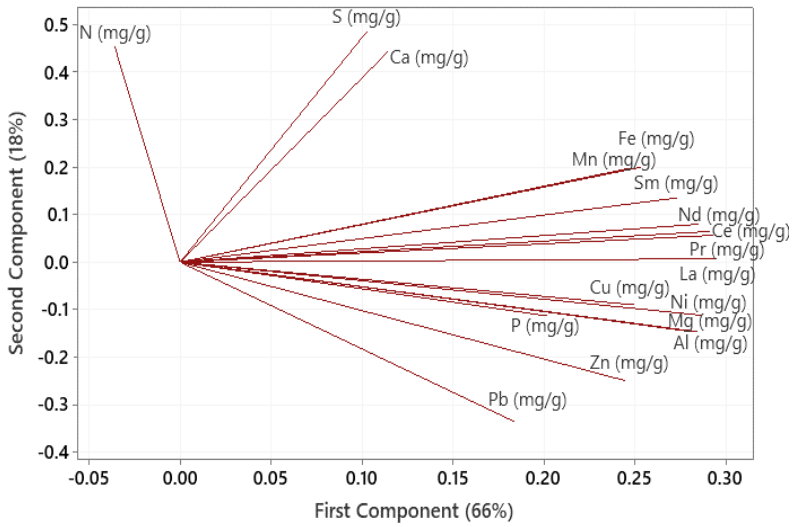

Figure 26: Loading plot that explains the grouping in Figure 25. The lines indicate which factors are controlling the principal components

To highlight differences in element composition between the three peat plateaus, the depth profiles for the macroelements S, Ca and Mg and the microelements Fe, Mn, Cu and Zn are shown in Figure 27 and Figure 28, respectively. Concentrations of S and Ca (Fig. 27A, B) were higher in all organic layers (excluding AL3) at Áidejávri than at Iškoras and Lakselv. Lakselv had the highest concentrations of Mg in all layers (Fig. 27C).

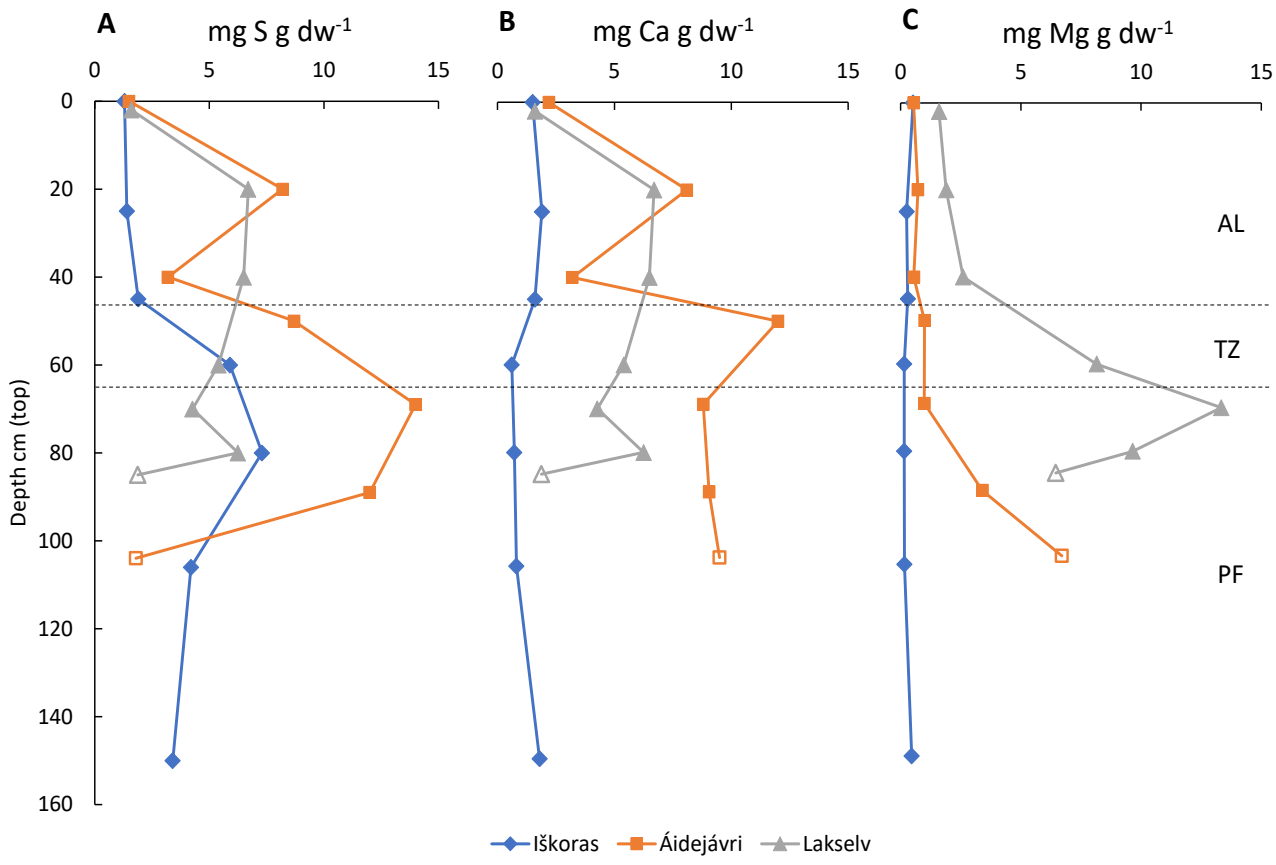

Figure 27: Depth profile for selected macroelements at the three sites. A: Sulphur. B: Calcium. C: Magnesium. Hollow markers are mineral soil

Highest concentrations of Fe, Mn, Cu and Zn were found at Lakselv (Fig. 28). The trend over depth at Lakselv shows a general increase peaking in PF1. This trend was similar to that of Mg (Fig. 27C) and inversely mirrors the total C-content (Fig. 22). Overall, Iškoras had the lowest concentrations of non-C elements with little variation across layers, which also mirrored C-content (Fig. 22) inversely. Áidejávri had more variation in non-C elements over depth than Iškoras. Especially the active layer showed large variation in S, Ca and Fe concentrations with depth (Fig. 27 and Fig. 28). Tabulated values for each element can be found in the Appendix (Table A 1).

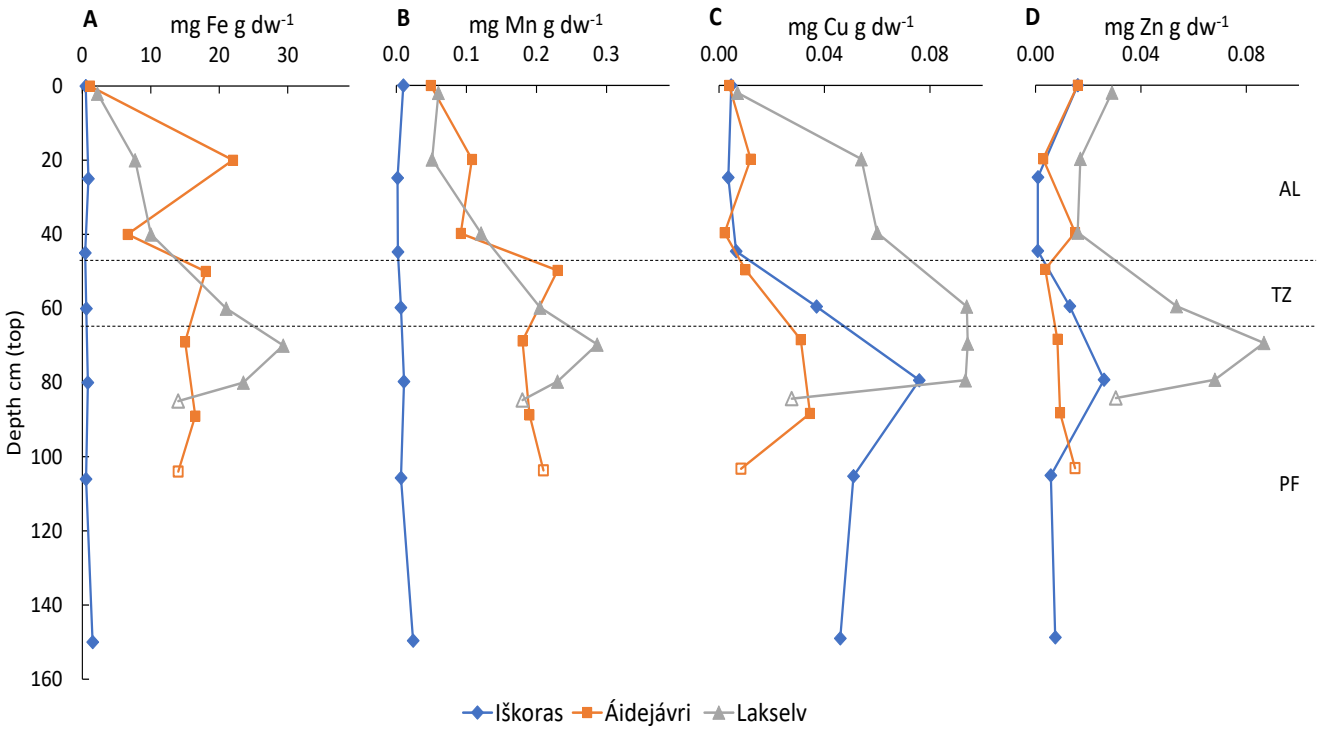

Figure 28: Depth profile for selected microelements at the three sites. A: Iron. B: Manganese. C: Copper. D: Zinc. Hollow markers are mineral soil. NB: different x-axis

To explore how the chemical composition affected C decomposition across peat plateaus, a PCA was performed, including CO_2 accumulation over 96 days averaged for all four incubation treatments (Ch. 3.2.4). Further, total C content and extractable DOC were included next to the macroelements N, P, S, Ca and Mg and the microelements Fe, Mn, Cu and Zn and pH. Values for PF3 were excluded because of their mineral influence.

The score plot reveals a clear clustering for sites for all layers except AL1 which groups separately. Component 1 explained 50% of the variability in the dataset and contributed most to the separation by site (Fig. 29). Component 1 was heavily impacted by C-variables (total C, CO_2 production and DOC), pH, macro- and microelements excluding N, S and Ca (Fig. 30). PC2 explained 21% of the variability and was mostly impacted by the macroelements N, S and Ca, which were generally higher at Áidejávri than Iškoras or Lakselv, thus explaining the grouping of Áidejávri. The grouping of the

top layer (AL1) samples is mainly caused by their higher C-content and corresponding low non-C element concentrations.

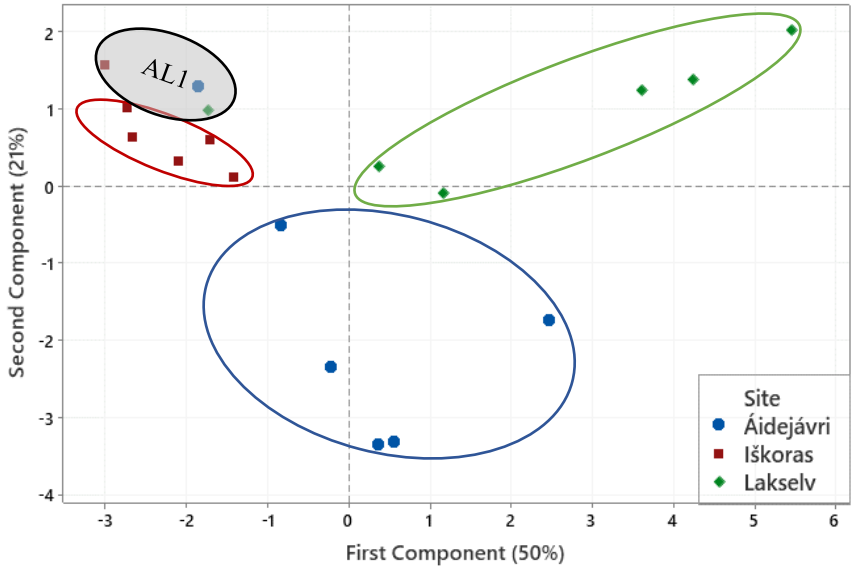

Figure 29: Score plot of a PCA with cumulative CO_2 production averaged across incubation conditions and peat chemistry. Points represent different peat layers (excluding FF3). Groupings are highlighted with circles

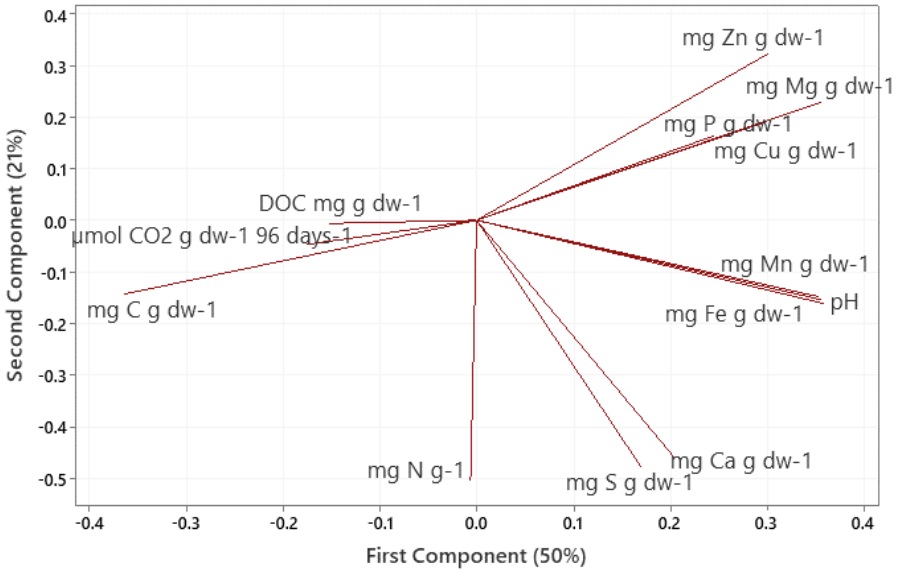

Figure 30: Loading plot that explains the grouping in Figure 29. The lines indicate which factors are controlling the principal components

3.2 Peat decomposition

Gas measurements with high temporal resolution were set up to capture gas kinetics and post-thaw metabolic patterns. Combined for the three peat plateaus, four incubation treatments and seven layers, a total of 112 individual times series of CO_2 production were recorded. Experiments with nutrient additions produced 33 additional times series which are presented in Ch. 3.2.6.

3.2.1 Gas kinetics

In general, highest CO_2 production was observed in loose oxic incubations (see Ch. 3.2.2, Fig. 33). Detailed kinetics for loose oxic incubations are presented for three different layers (AL1, TZ and PF2) in Figure 31. For all three peat plateaus, most CO_2 accumulated in AL1, following quasi-linear, zero-order kinetics (Fig. 31A). Áidejávri had the highest CO_2 production rate (0.31 µmol CO_2 g dw^{-1} d^{-1}), closely followed by Iškoras (0.29 µmol CO_2 g dw^{-1} h^{-1}). Lakselv had less than half of this production rate (0.13 µmol CO_2 g dw^{-1} h^{-1}).

CO_2 accumulation kinetics of TZ samples differed from those of AL1 in that CO_2 production rates were smaller and non-linear for Iškoras (Fig. 31B). The rate of CO_2 accumulation in the TZ sample from Iškoras was initially slower than from Áidejávri and Lakselv, but accelerated exponentially after 130 h, reaching a maximum CO_2 production rate of 0.51 µmol CO_2 g dw^{-1} h^{-1}, which was higher than the oxic decomposition rate observed for any of the AL1 samples irrespective of site. The sigmoid kinetics of product accumulation indicated microbial growth. This resulted in Iškoras having the highest final CO_2 accumulation of the three peat plateaus after 17

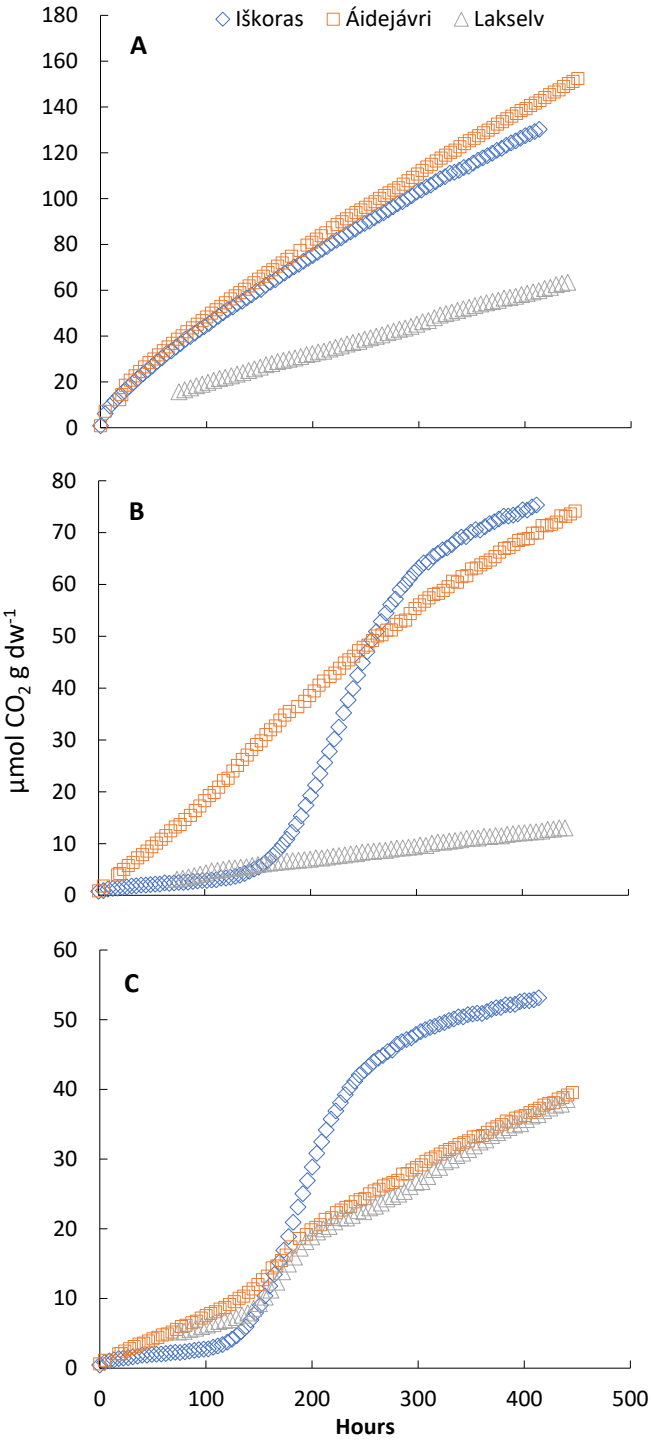

Figure 31: Comparison of CO_2 kinetics over 19 days across sites for the treatment loose oxic. A: Top active layer (AL1). B: Transition zone (TZ). C: Middle permafrost layer (PF2). Initial data for Lakselv are missing due to instrument failure. Note different scales on y-axis

days of incubation. By contrast, TZ samples form Áidejávri and Lakselv accumulated CO_2 linearly, and at a smaller rate than their respective AL1 samples (0.17 and 0.03 µmol CO_2 g dw^{-1} h^{-1} for Áidejávri and Lakselv, respectively).

In the layer PF2, all three sites showed some intermittent exponentiality in CO_2 accumulation but to varying degrees (Fig. 31C). Again, Iškoras had the highest concentration at the end of the incubation and the steepest slope during the exponential phase (0.40 µmol CO_2 g dw^{-1} h^{-1}). Also, PF2 of Áidejávri and Lakselv showed exponentiality around 150 h reaching rates of 0.14 and 0.21 µmol CO_2 g dw^{-1} h^{-1}, respectively, but the period of exponentiality was much more short-lived than with Iškoras PF2. CO_2 production thereafter was stable with rates of 0.08 µmol CO_2 g dw^{-1} h^{-1} for both Áidejávri and Lakselv.

To illustrate the effect of incubation conditions (oxic, anoxic, loose, slurry) on C mineralisation in PF peat, Figure 32 compares CO_2 kinetics of PF2 for different the incubation conditions across the three peat plateaus. The PF2 layer was chosen since this layer was also used for the experiments with nutrient additions (Ch. 2.3.4), and because the cumulative CO_2 production after 96 days among the sites were similar (Fig. 33).

Independent of site, permafrost (PF2) accumulated markedly more CO_2 under oxic than anoxic conditions (Fig. 32). Yet, Iškoras PF2 showed some exponentiality also under anoxic conditions (Fig. 32A), but both anoxic treatments (loose and slurry) had longer lag phases and less increase in CO_2 production than the oxic treatment. In comparison, PF2 from Áidejávri and Lakselv showed almost no exponentiality in product accumulation irrespective of incubation conditions. Incubating PF2 material as a constantly stirred, oxic slurry resulted in larger CO_2 production than oxic loose conditions for

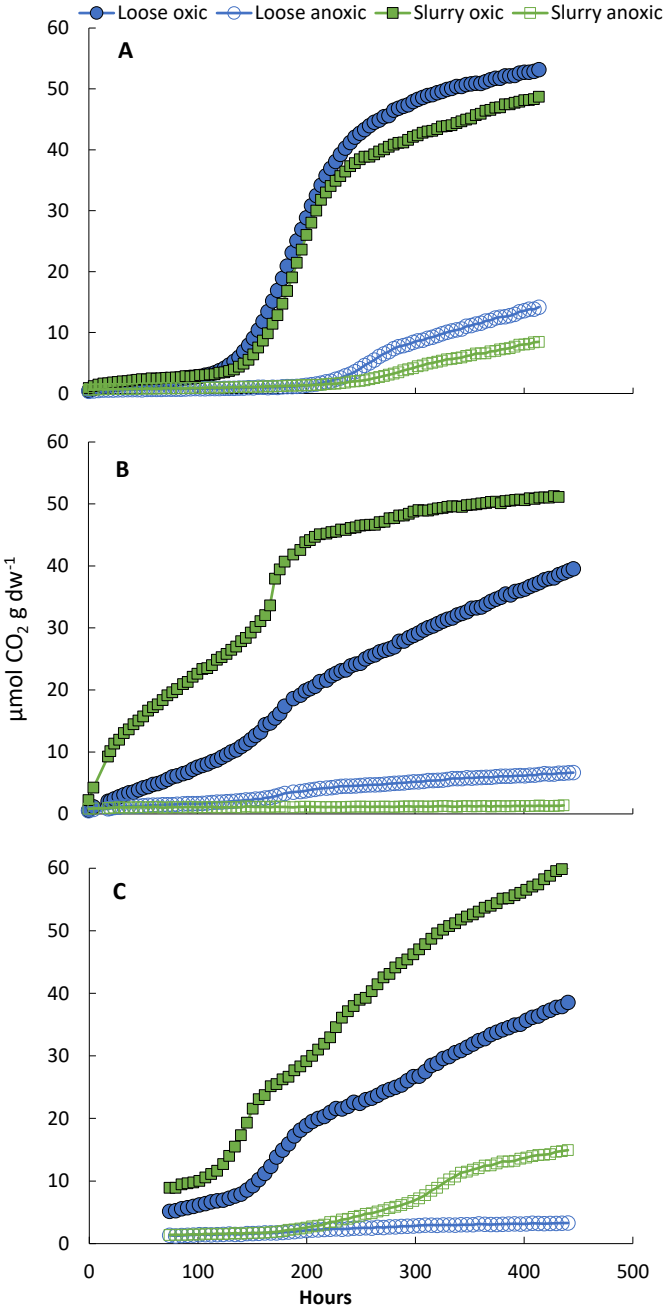

Figure 32: Comparison of CO_2 kinetics over 19 days for the layer PF2 across all four treatments. A: Iškoras. B: Áidejávri. C: Lakselv (no data available until after 70 hours due to instrument failure)

Áidejávri and Lakselv. At Iškoras stirred slurries produced less CO_2 than loose material both oxically and anoxically. Stirred anoxically, Áidejávri produced less CO_2 than loose material, whereas the opposite was the case for anoxically incubated Lakselv PF2.

Long-term kinetics are shown in the Appendix and revealed differences in accumulation patterns (Fig. A1, A2, A3, A4, A5, A6). Overall, changes in gas accumulation were relatively small beyond 19 days of high-resolution gas monitoring. However, there were noticeable differences between layers and peat plateaus. In the top AL (AL1), samples incubated as oxic slurries showed an abrupt halt in CO_2 accumulation and O_2 consumption towards the end of the high-resolution incubations, whereas consumption/accumulation trends continued in deeper AL samples. This was less pronounced in incubations with loose peat. Deeper layers (TZ and PF samples) at Iškoras that had shown sigmoid consumption/accumulation trends of O_2 and CO_2, respectively, but flattened out during the long-term incubation. Áidejávri samples showed a conspicuous increase in CO_2 production without corresponding O_2 uptake at the end of the long-term measurements in all layers except AL1 and PF3 for both loose and slurry treatments.

3.2.2 Cumulative Carbon Decomposition

To compare the overall CO_2 production across peat plateaus and depths, Figure 33 shows the cumulative CO_2 production over 96 days. All three peat plateaus showed highest cumulative CO_2 production in oxically incubated AL1 samples (both slurry and loose). The cumulative CO_2 production in AL1 for loose oxic was highest at Iškoras which was 1.3 and 2 times higher than at Áidejávri and Lakselv, respectively. Cumulative CO_2 production decreased strongly throughout the active layer (more so under oxic conditions), before increasing again in the TZ (except for Lakselv) and reaching a secondary maximum in the upper permafrost layer. In the top permafrost layer (PF1) for the loose oxic treatment, Áidejávri had the highest cumulative CO_2 production, which was 1.8 and 4.5 times higher than that at Iškoras and Lakselv, respectively.

Both Iškoras and Lakselv showed relatively small differences in cumulative CO_2 production between slurry and loose treatments, but O_2 availability had some effect in AL1 and PF layers (Fig. 33A and Fig. 33C, respectively). Lakselv had the lowest CO_2 accumulation of the three sites. Áidejávri showed most variability with depth among the four treatments and the cumulative CO_2 production in PF1 was as high as in AL1 (Fig. 33B). Also, the difference between slurry oxic and loose oxic incubation appeared to be largest for Áidejávri, especially in TZ and PF1. Taking CO_2 accumulation of the top active layer (AL1) as a reference, permafrost decomposability at Iškoras (PF1) reached 42% of that of AL1, Áidejávri (PF1) 104% and Lakselv (PF2) 59%, illustrating that old permafrost material can have a remarkably high decomposition.

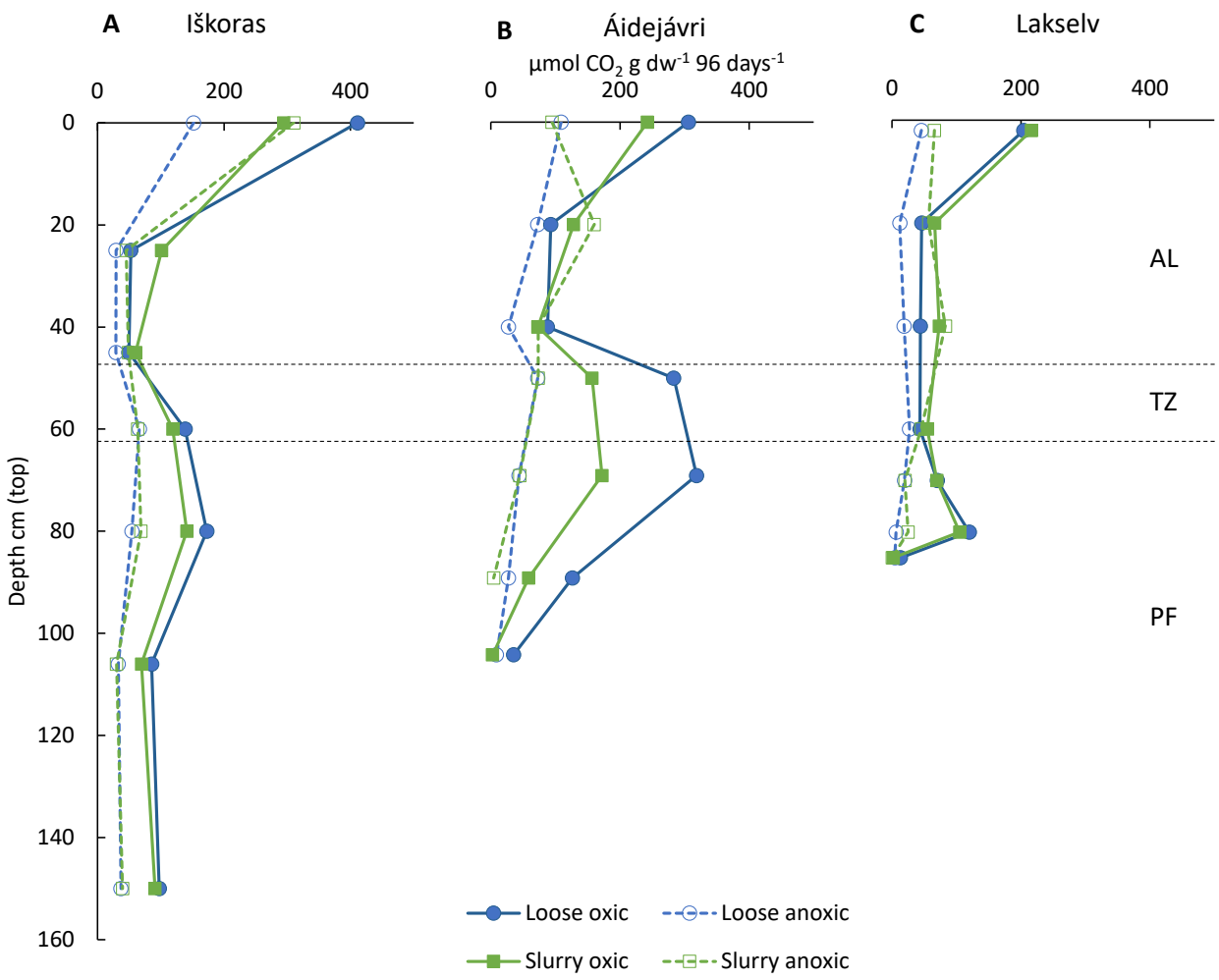

Figure 33: CO_2 accumulation over depth during 96 days under different incubation conditions. Stipulated lines indicate the position of the measured samples in the peat profile as AL (AL1, AL2 and AL3), TZ and PF (PF1, PF2 and PF3). A: Iškoras. B: Áidejávri. C: Lakselv

CO_2 production rates from oxic and anoxic treatments are summarised in Table 3 and time specific rates for different phases of product accumulation are given in the Appendix (Table A 5, A 6). Interestingly, anoxic incubations of Iškoras peat showed the same or higher CO_2 production rates than oxically incubated samples from Áidejávri (expect AL2) and Lakselv (expect for AL3 and PF2), illustrating high decomposability of Iškoras peat. For TZ and PF1 peat incubated oxically, the highest rates were observed at Áidejávri while for PF2 at Lakselv.

Table 3: Depth profile of CO_2 production averaged for loose and slurry incubations over 96 days of oxic and anoxic incubation at three peat plateaus.

Layer	CO_2 (µmol g dw^{-1} h^{-1})					
	Iškoras		Áidejávri		Lakselv	
	Oxic	Anoxic	Oxic	Anoxic	Oxic	Anoxic
AL1	0.153	0.100	0.119	0.044	0.091	0.024
AL2	0.033	0.016	0.048	0.051	0.024	0.015
AL3	0.024	0.017	0.035	0.022	0.025	0.022
TZ	0.056	0.028	0.096	0.032	0.021	0.016
PF1	0.068	0.027	0.107	0.019	0.030	0.009
PF2	0.034	0.014	0.040	0.007	0.049	0.007
PF3	0.041	0.017	0.008	0.002	0.003	0.001

3.2.3 Site Specific Differences

Figure 34 shows differences among peat plateaus in accumulated CO_2 after 17, 62 and 96 days averaged over the entire peat column and all incubation treatments. The deepest layer (PF3) was omitted as two sites (Áidejávri and Lakselv) had mineral soil in this layer. Iškoras and Áidejávri showed consistently higher average CO_2 production than Lakselv, irrespectively of incubation time. Due to high variability among the treatments, there was no significant difference between average CO_2 production at the three sites independent of cumulation period. However, the increase in average cumulative CO_2 production over time appeared to be higher at Lakselv and Áidejávri than at Iškoras. Both increased by a factor of around 2.5 between 17 days and 96 days, whereas Iškoras increases by a factor of 2 in the same period.

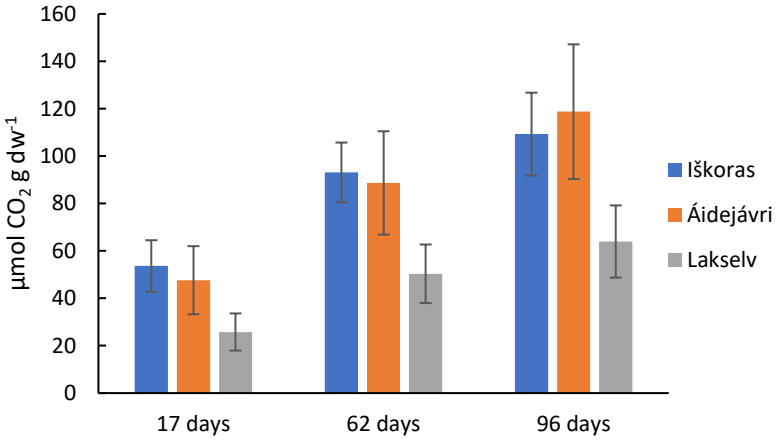

Figure 34: Cumulative CO_2 production averaged across all treatments (oxic, anoxic, loose, slurry) and layers excluding PF3 after 17, 62 and 96 days. Error bars are SE

To investigate whether the total C content could explain differences in CO_2 production, the average of cumulative CO_2 was normalised for C content (µg CO_2-C/mg C_{tot}). The CO_2 accumulation still

was lower at Lakselv than at Iškoras or Áidejávri. Iškoras and Áidejávri had similar CO_2 accumulation after normalisation (data not shown).

3.2.4 Depth Specific Differences

To show the general differences in decomposition activity across depth, the average of cumulative CO_2 production across all treatments was calculated for each layer after 17 and 96 days (Fig. 35). Iškoras and Áidejávri showed the same trend with largest CO_2 accumulation in AL1, TZ and PF1 (Fig. 35). AL1 produced more CO_2 at Iškoras after both 17 and 96 days than at Áidejávri, but the relative increase in decomposition activity over time was similar at both sites. In TZ and PF1 samples, the average cumulative CO_2 production was similar at the two sites after 17 days, but the relative increase after 96 days was higher at Áidejávri than at Iškoras. Lakselv showed a different pattern with highest averaged cumulative CO_2 production in AL1 and second highest in PF2 while the layers between AL1 and PF2 had lower CO_2 production. This trend was seen after both 17 and 96 days.

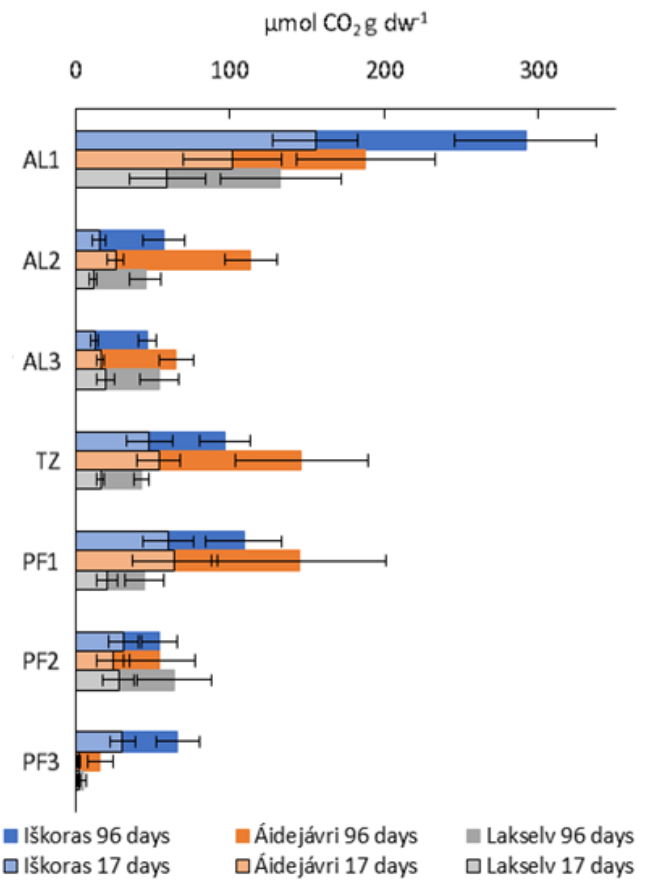

Figure 35: Cumulative CO_2 production averaged across incubation treatments (oxic, anoxic, loose, slurry) in different layers. Shown are stacked values for 17 and 96 days of incubation. Error bars are SE

3.2.5 Treatment Specific Differences

To generalise treatment effects across sites, the average of cumulative CO_2 production across layers (excluding PF3) was calculated for the different incubation conditions (Fig. 37). After 17 days, average CO_2 production was largest in oxic slurries irrespective of site. After 96 days this changed for Iškoras and Áidejávri, where loose oxic incubation accumulated more CO_2 than stirred incubation, while Lakselv still had highest production in oxic slurries.

The slurries were stirred the first 19 days of incubation after which they were shaken weekly. This is reflected by markedly higher CO_2 accumulation throughout the first 17 days (Fig. 37). The lack of continuous stirring after 19 days may have resulted in O_2 limitation in the slurries thus explaining lower CO_2 accumulation between day 17 and 96 in the slurries. Stirred samples depleted O_2 faster

than loose samples in the first phase of the incubation (0 to 19 days) and may have resulted in O_2 limitation in the second incubation phase (Appendix A 1, A 3, A 5).

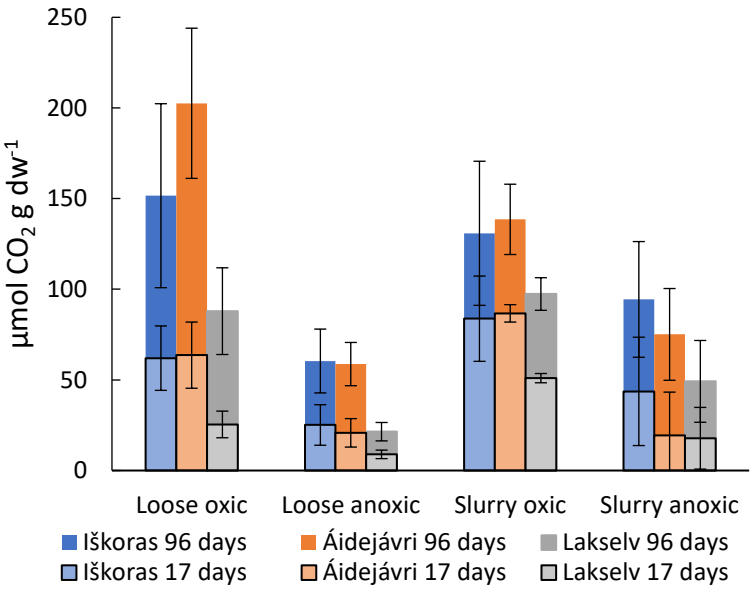

Figure 37: Effect of incubation treatment on CO_2 accumulation averaged over all layers (excluding PF3) after 17 and 96 days for all three sites. Error bars are SE

An additional parameter to evaluate the effect of incubation treatment on C decomposition is DOC accumulation over time. Carbon in peat is released upon mineralisation as either gases (CO_2 or CH_4) or DOC. However, the present study cannot distinguish DOC production by microbial decomposition and physical release by desorption from the peat matrix in the stirred slurries. Figure 36 shows the

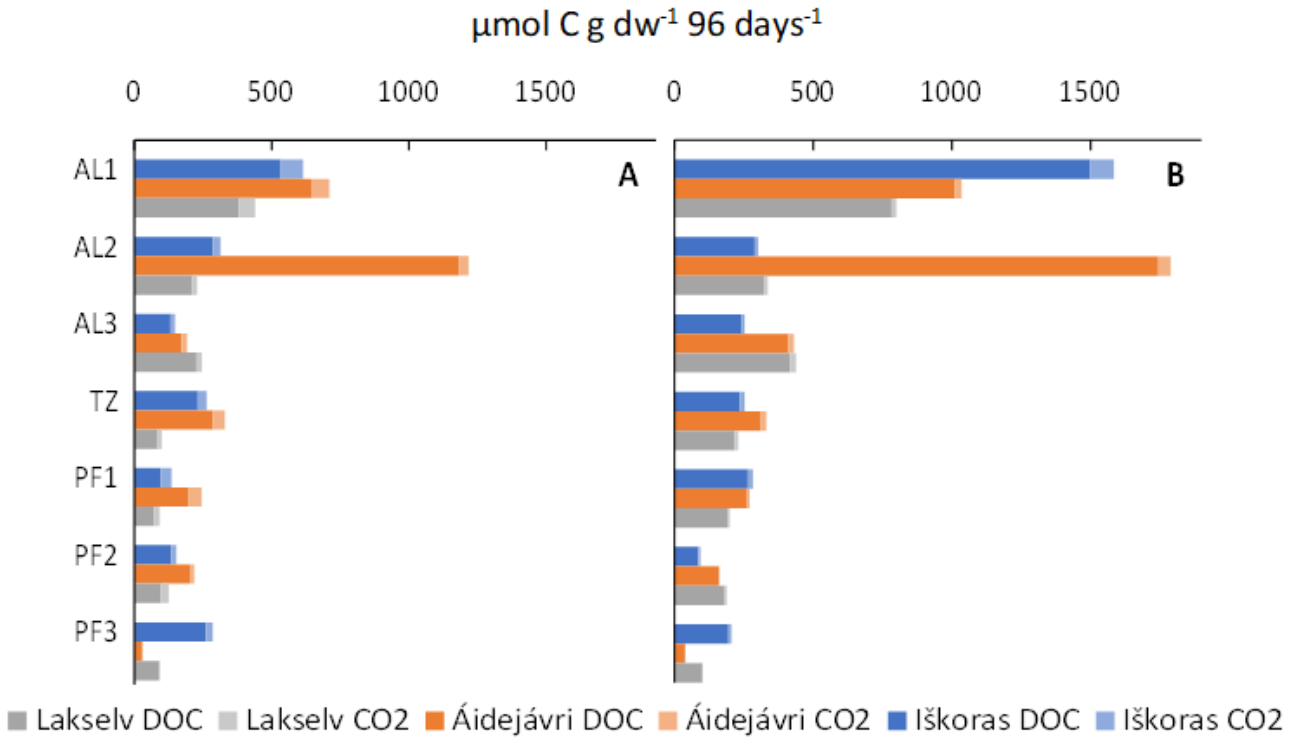

Figure 36: Combined cumulative CO_2-C production after 96 days and net DOC-C accumulation calculated as the difference between DOC measured on day 0 and DOC after 96 days at all three peat plateaus over all layers. A: measured in oxic slurries. B: measured in anoxic slurries

net DOC accumulation after 96 days of incubation for both oxic and anoxic slurries. DOC was measured three times during the incubations (after 1 h, 19 days and at the end of the incubation after ~96 days) in slurry treatments only. To evaluate the combined C-release from the peat slurries incubated under oxic and anoxic conditions, net DOC accumulation and cumulative CO_2 production were stacked and plotted per layer (Fig. 36). In general, the anoxic slurries released more C than the oxic slurries, particularly in the active layer. The highest C-release was seen in AL2 at Áidejávri for both oxic and anoxic slurries and AL1 at Iškoras under anoxic conditions. In general, the C-release measured as CO_2 production was small compared to the release of DOC.

3.2.6 Peat Decomposition with Nutrient Additions

The first nutrient experiment manipulated the concentration of native DOC as explained in Ch. 2.3.4. The setup was successful in that it created three distinct initial concentration levels of native DOC spanning from 130 to 345 µmol DOC g dw^{-1} (Fig. 38). The effect of initial DOC content on average CO_2 production was largest after 17 days and decreased after 69 days (Fig. 38). The relationship between native DOC concentration and CO_2 accumulation was not one-to-one. An 86% increase of native DOC from 'low' to 'regular' resulted in a 67% increase of CO_2 accumulation after 17 days and 39% after 62 days. The increase in native DOC from 'regular' to 'high' was 43% and this resulted in a CO_2 increase by 20% and 7% after 17 and 62 days, respectively.

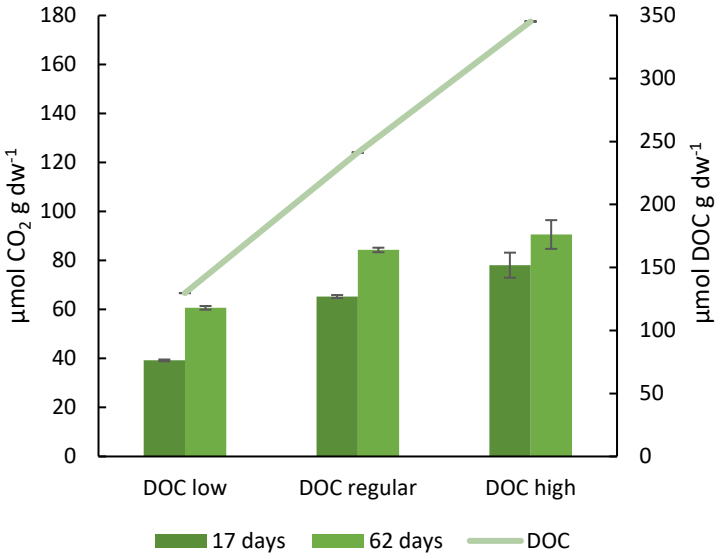

Figure 38: Average (n=3) CO_2 production (bars) for the three treatments in the DOC manipulation experiment after 17 and 62 days. The line shows the experimental gradient in initial DOC concentration. Error bars are SE

The second experiment tested nutrient limitations of C decomposition by adding selected nutrients (Ch. 2.3.4). This experiment was performed in collaboration with Nora Nedkvitne and included a treatment in which Hg was added alone or in combination with all other nutrients. The 'Mercury'

treatment is included in Figure 39 to show that the concentration of added Hg was not inhibitory, and should therefore not invalidate the treatment 'All' which also contained Hg (Table 2).

Average CO_2 accumulation after 17 and 62 days for the eight treatments is presented in Figure 39. The two treatments which had received readily decomposable C in form of glucose ('Carbon' and 'All') showed highest CO_2 production. After 17 days the CO_2 accumulation in the two treatments containing glucose was not significantly different from each other. This changed after 62 days, when the treatment 'All' (glucose in addition to all other nutrients) accumulated 1.3 times more CO_2 than the treatment with just glucose. All other nutrient treatments accumulated less CO_2 which was not significantly different from the 'Control', suggesting that non-C nutrients had little to no effect on C decomposition if not combined with glucose.

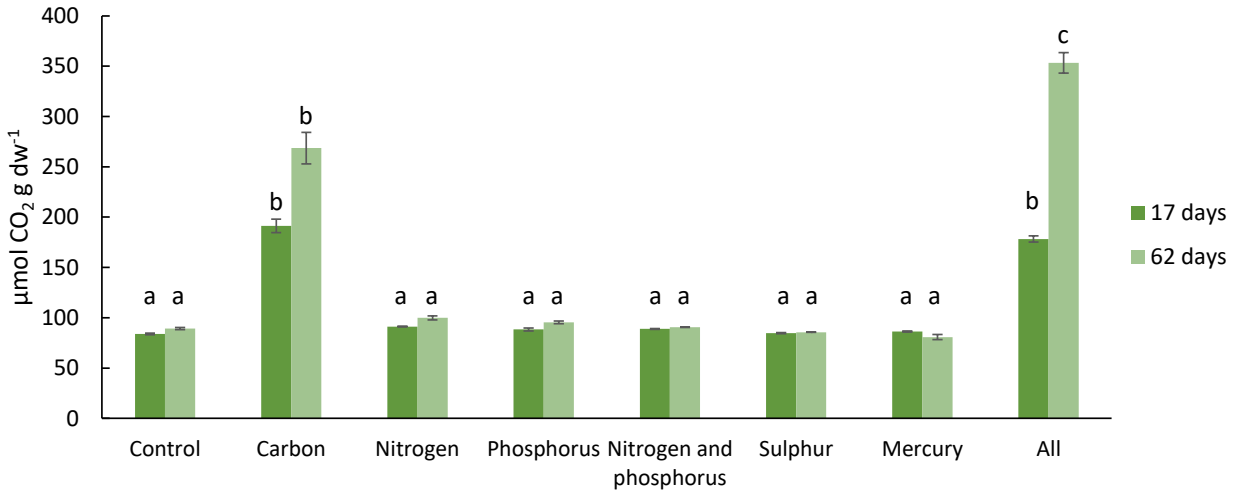

Figure 39: Average (n=3) CO_2 production of Iškoras PF2 after 17 and 62 days of incubation in the presence of nutrients. Error bars are SE. Different letters denote statistically significant differences between treatments

Figure 43 shows the average CO_2 kinetics for the two treatments with C addition and the Control. All other nutrient treatments showed kinetics similar to those of the 'Control' and are therefore not shown. The average CO_2 production rate at the end of the high-resolution incubation was highest in the 'Carbon' treatment which can be also seen in Figure 39 after 17 days even though the treatment 'All' had higher accumulation after 62 days. In Figure 43, the first treatment to experience exponential increase in CO_2 production was 'All' after ~100 hours. The time lag for exponential CO_2 accumulation in the 'Carbon' and 'Control' treatments was approximately the same but somewhat larger than the one of 'All' in which exponential increase in CO_2 production started after around 140 hours.

The lowest CO_2 production was found in 'Control' which also had the flattest slope in product accumulation. The exponential production started to flatten out after ~250 hours followed by a small, constant production. The 'Carbon' treatment showed the same trend after ~250 hours, but the

exponential slope was much steeper and therefore more CO_2 accumulated. The steepest slope was found in 'All' and it lasted until around 160 hours. But the exponential production was more short-lived and therefore less CO_2 accumulated than in the 'Carbon' treatment. Together, these data point at different microbial C use efficiencies in the nutrient treatments which, however, were beyond the scope of this thesis.

Prolonged incubation (62 days) resulted in significantly more CO_2 accumulation in 'All' as compared with 'Carbon' (Fig. 39). This illustrates that the effect of additional nutrients (next to C) on C decomposition is time dependent. To find out which elements limit microbial growth and C decomposition immediately after thawing, additional experiments with single nutrient additions in combination with C addition would be necessary.

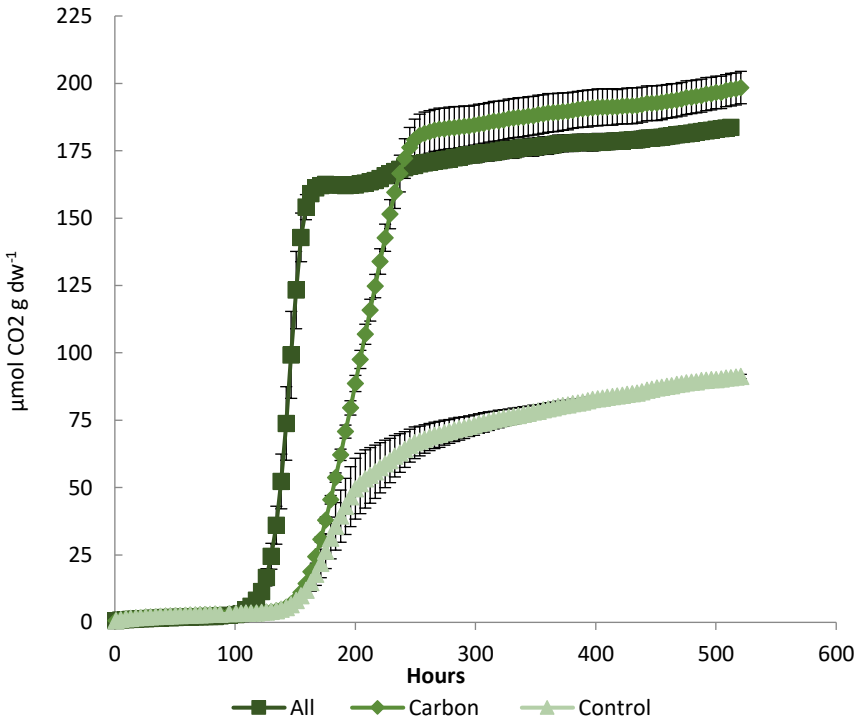

Figure 40: Average (n=3) CO_2 production kinetics for three treatments (All, Carbon, and Control) in the nutrient addition experiment. Error bars are SE

3.3 Methane and Nitrous Oxide

On a molar basis, CH_4 accumulation was by 2 to 5 orders of magnitude smaller than that of CO_2 independent of peat plateau. Even though CH_4 has a larger global warming potential than CO_2, methanogenesis in these peat samples cannot be considered a significant pathway of C degradation. Moreover, there was CH_4 release also under oxic conditions (Fig. 42). This raises the question if the CH_4 accumulating during incubation was produced during C mineralisation or accumulating due to slow, physical release of CH_4 stored in the peat matrix. Assuming that biogenic CH_4 production is

strictly anaerobic, we can subtract CH_4 accumulation curves obtained under oxic conditions from those observed under anoxic conditions, and would arrive at even smaller, biogenic CH_4 production rates (not shown).

3.3.1 Initial Release of Gas upon Thawing

To investigate the physical release of gases stored in permafrost peat upon thawing, initial release of gas from TZ and PF layers of Iškoras and Áidejávri during thawing was measured (Fig. 41). No data are available for Lakselv due to a temporary breakdown of the gas analytics. The initial release of CO_2 and CH_4 during thawing of permafrost peat was higher for Iškoras than Áidejávri. For both peat plateaus, the CO_2 release was larger in TZ and top PF than deeper PF layers, but overall small (0.5 - 4.5 µmol CO_2 g dw^{-1}) relative to the observed CO_2 accumulation in these layers (0.2 - 217.4 µmol CO_2 g dw^{-1} 96 $days^{-1}$).

Iškoras permafrost peat released more CH_4 during thawing than Áidejávri, but there were no differences between layers (Fig. 42). CH_4 release from Áidejávri permafrost peat during thawing was more variable over depth and largest in PF2. The release of CH_4 was one order of magnitude smaller

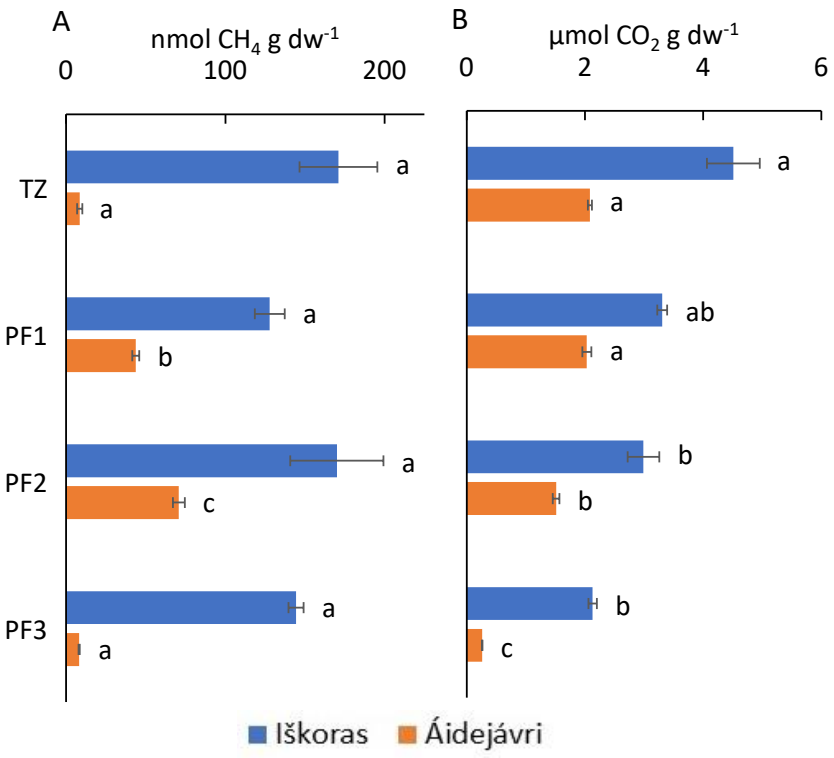

Figure 41: Average (n=4) CH_4 and CO_2 accumulation during over-night thawing of TZ and PF samples. Bottles were flushed with He before thawing to ensure anoxic conditions and equal gaseous concentrations. No data are available for Lakselv due to a technical breakdown of the incubator. Error bars are SE. Different letters denote statistically significant differences between layers at Iškoras and Áidejávri. A: CO_2 accumulation. B: CH_4 accumulation

than that of CO_2 but the initially released CH_4 was large relative to CH_4 production observed during incubation.

3.3.2 Methane Accumulation During Incubation

To show differences among peat plateaus, layers and incubation treatments, cumulative CH_4 production after 96 days is presented in Figure 42. All three peat plateaus accumulated some CH_4 in stirred, anoxically incubated Al samples (Iškoras and Áidejávri in AL1 and Lakselv in AL3), but overall, CH_4 release by AL samples was small. More CH_4 accumulated in TZ and PF samples, revealing marked differences between peat plateaus. Iškoras showed no difference in CH_4 release between oxic/anoxic or loose/slurry treatments, suggesting that CH_4 release was entirely abiotically driven. Conversely, Áidejávri and Lakselv accumulated more CH_4 under anoxic conditions (both loose and in slurries) than under oxic conditions, implying that CH_4 accumulation observed for permafrost samples from Áidejávri and Lakselv was, at least in part, biogenically.

It is noteworthy that the post-thaw CH_4 accumulation over 96 days in Iškoras samples was smaller than the release of CH_4 measured during thawing, while the CH_4 accumulation at Áidejávri exceeded

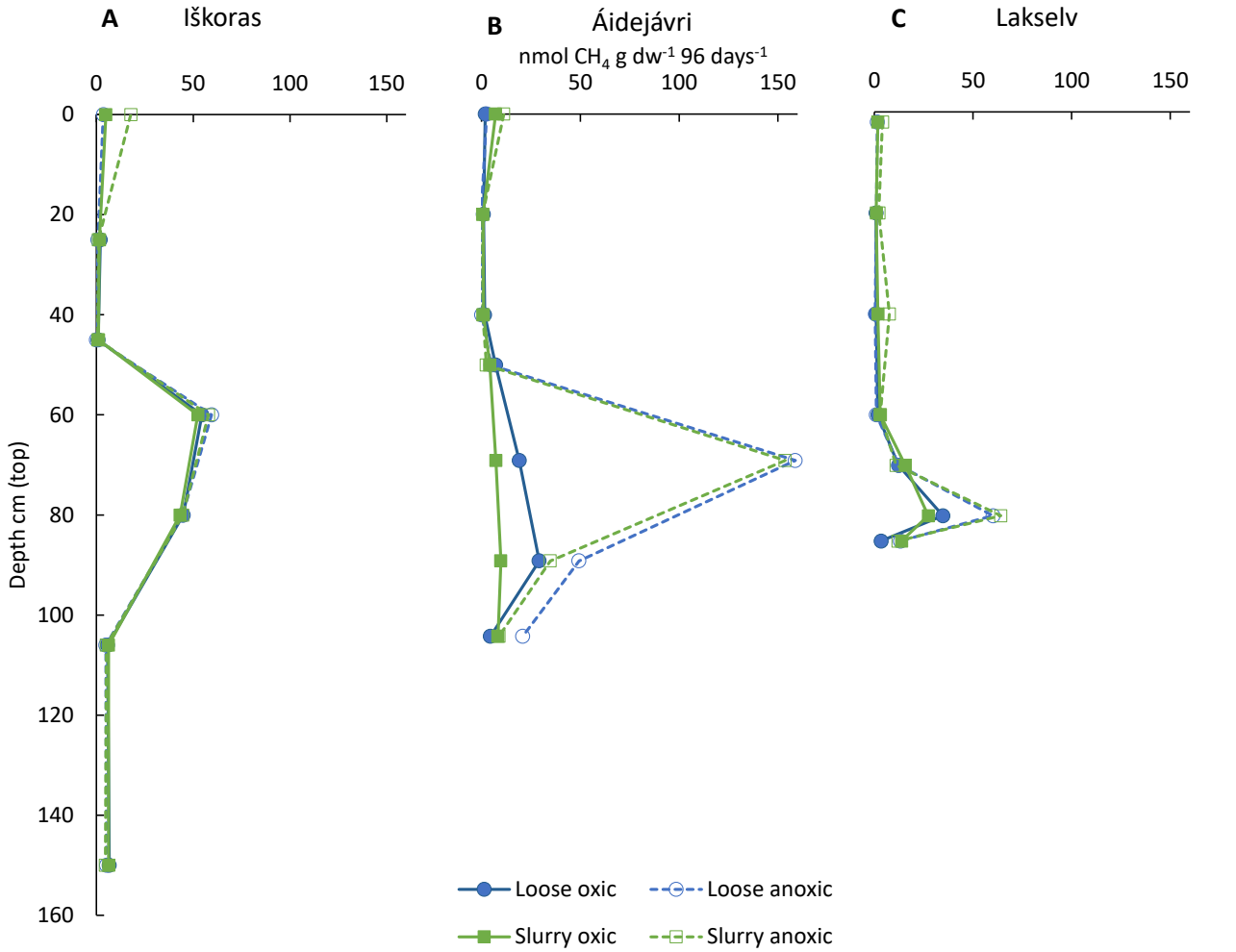

Figure 42: Cumulative CH_4 over depth and 96 days under different incubation conditions (treatments). Stipulated lines indicate the position of the data points in the peat profile as AL (AL1, AL2 and AL3), TZ and PF (PF1, PF2 and PF3). A: Iškoras. B: Áidejávri. C: Lakselv

the initial release of CH_4. This supports the idea that CH_4 accumulation measured at Iškoras was due to desorption of stored CH_4, while it was *de novo* produced in samples from Áidejávri and Lakselv.

To further explore if CH_4 accumulation can be attributed to release or production of CH_4, anoxic gas kinetics (loose and slurries) of the first 17-19 days were compared in TZ, PF1 and PF2 between peat plateaus (Fig. 43). Samples from Iškoras showed the same 'saturation' kinetics in all three layers, no matter whether the samples were incubated stirred or unstirred, oxically or anoxically (Fig. A 1). Most CH_4 was released in the beginning of the incubation after which accumulation slowed down, strongly suggesting that CH_4 release was not due to methanogenesis.

In contrast, gas kinetics in samples from Áidejávri showed exponential CH_4 accumulation (Fig. 43), especially in anoxic loose PF1. Also, the anoxic slurries of Áidejávri showed same exponentiality even though the lag phase lasted longer than in loose samples. As seen in Figure 42, the cumulative CH_4 release after 96 days was the same for anoxically loose and slurry for PF1, resulting in similar CH_4 accumulation for loose and stirred treatments despite differences in kinetics. Overall Áidejávri samples showed sigmoid product accumulation patterns suggesting methanogenesis and a somewhat inhibitory effect of stirring thereon (slurries were only stirred continuously until day 19, after which they were shaken once a week).

Lakselv had the lowest CH_4 accumulation among the three peat plateaus and CH_4 accumulation kinetics showed no exponentiality (Fig. 43). The largest release was observed in PF2, which was also observed after 96 days (Fig. 42). The gas kinetics followed quasi-linear, zero-order kinetics in all layers, and the largest rate was observed anoxically incubated loose PF2. The linear gas kinetics and the difference among oxic and anoxic incubations suggests however, that also Lakselv PF produced some CH_4 by methanogenesis.

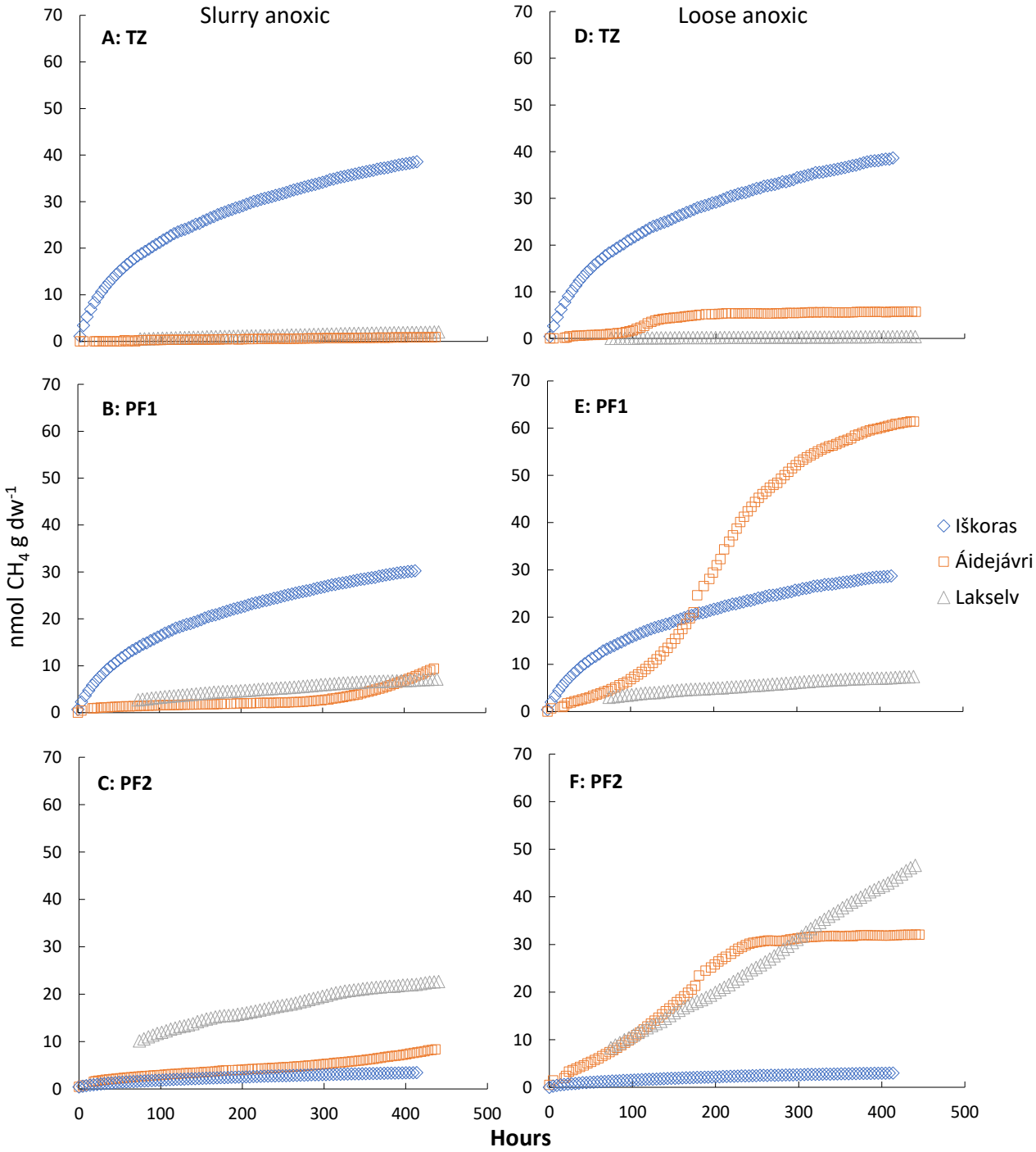

Figure 43: Comparison of CH_4 accumulation kinetics across peat plateaus (until day 19) for two treatments; left panel: slurry anoxic; right panel: loose anoxic, for samples from TZ, PF1, and PF2. A: Slurry anoxic TZ. B: Slurry anoxic PF1. C: Slurry anoxic PF2. D: Loose anoxic TZ. E: Loose anoxic PF1. F: Loose anoxic PF2

3.3.3 Nitrous Oxide Production

Nitrous oxide production was small and only seen in certain layers incubated anoxically. The N_2O accumulation reflects the net effect of N_2O production and consumption and N_2O is commonly consumed by denitrification upon depletion of other N oxyanions. Three incubations showed N_2O accumulation exceeding 5 nmol N_2O g dw^{-1} 96 d^{-1} (Fig. 44). All three were anoxic incubations of AL samples. No measurable N_2O net production was detected in permafrost samples. N_2O net production

occurred during the first 200 h of anoxic incubation, indicating that some NO_3^- or NO_2^- was present in the AL peat. There were differences in the ability to consume N_2O. Loose anoxic AL3 from Lakselv consumed accumulated N_2O quantitatively, whereas AL2 from Iškoras did not, indicating impaired functionality of N_2O reductase. The experiments were not designed to test denitrification potentials or denitrification product stoichiometries, but the preliminary findings here suggest that there are functional differences between denitrifying communities in AL at Iškoras and Lakselv.

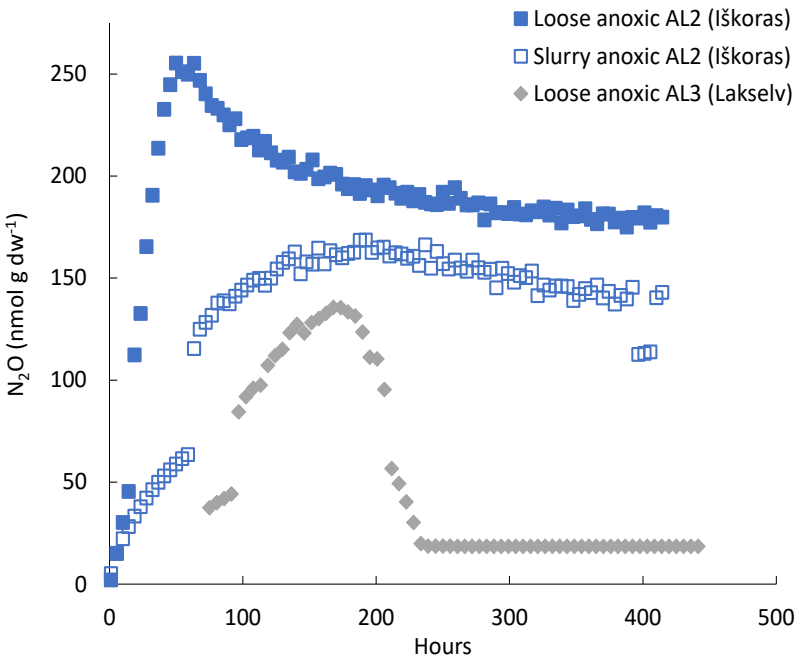

Figure 44: N_2O net accumulation over 19 days for three samples showing N_2O production

3.3.4 Nutrient Addition

Nutrient addition to Iškoras PF2 samples did not significantly affect CH_4 or N_2O release. Methane accumulation in the experiments with nutrient additions was in the range observed in the oxic slurries of Iškoras permafrost samples (data not shown). The N_2O emissions were below 36 nmol N_2O g dw^{-1} 62 d^{-1} and showed no significant effect of nutrient treatment.

4 Discussion

Carbon degradation varied across the three peat plateaus. Iškoras had the most dynamic post-thaw CO_2 kinetics, while permafrost layers from Áidejávri showed the largest CO_2 accumulation over 96 days, both relative to its active layer and the permafrost at other peat plateaus. Lakselv produced least CO_2, and degradation appeared to be highly dependent on O_2 with no effect of slurry/loose incubation. This study seeks to identify factors causing these differences.

4.1 Differences in Peat Chemistry

The three peat plateaus differed in peat chemistry. Iškoras had the highest C content (Fig. 22) and was otherwise poor in minerals (Fig. 27, 28). Among the three peat plateaus, Iškoras had the highest C/N and C/P ratios (Fig. 24) and the lowest pH (Fig. 22). Áidejávri had C contents similar to those at Iškoras but with lower C/N ratios, which may point towards more ombrotrophic conditions during peat formation (Andersson et al., 2012). Lakselv had the lowest C content and a high content of minerals. In the following, different chemical properties will be interpreted and discussed in relation to measured C degradation.

4.1.1 Carbon Stability, $\delta^{13}C$ and C/N ratios

Stable isotope natural abundance in the active layer has been previously used to evaluate peat plateau degradation (Alewell et al., 2011; Krüger et al., 2014). The $\delta^{13}C$ value of the top peat layer (AL1) represents recent input of C from vegetation and appeared to be the same at Áidejávri and Lakselv, while $\delta^{13}C$ was slightly higher in AL1 at Iškoras. All three top layers were enriched in ^{13}C, likely reflecting increased oxic decomposition with preferential loss of ^{12}C. The $\delta^{13}C$ signal deeper in the active layer was relatively more depleted and likely reflects anoxic decomposition in mires before permafrost uprise. Anoxic conditions are believed to have either no isotope signal because of opposite fractionation during CO_2 and CH_4 production or decreased $\delta^{13}C$ values because of enrichment of decomposition products low in $\delta^{13}C$ such as lignin and other phenolic compounds (Alewell et al., 2011). Maxima in $\delta^{13}C$ along the active layer profile have been used as indicators for permafrost uplift and associated change from minerotrophic to ombrotrophic vegetation or increased decomposition (Krüger et al., 2014). The absence of a distinct $\delta^{13}C$ maximum in the active layers studied here may indicate that decomposition was not enhanced after uplift because O_2 diffusion deeper into the active layer was limited or that the pre-permafrost peat material was already degraded. It has to be mentioned however, that the depth resolution of $\delta^{13}C$ measurements in the active layer may not be high enough to detect local maxima as seen in the study by Krüger et al. (2014) of Swedish peat plateaus. There were marked differences in $\delta^{13}C$ between the three peat plateaus with OM being more ^{13}C depleted at Lakselv than at Iškoras, while $\delta^{13}C$ at Áidejávri fluctuated between the values

at Lakselv and Iškoras (Fig. 23A). Given that Lakselv had the lowest CO_2 production in the incubations, the lower $\delta^{13}C$ values in this peat are indicative for more degraded peat and support the idea that peat at Lakselv is more degraded than at Áidejávri or Iškoras. The zig-zag pattern of $\delta^{13}C$ through the permafrost layers at the latter two sites is difficult to interpret, but may indicate pre-permafrost degradation or periodic cryoturbation (Alewell et al., 2011).

Another way to assess the C stability is to evaluate the C/N ratio. Fresh plant material has a wide C/N ratio which increasingly narrows during decomposition as C is more easily lost than N, particularly in N-poor environments. The C/N ratio therefore gives an indication of C quality, and the C/N ratio in permafrost reflects the decomposability from before permafrost formation assuming no decomposition occurs in frozen soil. A high C/N ratio indicates low decomposition and high content of easily decomposable C (Schädel et al., 2014; Treat et al., 2016). Assuming this is also applicable to the peat plateaus in Finnmark, this could explain the highest cumulative CO_2 production in AL1 from Iškoras (Fig. 33) by its high C/N ratio (Fig. 24).

If the generally higher C/N ratios at Iškoras reflect historically less decomposition and hence more readily available C for decomposition, this would explain why the C content at Iškoras was higher and more stable throughout the peat profile (Fig. 22). More bioavailable C in Iškoras permafrost would then also explain the initially higher post-thaw decomposition after 17 days (Fig. 34) and the microbial growth dynamics seen as sigmoid product accumulation curves (Fig. 31). No such growth dynamics were seen in permafrost samples from Áidejávri and Lakselv. However, the high C/N ratio at Iškoras cannot be the only explanation, as Lakselv and Áidejávri had similar C/N ratios but showed differences in CO_2 production, with much higher CO_2 production in samples from Áidejávri than Lakselv. Notwithstanding, the low C/N ratios of Lakselv peat support the finding that low $\delta^{13}C$ values indicate high pre-permafrost decomposition and hence low OM quality.

The C/N ratios mirrored to some extend $\delta^{13}C$ with depth and correlated with $\delta^{13}C$ at Lakselv but not at Áidejávri and Iškoras. C/N ratios at Iškoras were much higher in the top layer than at the other two sites and declined more with depth as expected from increasing decomposition with age of peat material. Differences in C/N ratio may also reflect differences in dominant vegetation. However, Kjellman et al. (2018) found that both Lakselv and Iškoras had a C/N ratio (20-40), reflecting long-term dominance by fen vegetation. Since Áidejávri has similar C/N ratios, it was likely also dominated by fen vegetation during peat formation. Therefore, changes in C/N ratio over depth are likely not due to vegetation change but reflect differences in decomposition state.

4.1.2 Age and Minerogenic Influence

The peatland at Iškoras is roughly 3000 years older than that at Lakselv (Kjellman et al., 2018) and with Áidejávri being further inland, this site could be even older. Also, the formation of permafrost started later at Lakselv compared to Iškoras and probably also Áidejávri (Kjellman et al., 2018). The age difference might play a role for the observed differences in decomposition activity between the peat plateaus. Lakselv, which has the youngest peat, showed less variation in cumulative CO_2 production along depth compared with the other peat plateaus (Fig. 35). This could indicate less formation of layers differing in degradation state in this younger peat.

The peat quality of the three peats may also have been affected by the time of permafrost formation. During peat plateau formation, the peat will be lifted due to ice expansion above the water table which can cause enhanced mineralisation (Kjellman et al., 2018). Uplift and perturbation can be estimated by combining the C/N ratios and $\delta^{15}N$ values over depth (Krüger et al., 2017). Conen et al. (2013) compared $\delta^{15}N$ and C/N ratios across undisturbed and disturbed mineral soil profiles (including organic layers) and found an empirical relationship between $\delta^{15}N$ and C/N ratios for undisturbed sites with a relatively small "uncertainty envelope" of ±2.4 ‰. Samples below this range have received and samples above lost N. Krüger et al. (2017) applied this concept to the active layer of Swedish peat plateaus and found good agreement between known perturbation and $\delta^{15}N$ versus C/N. Points above the envelope were interpreted as signals for permafrost uplift, while points below as indicative for mixing by cryoturbation. However, Kjellman et al. (2018), studying peat plateaus at Finnmark found that this approach was not always consistent with the record of plant macrofossils.

Figure 45A shows the $\delta^{15}N$ versus C/N values of the three peat plateaus studied in the present work relative to the uncertainty envelope, and a classification of the studied peat layers as either unperturbed or perturbed. Samples with perturbation suggesting permafrost uplift (dashed markers) or cryoturbation (hollow markers) were evident at all three peat plateaus but to varying degrees (Fig. 45). The Iškoras core showed signs of perturbation in the bottom and the top of the active layer. The top active layer (AL1) could indicate permafrost uplift and increased mineralisation while the bottom active layer (AL3) showed signs of cryoturbation. Similar results were found by Kjellman et al. (2018) for a core from Iškoras taken only few meters away. Áidejávri showed signs of perturbation in all layers except the middle active layer (AL2). Perturbation in top active layer (AL1) can be attributed to mineralisation while all samples below AL2 were found below the uncertainty envelope

which indicates cryoturbation. At Lakselv cryoturbation was indicated only in the deeper layers (PF1 and PF2).

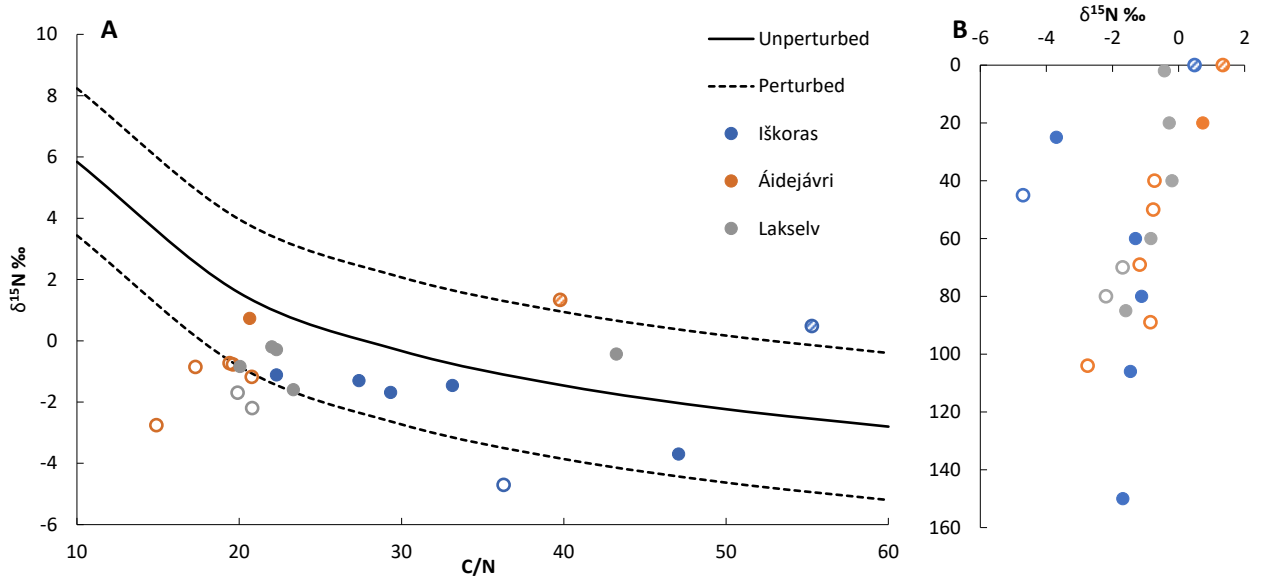

Figure 45: Correlation between $\delta^{15}N$ values and C/N ratio across depth profiles at the three peat plateaus Iškoras, Áidejávri and Lakselv. A: The solid line shows the relationship between $\delta^{15}N$ values and C/N ratio given by Conen et al. (2013) to distinguish unperturbed and perturbed samples. Unperturbed samples are shown by closed markers and are within the uncertainty envelope ±2.4‰ $\delta^{15}N$ of unperturbed samples (solid and dashed lines). Perturbed samples are outside the dashed line (±2.4‰ $\delta^{15}N$). As described in Krüger et al. (2017), samples above the uncertainty envelope indicate increase of mineralisation due to permafrost uplift (dashed markers) and samples below cryoturbation (hollow markers). B: Classification from A shown as depth profile

Based on plant macrofossils, Kjellman et al. (2018) found that a core taken at Lakselv showed a high degree of pre-permafrost decomposition as macrofossils were difficult to identify. This could indicate that the peat at Lakselv was already decomposed before permafrost formation started which also would explain its lower C content. This would mean that the permafrost peat at Lakselv is more recalcitrant, which matches the lower post-thaw decomposition activity observed in permafrost from this peat plateau. This is further supported by the low $\delta^{13}C$ values and low C/N ratios at Lakselv. The decomposition state of peat before permafrost formation would have been highly dependent on hydrological conditions during peat formation. The peat at Lakselv might have been dry during periods before permafrost formation which would explain its higher degradation status. Nothing is known about differences in hydrological conditions during peat formation between the three sites, but the peat at Lakselv is shallow and the catchment area is small compared to Iškoras and Áidejávri, which might result in a less stable hydrological regime with intermittent drainage and drier conditions at Lakselv (Sebastian Westermann, pers. com.).

Another explanation for the lower C content at the Lakselv peat plateau is the minerogenic influence of the surrounding bedrock and the closeness of the sea. Kjellman et al. (2018) reported high mineral and low C content for a peat at Lakselv that was formed at the end of the Holocene thermal maximum around 4000 cal. yr. BP. This peat was located at ~0.6 m depth which would roughly correspond to

the PF1 layer of the Lakselv core studied here. This would explain the low C content and the inversely high content of some macro-, micro and trace elements by enhanced decomposition during the Holocene thermal maximum, probably caused by water table draw down and matches the perturbation indicated by the $\delta^{15}N$ versus C/N relationship seen for this layer in Figure 45. The peat plateau at Lakselv is likely also affected by its proximity to the sea depositing minerals during sea spray events. Also, Lakselv has the highest mean annual temperature among the three studied peat plateaus. Taken together, this may explain the observed higher recalcitrance of peat from this site by more frequent perturbations during peat formation, resulting in overall poorer peat quality, also in the permafrost layer.

Kjellman et al. (2018) also found some minerogenic influence at Iškoras at ~0.4-0.8 m depth (5400-3500 cal. yr. BP). In the present study, the total C content decreased at around 0.6 m (TZ) at Iškoras, and other elements were found in higher concentrations, such as S, Cu and Zn. At Iškoras the C/P ratio was very high, ~1600, in AL2 and AL3, which can only be explained by the scarcity of pedo- and atmogenic P at this mountainous inland site. The peat at Iškoras is deep and the catchment area larger than at Lakselv which could imply more stable hydrological conditions resulting in less decomposed peat before permafrost formation.

The peat depth at Áidejávri varies between 0.7 and 3 m (Sebastian Westermann, pers. com.). The peat core retrieved in the present study was shallow (1.1 m) and might have experienced dry conditions with increased C degradation before permafrost formation. The top layers of the Áidejávri peat plateau might also be affected by mineral dust input from a nearby first-order road. To further test the effect of peat thickness and historical dry spells on present day C degradability, more cores would have to be investigated from the same peat complex and related to peat age and other physical and biogeochemical markers.

4.1.3 Iron and DOC Release

In thermokarst ponds at Áidejávri and Lakselv surface films were observed (Fig. 46). These films were seen in younger and colder lakes fed with water from freshly thawed permafrost, whereas older and warmer lakes do not show such surface films. This could indicate that peat plateaus at both sites release Fe upon thawing forming iron(III)–organic complexes (Kleja et al., 2012). This is supported by the high Fe content in the peat plateaus which was on average 18 and 21 times higher at Áidejávri and Lakselv, respectively, than at Iškoras. Iron can trap organic C in soils, which can limit C mobilisation and degradation (Patzner et al., 2020). This could explain some of the variation seen among the three sites where cumulative CO_2 production on average increased more in samples from Áidejávri and Lakselv from day 17 to day 96 than in samples from Iškoras (Fig. 34). Carbon trapped

by Fe^{3+} could also be released after thawing if water logging leads to reducing conditions and Fe^{3+} reduction (Patzner et al., 2020).

Figure 46: Photograph by Sebastian Westermann from Áidejávri. Small thermokarst with freshly thawed permafrost at 4°C with surface film

Commonly, there is a positive relationship between pH and extractable DOC in peat soil (Evans et al., 2012). Surprisingly, the release of DOC and pH measured in the slurries after 1 h of stirring showed an opposite trend with highest DOC concentrations at Iškoras which had the lowest pH. Peat at Iškoras is very poor in base cations (Fig. 27) which may explain the low pH. However, Iškoras also had the lowest content of mobilizable Fe, which is known to complex DOC. All slurry samples for DOC analysis were filtered through 0.45 µm and analysed by combustion and it is conceivable that some of the released DOC from the Fe-rich Áidejávri and Lakselv samples was retained in the filter and thus escaped analysis. Another explanation to the high amount of extractable DOC at Iškoras, especially in TZ and PF layers could be a potentially higher concentration of DOC in the permafrost (Fig. 22). This would be in line with a higher decomposability of peat at Iškoras as seen in the incubated PF samples.

4.2 Gas Production

The gas measurements in this study represent the potential production of CO_2, CH_4 and N_2O under oxic and anoxic as well as loosely packed and stirred conditions at 10°C and cannot be transferred directly to *in situ* conditions. Estop-Aragones et al. (2018) argued that *ex situ* incubations overestimate the C fluxes from deeper layers in anoxic peats. This is due to poor representation of

concentration gradients of end products and missing rates of diffusive transport in batch incubations. This being said, only few permafrost studies have measured C degradability of freshly thawed permafrost peat (Panneer Selvam et al., 2017; Treat et al., 2014; Waldrop et al., 2021). Most studies focus on active layer (Sjögersten et al., 2016; Treat et al., 2015; Voigt et al., 2017a) or collapsed peat plateaus (Estop-Aragones et al., 2018).

4.2.1 Degradability over Depth

In the active layer, the highest CO_2 production rates were found in AL1, below which they declined with depth. This was true for all three peat plateaus, except for the anoxic incubations at Áidejávri and Lakselv (Table 3). Highest CO_2 accumulation in the top active layer and a decrease with depth is commonly observed and has been attributed to input of fresh OM from plants at the top of the active layer and increasing recalcitrance of peat with depth. Sjögersten et al. (2016) found a positive relationship between CO_2 release and concentrations of carbohydrates (O-alkyls), aromatics and phenolics in active layer samples from Swedish and Canadian peat plateaus. They reported average CO_2 production rates ranging from 0.15 in the bottom to 0.62 µmol g dw^{-1} h^{-1} in the top active layer for oxic incubations at 15°C at field capacity. To compare the rates found in the present study with those of Sjögersten et al. (2016), rates given in Table 3 were adjusted to a temperature of 15°C using a Q_{10} of 2 (Schädel et al., 2016), resulting in oxic decomposition rates of 0.14-0.23, 0.04-0.07 and 0.04-0.05 µmol CO_2 g dw^{-1} h^{-1} for AL1, AL2 and AL3, respectively, across the three sites, which is considerably lower than those reported by Sjögersten et al. (2016). No functional groups of peat OM were measured in the present study, but the comparison in CO_2 production rates suggests that the Norwegian peat plateaus peat plateaus have a poorer quality in the active layer compared to peat plateaus in Sweden and Canada.

In the present study, cumulative CO_2 production increased from the bottom of the active layer to the permafrost, suggesting that permafrost peat has a considerable potential for post-thaw CO_2 release. Few studies have compared CO_2 production of active layer and permafrost peat, and the ones that have did not observe any effect of depth (Treat et al., 2014; Waldrop et al., 2021).

Treat et al. (2014), determining C degradation potentials in Alaskan peat plateaus, provides one of the few studies that have incubated peat permafrost from a frozen core thawed in the laboratory. The cumulative CO_2 production measured after incubating for 30 days at 20°C did not differ between the active layer (middle or bottom) and permafrost (minimum 20 cm below the permafrost top). In the present study, these depths would correspond to AL2 or AL3 for the active layer and PF2 or PF3 for the permafrost. The cumulative CO_2 production reported by Treat et al. (2014) for the Alaskan peat plateau was roughly 4 and 2 mg CO_2-C g C^{-1} 30 d^{-1} for oxic and anoxic incubation, respectively,

which is higher than the rates found for AL2/AL3 and PF2/PF3 in the present study (0.3-2.6 and 0.03-2.2 mg CO_2-C g C^{-1} 30 d^{-1} for oxic and anoxic conditions, respectively). This was true both when using average CO_2 production rates for the entire 96 days of incubation (Table 3) or the larger CO_2 production rates observed during stable production within the first 19 days of incubation (Table A 5). All rates were scaled to 30 days of incubation, besides correcting for temperature (Q_{10} = 2) and C-content. Of all the samples comparable in depth (AL2, AL3, PF2 and PF3) to Treat et al. (2014), incubated either oxically or anoxically, only the anoxically incubated AL2 sample from Áidejávri had a CO_2 production rate (2.2 mg CO_2-C g C^{-1} 30 d^{-1}) comparable with those reported by Treat et al. (2014).

Waldrop et al. (2021) also incubated frozen permafrost peat from an Alaskan peat plateau thawed in the laboratory. Samples were incubated under both oxic and anoxic conditions at 5°C for 6 months. The peat plateau cores were divided based on peat horizons (fibric, mesic, humic and mineral) and pooled and homogenised after thawing for each horizon. The incubations showed no difference in cumulative CO_2 production across the horizons and CO_2 accumulation was therefore given as an average over the whole depth. Average oxic (831µmol CO_2 g C^{-1} 6 $month^{-1}$) and anoxic (214 µmol CO_2 g C^{-1} 6 $month^{-1}$) CO_2 accumulation rates were higher than those observed of the present study when extrapolating the cumulative CO_2 production over 96 days to 6 months using average CO_2 production rate (Table 3) and correcting for temperature (Q_{10} = 2) and C-contentyielding12.6 - 634.8 µmol CO_2 g C^{-1} 6 $month^{-1}$ for oxic and 3.9 - 415.7 µmol CO_2 g C^{-1} 6 $month^{-1}$ for anoxic incubations across all peat plateaus and layers. The higher cumulative CO_2 production and the lack of a horizon effect reported in Waldrop et al. (2021) might be due to the homogenisation of samples prior to incubation which may have increased the availability of labile C in the peat.

In summary, the potential C-degradation seemed to be smaller in the Norwegian peat plateaus compared with peat plateaus in Alaska and Canada. This could suggest that the peat quality is poorer in the Norwegian peat plateaus. Peat plateaus in Alaska are known to have more vegetation with shrubs and more extreme temperature regimes because of their continental climate. Also, permafrost formation might have started later in Alaska than in Norway (Sebastian Westermann, pers. com.). These are all factors that can affect peat quality. In general, it is difficult to compare C degradation across published studies because incubation conditions differ and information about peat formation and substrate type is lacking. The present study shows that three peat plateaus situated within the same geographical region differ greatly in peat and permafrost formation history and hence peat quality and degradability.

The present study also found a depth trend for DOC released during incubation (Fig. 36). DOC release was larger in active layer than in permafrost samples, which could indicate higher OM degradability.

Wang et al. (2013) also found decrease in DOC release with depth in incubated permafrost peat. While the DOC release can be linked to the degradation status of the peat, it is more difficult to say something about the degradability of the DOC itself. Panneer Selvam et al. (2017) found in incubations of thawed cores from a Finnish peat plateau, that DOC from the active layer had a lower initial degradation potential than DOC from thawed permafrost. This agrees with the finding in the present study that CO_2 accumulation in permafrost samples was faster than that of deeper active layer samples (Fig. 35) despite releasing less DOC (Fig. 36), suggesting that 'old' permafrost DOC is more degradable than 'new' DOC in the active layer. This trend was especially evident at Áidejávri where CO_2 accumulation in PF1 exceeded that of AL1 (Fig. 33), despite releasing more DOC in the active layer. The DOC release in AL2 was remarkably high at Áidejávri (Fig. 36) which coincided with high concentrations of S, Ca and Fe (Fig. 27 and 28).

4.2.2 Effect of Incubation Conditions on Microbial Degradation Potential

On average, CO_2 accumulation (excluding PF3) from anoxic incubations were 54%, 39% and 38% of that in oxic incubations at Iškoras, Áidejávri and Lakselv, respectively. The incubation study by Waldrop et al. (2021) with arctic Alaskan peat found that CO_2 accumulation after 6 months at 5°C under anoxic conditions accounted for 26% of that measured under oxic conditions. This is in agreement with other studies which found that O_2 availability is critical for CO_2 production after permafrost thaw (Estop-Aragones et al., 2018; Schädel et al., 2016).

When combining CO_2 and DOC release, C release was highest for anoxic incubations (Fig. 36). This was especially evident for active layer samples, but also deeper permafrost layers released more DOC under anoxic than oxic conditions. This may be partly due to less DOC mineralisation under anoxic conditions but does not explain why overall more C is released under anoxic conditions. DOC release was measured in stirred slurries, which increased in pH until day 19 before it decreased again towards the end of the incubation (Table A 7). Initial pH raise in the incubations may have released extra DOC by desorption which supports microbial growth, which in turn could contribute to new DOC formation. The release of DOC from peat plateaus is of concern because DOC is easily lost along water paths and can potentially increase the CO_2 production downstream given its high degradability under oxic conditions.

A study incubating thawed, loose peat from a permafrost region in Tibet also found higher DOC release from peat incubated anoxically (Wang et al., 2013), but the difference between oxic and anoxic DOC release was smaller than that was found in the present study. Preston et al. (2011) reported that water saturation in peat microcosms increased DOC concentrations significantly compared to field conditions. The experiment was not with permafrost affected peat and did not have

complete anoxic conditions, but nevertheless supports the finding that O_2 limitation can increase extractable DOC.

Oxygen availability also had a clear effect on CH_4 production, especially at Áidejávri and to a lesser degree at Lakselv. At Iškoras no effect of O_2 was seen on CH_4 release, indicating physical release of stored CH_4 rather than post-thaw biogenic CH_4 production. Studies have found CH_4 release from organic permafrost to be only a small fraction of total gaseous C release irrespective of O_2 availability (Schädel et al., 2016). In the present study, CH_4 emissions accounted for 0 - 0.94% of total gaseous C release (CO_2+CH_4) over 96 days (excluding the minerally influenced PF3). Áidejávri and Lakselv had highest CH_4 release contributing 0.94% and 0.79% to gaseous C loss, respectively, in anoxically incubated PF2 peat. Treat et al. (2014) found CH_4 emissions in incubations at 20°C accounting for 0.04% and 0.43% of total C emissions over 30 days under oxic and anoxic incubation conditions, respectively. The absolute CH_4 release under oxic conditions was half of that under anoxic at 20°C but it is not clear whether this was produced during C mineralisation or accumulating through physical release. Schädel et al. (2016) found in a meta study that CH_4 release in anoxic incubations was ~5.7% of total C release across all observations in different permafrost affected ecosystems (peat plateaus, boreal forest and tundra). Studies using different incubation temperatures were reviewed and it was found that increase in temperatures increases the ratio of oxic to anoxic C release (CO_2+CH_4).

Field studies have found no or very little CH_4 emissions from peat plateaus which could indicate that CH_4 produced *in situ* in permafrost is oxidized in the active layer before reaching the peat surface. Measured field fluxes at an Alaskan peat plateau detected no CH_4 surface flux (Waldrop et al., 2021), and *in situ* measurements of CH_4 emission in Northeast European Russia were close to zero in vegetated peat plateau (Voigt et al., 2017a). The latter study found a significant warming effect with open-top chambers resulting in an increase of CH_4 fluxes in the soil column.

Studies of non-peat permafrost sites have found that CH_4 release is highly dynamic throughout the year. A study of three Arctic sites found that spring-thaw and autumn-freeze contribute about a quarter of the annual CH_4 emission, and that emissions were significantly higher during autumn-freeze than spring thaw (Bao et al., 2021). Another study found that CH_4 emissions increased and reached a maximum during the freeze-in period, creating a burst of CH_4 emission (Mastepanov et al., 2008). The highest CH_4 release observed in the present study was immediately after thawing by physical release (Fig. 41). In fact, there was more CH_4 released during overnight-thawing of Iškoras permafrost samples than accumulating during 96 days anoxic incubation, supporting the idea that CH_4 accumulation throughout the entire incubation period was due to physical desorption and not

methanogenesis. Nevertheless, the flush of CH_4 release upon thawing of Iškoras permafrost samples suggests that the Iškoras peat was actively forming CH_4 before permafrost emerged.

Carbon degradation was also influenced by physical disintegration as seen by differences in loosely packed peat at field capacity and peat suspended in water and constantly stirred. Permafrost samples from Áidejávri showed no difference in CH_4 accumulation after 96 days between loose and slurry anoxic incubations (Fig. 42), but when looking at the CH_4 kinetics (Fig. 43), it is evident that CH_4 production was affected by stirring in the beginning of the incubation. Loosely incubated permafrost samples had a shorter lag phase before exponential increase in CH_4 than stirred samples. After ~62 days, both loose and slurry anoxic incubations from PF1 showed a second exponential increase in CH_4 (Fig. A 4), probably because stirring ended after 19 days when placing all bottles for longer-term incubation without stirring. This may have resulted in a shift towards actively growing methanogens in both loose and slurry incubations. Sjögersten et al. (2016) found a strong relationship between the CH_4 release and microbial community structure in the active layer. This is likely also the case for permafrost layers which could indicate that the microbial community structure among the three peat plateaus was quite different. The apparent absence of biogenic CH_4 formation in permafrost peat from Iškoras may reflect the larger age of this permafrost, which probably has resulted in a loss of genetic potential for methanogenesis.

While the CH_4 production in permafrost samples from Áidejávri and Lakselv appeared to be supressed by constant stirring in the beginning, the opposite was the case for CO_2. The constantly stirred slurries were included to obtain incubation condition without diffusion constraints and to ensure full oxygenation for aerobic metabolism, and as expected constant stirring of slurries increased CO_2 production and O_2 consumption as compared to loosely placed peat in the first phase of incubation (Fig. 32). However, the addition of water to the slurries decreased the head space volume which meant that the absolute amount of O_2 present in the oxic slurry treatments was smaller than in the oxic incubations with loose peat. The smaller amount of O_2 and the higher O_2 consumption in constantly stirred incubations resulted in slurries experiencing O_2 limitation earlier than loose incubations. After 19 days, slurries were set to incubation without stirring and only shaken once a week which further limited O_2 availability later during incubation. In consequence, slurry incubations accumulated more CO_2 in the beginning and less towards the end of the incubation compared to loose peat. This was most obvious for Áidejávri and Lakselv where more CO_2 accumulation was observed in slurry than loose incubations in the beginning (Fig. 32) even though the CO_2 accumulation after 96 days was either higher in loose or the same in slurries and loose incubations (Fig. 33). It does not seem that initial oxic conditions increased subsequent anoxic C degradation.

Differences in gas kinetics for both CO_2 and CH_4 among the three peat plateaus may also have been driven by differences in the microbial community composition. An incubation study with permafrost soil from the Tibetan Plateau found that CO_2 release after thawing showed a positive relationship with C degradation functional gene abundance (Chen et al., 2020), however without showing any change in the total microbial community composition. The higher abundance of genes linked to C degradation matched an increase in respective enzyme activities and thus increased microbially driven C degradation. In general, high-altitude ecosystems differ from high-latitude ecosystems by having lower contents of OM and ice, and most likely the microbial community in the Tibetan permafrost would be different from that of the Norwegian peat plateaus (Wang & Xue, 2021). It is not known whether permafrost thawing results in a microbial succession in response to increased substrate availability. In the present study, there were clear differences in the kinetics of gaseous product accumulation, both for CO_2 and CH_4. Thawed permafrost peat from Iškoras supported exponential CO_2 accumulation and PF peat from Áidejávri exponential CH_4 accumulation, strongly indicating microbial growth which will result in community change eventually. Detailed molecular studies would be needed to elucidate whether community change will lead overall more degradation of permafrost C, or to a shift in the CO_2/CH_4 ratio under anoxic conditions.

4.2.3 Nutrients

Permafrost peat from Iškoras was chosen for additional experiments with nutrient additions. The DOC manipulation experiment showed that CO_2 production depends directly on the initial concentration of native DOC (Fig. 38). However, the relationship was not one-to-one, which means that only a fraction of the DOC extractable after thawing is bioavailable. This was also clear when looking at the gas kinetics over 96 days, which showed clear signs of C limitation with accumulation levelling off over time. It is noteworthy, that the DOC manipulation had no measurable effect on anoxic respiration as initial accumulation rates were minute (not shown). After switching the experiment to oxic conditions, O_2 was quickly taken down and the treatment ‘high’ DOC experienced O_2 limitation towards the end of the incubation (Fig. A 8). This may explain in part why the difference in CO_2 accumulation among the three DOC treatments decreased over time and the difference between ‘regular’ and ‘high’ decreased from 20% after 17 days to 7% after 62 days (Fig. 38).

The nutrient addition experiment showed an opposite trend with increasing difference in CO_2 accumulation among the treatments over time. This was true for the ‘Carbon’ and the ‘All’ treatments both of which seemed to alleviate C-limitation. These two treatments were also more affected by O_2 and nutrient limitation. After 62 days, the ‘All’ treatment had accumulated more CO_2 than the ‘Carbon’ treatment, suggesting that other nutrients than C limited C-degradation in Iškoras permafrost peat even though C was the initial limitation for microbial growth.

Neither DOC manipulation nor nutrient addition influenced CH_4 release. Sjögersten et al. (2016) found that thawing permafrost and thermokarst formation is unlikely to emit large quantities of CH_4 if no labile substrate is added. This study only looked at active layer peat and can therefore not be compared with the DOC manipulation or the nutrient experiment in the present study which was carried out with permafrost material. But considering the cumulative CH_4 production after 96 days (Fig. 42), none of the three sites in this study showed CH_4 production in the active layer. Possibly the incubation period after nutrient addition was too short to trigger CH_4 formation. In general, it seems difficult to trigger CH_4 formation from thawed permafrost without substrate additions. For instance, CH_4 formation in long-term incubations of West-Siberian permafrost with repeated glucose addition did not see any effect on CH_4 release until after one year of incubation (Maija Marushchak, pers. com.). This calls for longer incubation times and more detailed investigations on conditions fuelling CH_4 production in thawed permafrost. Additionally, it would be interesting to setup an experiment for Áidejávri with C addition, since the permafrost peat at this site showed clear signs of microbial CH_4 release without nutrient addition.

5 Summary and Conclusion

This study quantified C degradability of OM from active layers and permafrost across three peat plateaus, using different incubation conditions at a constant temperature (10°C). Observed C degradation varied among the three sites, reflecting differences in peat quality; peat at Lakselv appeared to be more decomposed than at Iškoras and Áidejávri, having a lower C content, being less stratified and having the lowest degradation potential. Judged from stable isotope markers, peat quality was already low before permafrost was formed at Lakselv. By contrast, peat from Iškoras had larger decomposition rates and higher C/N ratios, contained more total C and gas kinetics suggested microbial growth which, taken together, reflects higher peat quality. The peat quality at Áidejávri resembled that at Lakselv in many aspects (C/N ratio, pH, ^{15}N, larger content of non-C elements), but the CO_2 production potential at Áidejávri was higher than at Lakselv and more like that found at Iškoras. This shows that inorganic peat chemistry alone cannot explain the potential for peat decomposition in thawing peat plateaus. One important additional factor seems to be the amount of iron released from permafrost which may affect C decomposition due to trapping of DOC. A manipulation experiment revealed that DOC stored in permafrost plays an important role for the immediate respiration response after thawing in the presence of O_2 but not under anoxic conditions. All samples released far more DOC throughout incubation than CO_2-C. Hence, DOC runoff and mineralisation in down-stream ecosystems may be even more important for the fate of C released by permafrost thawing than decomposition in the peat plateau. Interestingly, more DOC was released under anoxic conditions, suggesting that the partitioning between on-site and off-site C mineralisation will depend on the hydrological regime during thermokarst formation.

Carbon degradability varied over depth with highest cumulative CO_2 production in the top of the active layer and a second maximum in top or mid permafrost. This was most pronounced at Áidejávri and Iškoras and shows that thawed permafrost in Norwegian peat plateaus can be a substantial source for CO_2 emission *in situ*. CO_2 production of thawed permafrost samples was by a factor of 2-19 times higher in the presence of O_2 than under anoxic conditions. Translated to field conditions this means that the global warming potential from degrading permafrost C will depend to a large degree on hydrological conditions; if freshly thawed permafrost is exposed to air, mineralisation will be fast, but slow when inundated. No biogenic CH_4 production was observed for permafrost samples over 96 days of anoxic incubation at Iškoras. In contrast, permafrost peat from Áidejávri and Lakselv showed measurable biogenic CH_4 production. However, rates were small, making it unlikely that permafrost thaw leads to substantial, instantaneous CH_4 emissions.

This study is the first of its kind determining degradation potentials in depth profiles of permafrost peat plateaus in Northern Norway under oxic and anoxic conditions. Measured degradation rates were

somewhat smaller than reported from comparable incubations of permafrost peat from Alaska; but with its high frequency of gas measurements and number of layers included, the present study provides new insights into potential C degradation rates and their controlling factors in thawing peat plateaus. The data may be valuable for calibrating geographically distributed model simulations of permafrost C climate feed backs.

6 References

Alewell, C., Giesler, R., Klaminder, J., Leifeld, J. & Rollog, M. (2011). Stable carbon isotopes as indicators for environmental change in palsa peats. *Biogeosciences*, 8 (7): 1769-1778. doi: 10.5194/bg-8-1769-2011.

Andersson, R. A., Meyers, P., Hornibrook, E., Kuhry, P. & Mörth, C.-M. (2012). Elemental and isotopic carbon and nitrogen records of organic matter accumulation in a Holocene permafrost peat sequence in the East European Russian Arctic. *Journal of Quaternary Science*, 27 (6): 545-552. doi: 10.1002/jqs.2541.

Bao, T., Xu, X., Jia, G., Billesbach, D. P. & Sullivan, R. C. (2021). Much stronger tundra methane emissions during autumn freeze than spring thaw. *Global Change Biology*, 27 (2): 376-387. doi: 10.1111/gcb.15421.

Borge, A. F., Westermann, S., Solheim, I. & Etzelmüller, B. (2017). Strong degradation of palsas and peat plateaus in northern Norway during the last 60 years. *The Cryosphere*, 11 (1): 1-16. doi: 10.5194/tc-11-1-2017.

Carter, J. F. & Barwick, V. (2011). *Good Practice Guide For Isotope Ratio Mass Spectrometry*, 978-0-948926-31-0. http://www.forensic-isotopes.org/: FIRMS.

Chadburn, S. E., Krinner, G., Porada, P., Bartsch, A., Beer, C., Belelli Marchesini, L., Boike, J., Ekici, A., Elberling, B., Friborg, T., et al. (2017). Carbon stocks and fluxes in the high latitudes: using site-level data to evaluate Earth system models. *Biogeosciences*, 14 (22): 5143-5169. doi: 10.5194/bg-14-5143-2017.

Chaudhary, N., Westermann, S., Lamba, S., Shurpali, N., Sannel, A. B. K., Schurgers, G., Miller, P. A. & Smith, B. (2020). Modelling past and future peatland carbon dynamics across the pan-Arctic. *Global Change Biology*, 26 (7): 4119-4133. doi: 10.1111/gcb.15099.

Chen, Y., Liu, F., Kang, L., Zhang, D., Kou, D., Mao, C., Qin, S., Zhang, Q. & Yang, Y. (2020). Large-scale evidence for microbial response and associated carbon release after permafrost thaw. *Global Change Biology*, 0 (0): 1-12. doi: 10.1111/gcb.15487.

Conen, F., Yakutin, M. V., Carle, N. & Alewell, C. (2013). δ^{15}N natural abundance may directly disclose perturbed soil when related to C:N ratio. *Rapid Commun Mass Spectrom*, 27 (10): 1101-1014. doi: 10.1002/rcm.6552.

de Wit, H. A., Valinia, S., Weyhenmeyer, G. A., Futter, M. N., Kortelainen, P., Austnes, K., Hessen, D. O., Räike, A., Laudon, H. & Vuorenmaa, J. (2016). Current Browning of Surface Waters Will Be Further Promoted by Wetter Climate. *Environmental Science & Technology Letters*, 3 (12): 430-435. doi: 10.1021/acs.estlett.6b00396.

Estop-Aragones, C., Cooper, M. D. A., Fisher, J. P., Thierry, A., Garnett, M. H., Charman, D. J., Murton, J. B., Phoenix, G. K., Treharne, R., Sanderson, N. K., et al. (2018). Limited release of previously-frozen C and increased new peat formation after thaw in permafrost peatlands. *Soil Biology & Biochemistry*, 118: 115-129. doi: 10.1016/j.soilbio.2017.12.010.

Evans, C. D., Jones, T. G., Burden, A., Ostle, N., Zielinski, P., Cooper, M. D. A., Peacock, M., Clark, J. M., Oulehle, F., Cooper, D., et al. (2012). Acidity controls on dissolved organic carbon mobility in organic soils. *Global Change Biology*, 18 (11): 3317-3331. doi: 10.1111/j.1365-2486.2012.02794.x.

Hofgaard, A. (2003). *Effects of climate change on the distribution and development of palsa peatlands: background and suggestions for a national monitoring project*. NINA Project Report 21.

Hugelius, G., Loisel, J., Chadburn, S., Jackson, R. B., Jones, M., MacDonald, G., Marushchak, M., Olefeldt, D., Packalen, M., Siewert, M. B., et al. (2020). Large stocks of peatland carbon and nitrogen are vulnerable to permafrost thaw. *Proceedings of the National Academy of Sciences*, 117 (34): 20438-20446. doi: 10.1073/pnas.1916387117.

IPCC. (2014). *Climate Change 2014: Synthesis Report. Contribution of Working Groups I, II and III to the Fifth Assessment Report of the Intergovernmental Panel on Climate Change*. In Team, C. W., Pachauri, R. K. & Meyer, L. A. (eds). IPCC, 978-92-9169-143-2. Geneva, Switzerland.

Jones, M. C., Harden, J., O'Donnell, J., Manies, K., Jorgenson, T., Treat, C. & Ewing, S. (2017). Rapid carbon loss and slow recovery following permafrost thaw in boreal peatlands. *Global Change Biology*, 23 (3): 1109-1127. doi: 10.1111/gcb.13403.

Kartverket. (2019). *Landareal Norge*: Geonorge. Available at: https://kartkatalog.geonorge.no/metadata/landareal-norge/1d6537ae-2f5c-4772-a864-6af00c54fcaa (accessed: 4th August 2020).

Kartverket. (2020). *Satelittdata - Sentinel-2 - Skyfri mosaikk WMS*: Geonorge. Available at: https://kartkatalog.geonorge.no/metadata/satelittdata-sentinel-2---skyfri-mosaikk-wms/18fa1fa7-a1de-4d9f-b484-6560844bd788 (accessed: 4th August 2020).

Keuper, F., Wild, B., Kummu, M., Beer, C., Blume-Werry, G., Fontaine, S., Gavazov, K., Gentsch, N., Guggenberger, G., Hugelius, G., et al. (2020). Carbon loss from northern circumpolar permafrost soils amplified by rhizosphere priming. *Nature Geoscience*, 13 (8): 560-565. doi: 10.1038/s41561-020-0607-0.

Kjellman, S. E., Axelsson, P. E., Etzelmuller, B., Westermann, S. & Sannel, A. B. K. (2018). Holocene development of subarctic permafrost peatlands in Finnmark, northern Norway. *Holocene*, 28 (12): 1855-1869. doi: 10.1177/0959683618798126.

Kleja, D. B., van Schaik, J. W. J., Persson, I. & Gustafsson, J. P. (2012). Characterization of iron in floating surface films of some natural waters using EXAFS. *Chemical Geology*, 326: 19-26. doi: 10.1016/j.chemgeo.2012.06.012.

Klimaservicesenter, N. *Seklima*. Available at: https://seklima.met.no/ (accessed: 1st of May 2021).

Krüger, J. P., Leifeld, J. & Alewell, C. (2014). Degradation changes stable carbon isotope depth profiles in palsa peatlands. *Biogeosciences*, 11 (12): 3369-3380. doi: 10.5194/bg-11-3369-2014.

Krüger, J. P., Conen, F., Leifeld, J. & Alewell, C. (2017). Palsa Uplift Identified by Stable Isotope Depth Profiles and Relation of $\delta^{15}N$ to C/N Ratio. *Permafrost and Periglacial Processes*, 28 (2): 485-492. doi: 10.1002/ppp.1936.

Lawrence, D., Fisher, R., Koven, C., Oleson, K., Swenson, S. & Vertenstein, M. (2018). *Technical Description of version 5.0 of the Community Land Model (CLM)*. Boulder, Colorado: National Center for Atmospheric Research.

Lindgren, A., Hugelius, G. & Kuhry, P. (2018). Extensive loss of past permafrost carbon but a net accumulation into present-day soils. *Nature*, 560 (7717): 219-222. doi: 10.1038/s41586-018-0371-0.

Martin, L. C. P., Nitzbon, J., Aas, K. S., Etzelmuller, B., Kristiansen, H. & Westermann, S. (2019). Stability Conditions of Peat Plateaus and Palsas in Northern Norway. *Journal of Geophysical Research-Earth Surface*, 124 (3): 705-719. doi: 10.1029/2018jf004945.

Marushchak, M. E., Pitkamaki, A., Koponen, H., Biasi, C., Seppala, M. & Martikainen, P. J. (2011). Hot spots for nitrous oxide emissions found in different types of permafrost peatlands. *Global Change Biology*, 17 (8): 2601-2614. doi: 10.1111/j.1365-2486.2011.02442.x.

Mastepanov, M., Sigsgaard, C., Dlugokencky, E. J., Houweling, S., Strom, L., Tamstorf, M. P. & Christensen, T. R. (2008). Large tundra methane burst during onset of freezing. *Nature*, 456 (7222): 628-630. doi: 10.1038/nature07464.

Molstad, L., Dörsch, P. & Bakken, L. R. (2007). Robotized incubation system for monitoring gases (O_2, NO, N_2O N_2) in denitrifying cultures. *J Microbiol Methods*, 71 (3): 202-211. doi: 10.1016/j.mimet.2007.08.011.

Molstad, L., Dörsch, P. & Bakken, L. (2016). Improved robotized incubation system for gas kinetics in batch cultures. doi: 10.13140/RG.2.2.30688.07680.

NGU. (2021a). *Berggrunn. Nasjonal berggrunnsdatabase*. Geological Survey of Norway. Available at: http://geo.ngu.no/kart/berggrunn/ (accessed: 29th March 2021).

NGU. (2021b). *Løsmasser. Nasjonal løsmassedatabase*. Geological Survey of Norway. Available at: http://geo.ngu.no/kart/losmasse/ (accessed: 29th March 2021).

Obu, J., Westermann, S., Bartsch, A., Berdnikov, N., Christiansen, H. H., Dashtseren, A., Delaloye, R., Elberling, B., Etzelmüller, B., Kholodov, A., et al. (2019). Northern Hemisphere

permafrost map based on TTOP modelling for 2000–2016 at 1 km^2 scale. *Earth-Science Reviews*, 193: 299-316. doi: 10.1016/j.earscirev.2019.04.023.

Panneer Selvam, B., Lapierre, J. F., Guillemette, F., Voigt, C., Lamprecht, R. E., Biasi, C., Christensen, T. R., Martikainen, P. J. & Berggren, M. (2017). Degradation potentials of dissolved organic carbon (DOC) from thawed permafrost peat. *Scientific Reports*, 7 (1): 45811. doi: 10.1038/srep45811.

Patzner, M. S., Mueller, C. W., Malusova, M., Baur, M., Nikeleit, V., Scholten, T., Hoeschen, C., Byrne, J. M., Borch, T., Kappler, A., et al. (2020). Iron mineral dissolution releases iron and associated organic carbon during permafrost thaw. *Nature Communications*, 11 (1): 6329. doi: 10.1038/s41467-020-20102-6.

Payette, S., Delwaide, A., Caccianiga, M. & Beauchemin, M. (2004). Accelerated thawing of subarctic peatland permafrost over the last 50 years. *Geophysical Research Letters*, 31 (18): L18208. doi: 10.1029/2004gl020358.

Preston, M. D., Eimers, M. C. & Watmough, S. A. (2011). Effect of moisture and temperature variation on DOC release from a peatland: Conflicting results from laboratory, field and historical data analysis. *The Science of the total environment*, 409 (7): 1235-1242. doi: 10.1016/j.scitotenv.2010.12.027.

Quinton, W. L. & Baltzer, J. L. (2012). The active-layer hydrology of a peat plateau with thawing permafrost (Scotty Creek, Canada). *Hydrogeology Journal*, 21 (1): 201-220. doi: 10.1007/s10040-012-0935-2.

Ringner, M. (2008). What is principal component analysis? *Nature Biotechnology*, 26 (3): 303-304. doi: 10.1038/nbt0308-303.

Schädel, C., Schuur, E. A. G., Bracho, R., Elberling, B., Knoblauch, C., Lee, H., Luo, Y., Shaver, G. R. & Turetsky, M. R. (2014). Circumpolar assessment of permafrost C quality and its vulnerability over time using long-term incubation data. *Global Change Biology*, 20 (2): 641-652. doi: 10.1111/gcb.12417.

Schädel, C., Bader, M. K. F., Schuur, E. A. G., Biasi, C., Bracho, R., Čapek, P., De Baets, S., Diáková, K., Ernakovich, J., Estop-Aragones, C., et al. (2016). Potential carbon emissions dominated by carbon dioxide from thawed permafrost soils. *Nature Climate Change*, 6 (10): 950-953. doi: 10.1038/nclimate3054.

Sjögersten, S., Caul, S., Daniell, T. J., Jurd, A. P. S., O'Sullivan, O. S., Stapleton, C. S. & Titman, J. J. (2016). Organic matter chemistry controls greenhouse gas emissions from permafrost peatlands. *Soil Biology and Biochemistry*, 98: 42-53. doi: 10.1016/j.soilbio.2016.03.016.

Spencer, R. G. M., Mann, P. J., Dittmar, T., Eglinton, T. I., McIntyre, C., Holmes, R. M., Zimov, N. & Stubbins, A. (2015). Detecting the signature of permafrost thaw in Arctic rivers. *Geophysical Research Letters*, 42 (8): 2830-2835. doi: 10.1002/2015gl063498.

Treat, C. C., Wollheim, W. M., Varner, R. K., Grandy, A. S., Talbot, J. & Frolking, S. (2014). Temperature and peat type control CO_2 and CH_4 production in Alaskan permafrost peats. *Global Change Biology*, 20 (8): 2674-2686. doi: 10.1111/gcb.12572.

Treat, C. C., Natali, S. M., Ernakovich, J., Iversen, C. M., Lupascu, M., McGuire, A. D., Norby, R. J., Roy Chowdhury, T., Richter, A., Šantrůčková, H., et al. (2015). A pan-Arctic synthesis of CH_4 and CO_2 production from anoxic soil incubations. *Global Change Biology*, 21 (7): 2787-2803. doi: 10.1111/gcb.12875.

Treat, C. C., Jones, M. C., Camill, P., Gallego-Sala, A., Garneau, M., Harden, J. W., Hugelius, G., Klein, E. S., Kokfelt, U., Kuhry, P., et al. (2016). Effects of permafrost aggradation on peat properties as determined from a pan-Arctic synthesis of plant macrofossils. *Journal of Geophysical Research: Biogeosciences*, 121 (1): 78-94. doi: 10.1002/2015jg003061.

Treat, C. C., Jones, M. C., Alder, J., Sannel, A. B. K., Camill, P. & Frolking, S. (2021). Predicted Vulnerability of Carbon in Permafrost Peatlands With Future Climate Change and Permafrost Thaw in Western Canada. *Journal of Geophysical Research: Biogeosciences*, 126 (5): e2020JG005872. doi: 10.1029/2020jg005872.

Turetsky, M. R., Wieder, R. K., Vitt, D. H., Evans, R. J. & Scott, K. D. (2007). The disappearance of relict permafrost in boreal north America: Effects on peatland carbon storage and fluxes. *Global Change Biology*, 13 (9): 1922-1934. doi: 10.1111/j.1365-2486.2007.01381.x.

Turetsky, M. R., Abbott, B. W., Jones, M. C., Anthony, K. W., Olefeldt, D., Schuur, E. A. G., Grosse, G., Kuhry, P., Hugelius, G., Koven, C., et al. (2020). Carbon release through abrupt permafrost thaw. *Nature Geoscience*, 13 (2): 138-143. doi: 10.1038/s41561-019-0526-0.

Voigt, C., Lamprecht, R. E., Marushchak, M. E., Lind, S. E., Novakovskiy, A., Aurela, M., Martikainen, P. J. & Biasi, C. (2017a). Warming of subarctic tundra increases emissions of all three important greenhouse gases – carbon dioxide, methane, and nitrous oxide. *Global Change Biology*, 23 (8): 3121-3138. doi: 10.1111/gcb.13563.

Voigt, C., Marushchak, M. E., Lamprecht, R. E., Jackowicz-Korczyński, M., Lindgren, A., Mastepanov, M., Granlund, L., Christensen, T. R., Tahvanainen, T., Martikainen, P. J., et al. (2017b). Increased nitrous oxide emissions from Arctic peatlands after permafrost thaw. *Proceedings of the National Academy of Sciences*, 114 (24): 6238-6243. doi: 10.1073/pnas.1702902114.

Waldrop, M. P., McFarland, J., Manies, K. L., Leewis, M. C., Blazewicz, S. J., Jones, M. C., Neumann, R. B., Keller, J. K., Cohen, L., Euskirchen, E. S., et al. (2021). Carbon Fluxes and Microbial Activities From Boreal Peatlands Experiencing Permafrost Thaw. *Journal of Geophysical Research-Biogeosciences*, 126 (3): e2020JG005869. doi: 10.1029/2020JG005869.

Wang, X. W., Song, C. C., Wang, J. Y., Miao, Y. Q., Mao, R. & Song, Y. Y. (2013). Carbon release from Sphagnum peat during thawing in a montane area in China. *Atmospheric Environment*, 75: 77-82. doi: 10.1016/j.atmosenv.2013.04.056.

Wang, Y. & Xue, K. (2021). Linkage between microbial shift and ecosystem functionality. *Global Change Biology*, 0 (0): 1-3. doi: 10.1111/gcb.15615.

Wilhelm, E., Battino, R. & Wilcock, R. J. (1977). Low-Pressure Solubility of Gases in Liquid Water. *Chemical Reviews*, 77 (2): 219-262. doi: 10.1021/cr60306a003.

WRB, I. W. G. (2014). *World Reference Base for Soil Resources 2014, update 2015. International Soil Classification System for Naming Soils and Creating Legends for Soil Maps*. World Soil Resources Reports 106, 978-92-5-108369-7. FAO, Rome.

Yang, Z., Fang, W., Lu, X., Sheng, G. P., Graham, D. E., Liang, L., Wullschleger, S. D. & Gu, B. (2016). Warming increases methylmercury production in an Arctic soil. *Environmental Pollution*, 214: 504-509. doi: 10.1016/j.envpol.2016.04.069.

Åkerman, H. J. & Johansson, M. (2008). Thawing permafrost and thicker active layers in sub-arctic Sweden. *Permafrost and Periglacial Processes*, 19 (3): 279-292. doi: 10.1002/ppp.626.

7 Appendix

Figure A 1: Iškoras

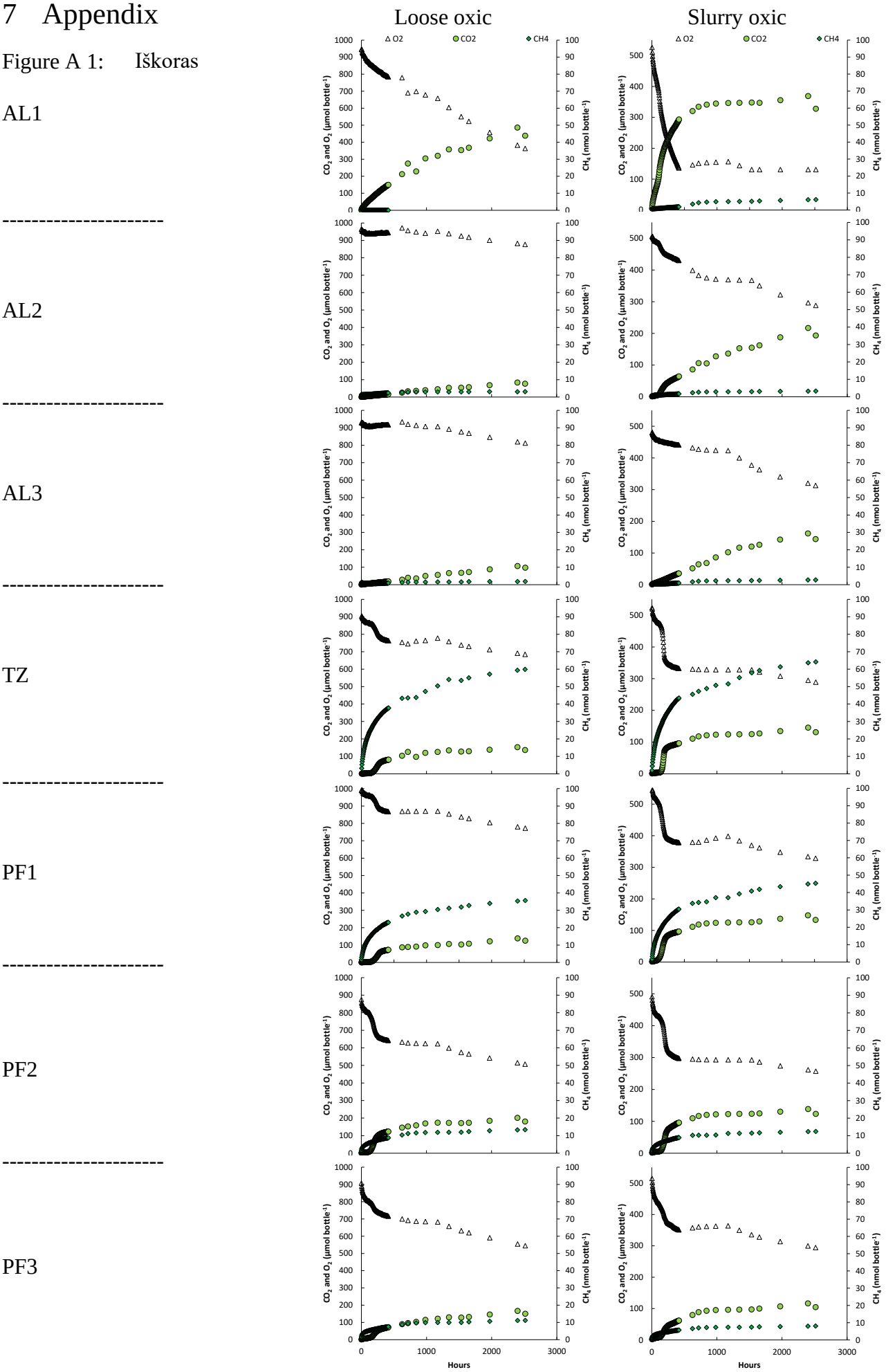

Figure A 2: Iškoras

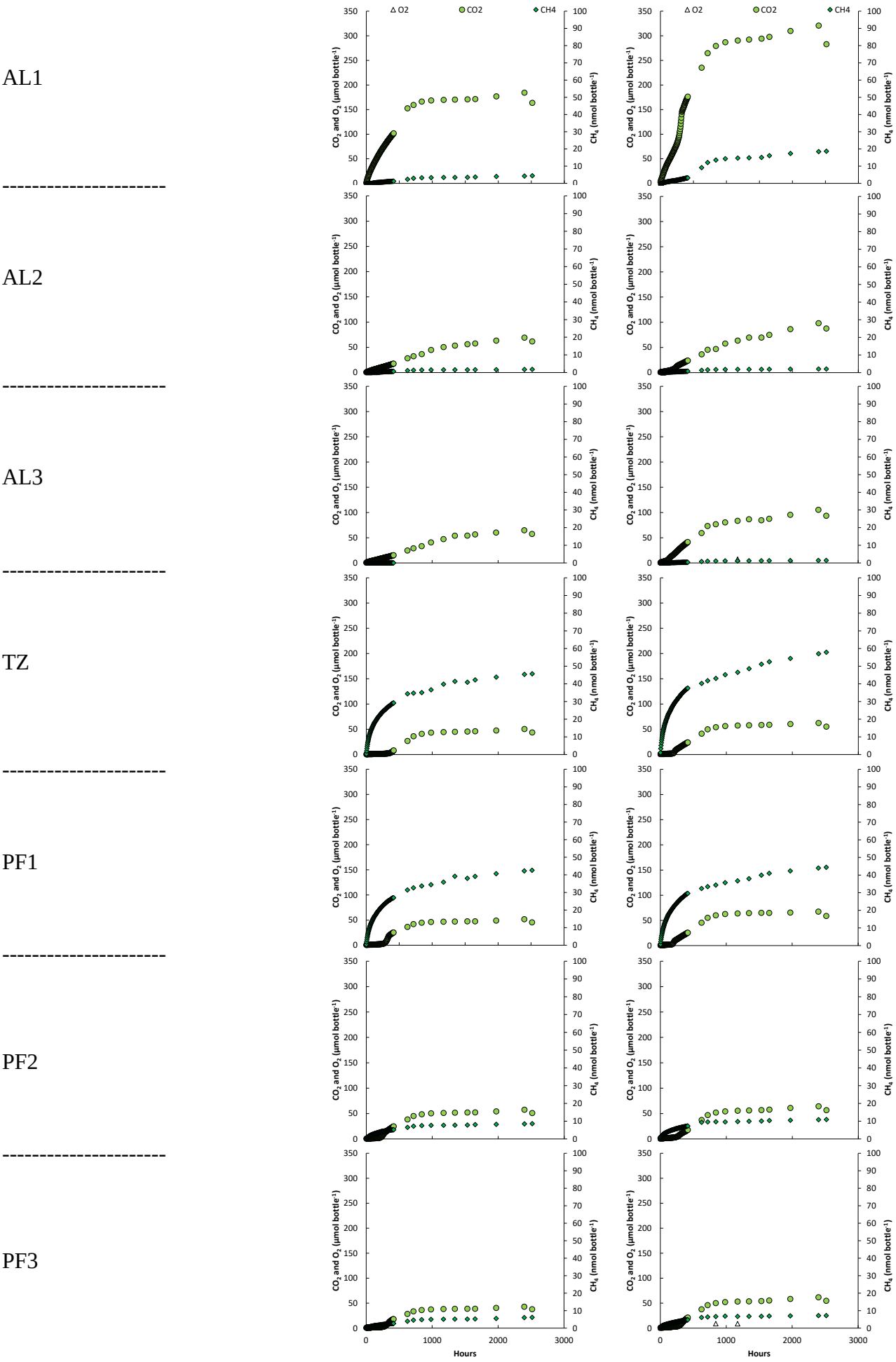

Figure A 3: Áidejávri

Loose oxic

Slurry oxic

AL1

AL2

AL3

TZ

PF1

PF2

PF3

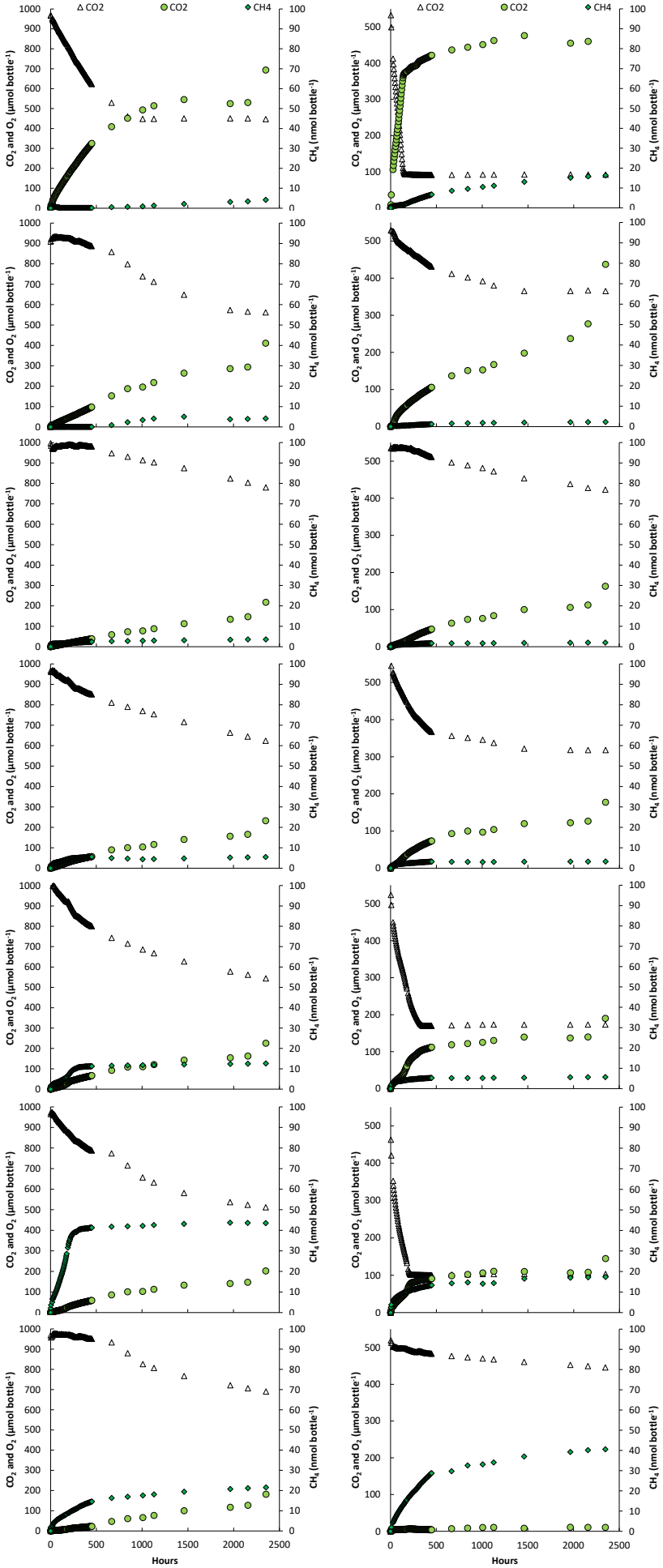

Figure A 4: Áidejávri

Loose anoxic

Slurry anoxic

AL1

AL2

AL3

TZ

PF1

PF2

PF3

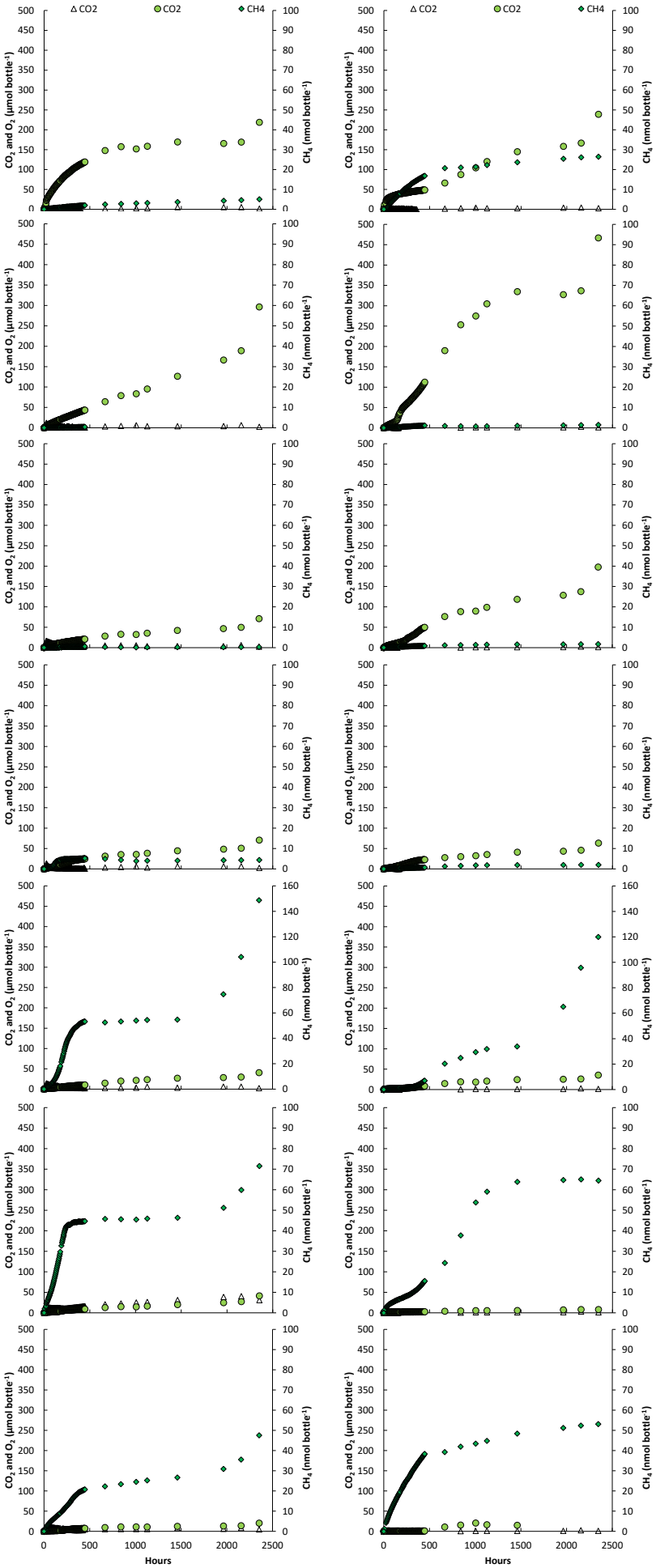

Figure A 5: Lakselv

Loose oxic

Slurry oxic

AL1

AL2

AL3

TZ

PF1

PF2

PF3

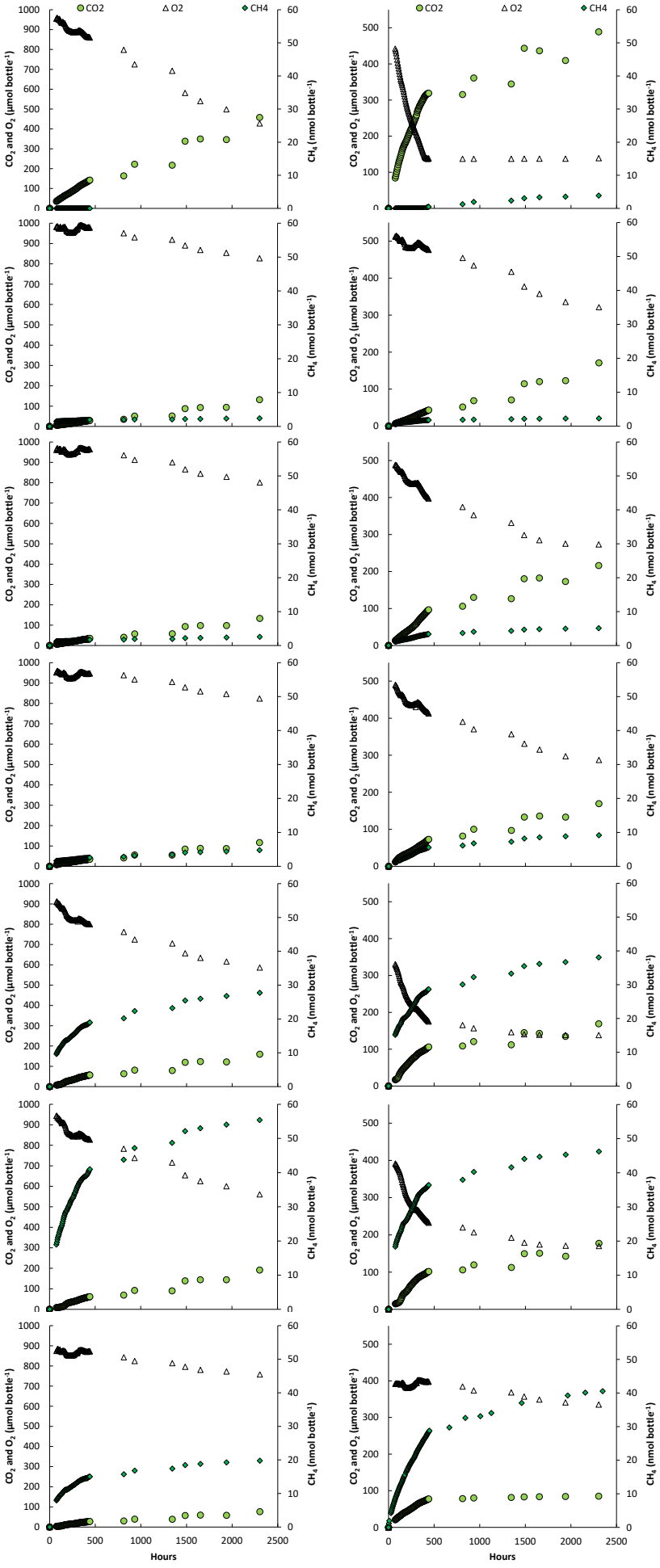

Figure A 6: Lakselv

Loose anoxic

Slurry anoxic

AL1

AL2

AL3

TZ

PF1

PF2

PF3

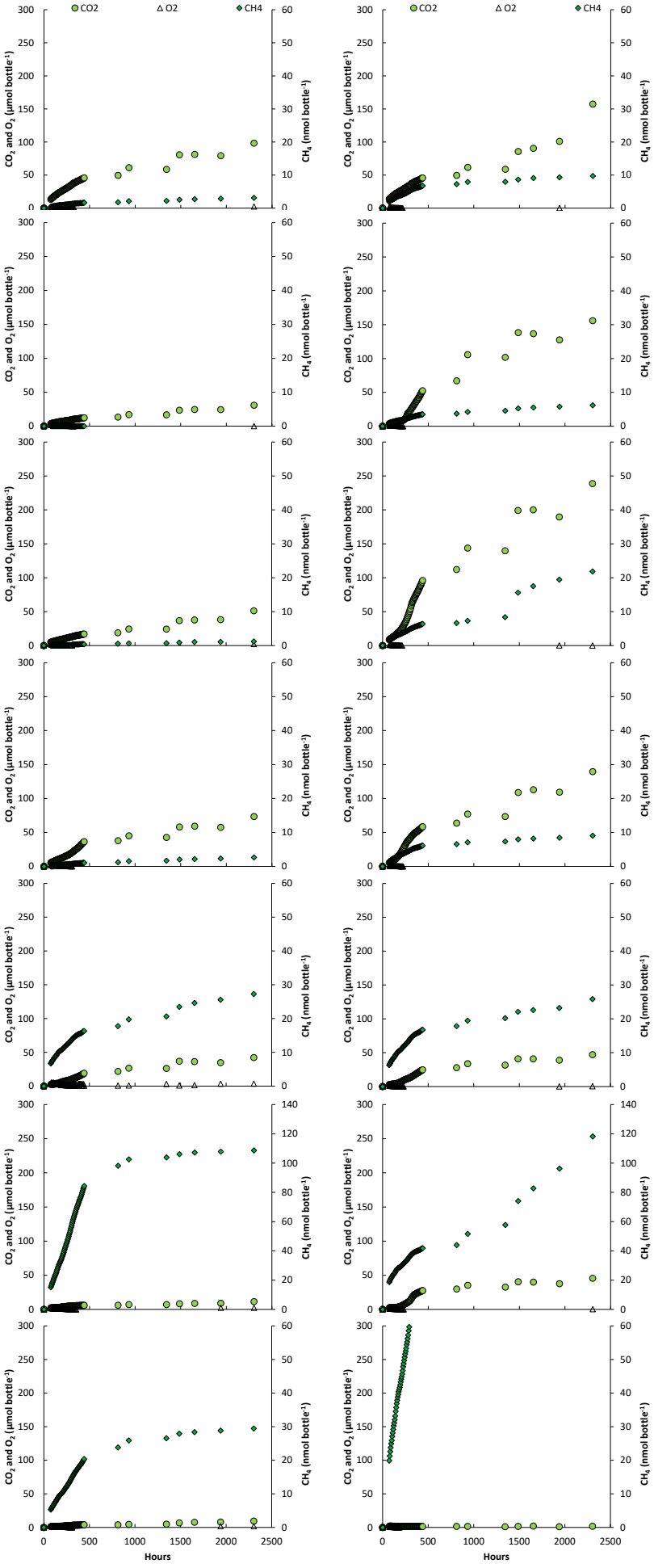

Figure A 7: Nutrient experiment

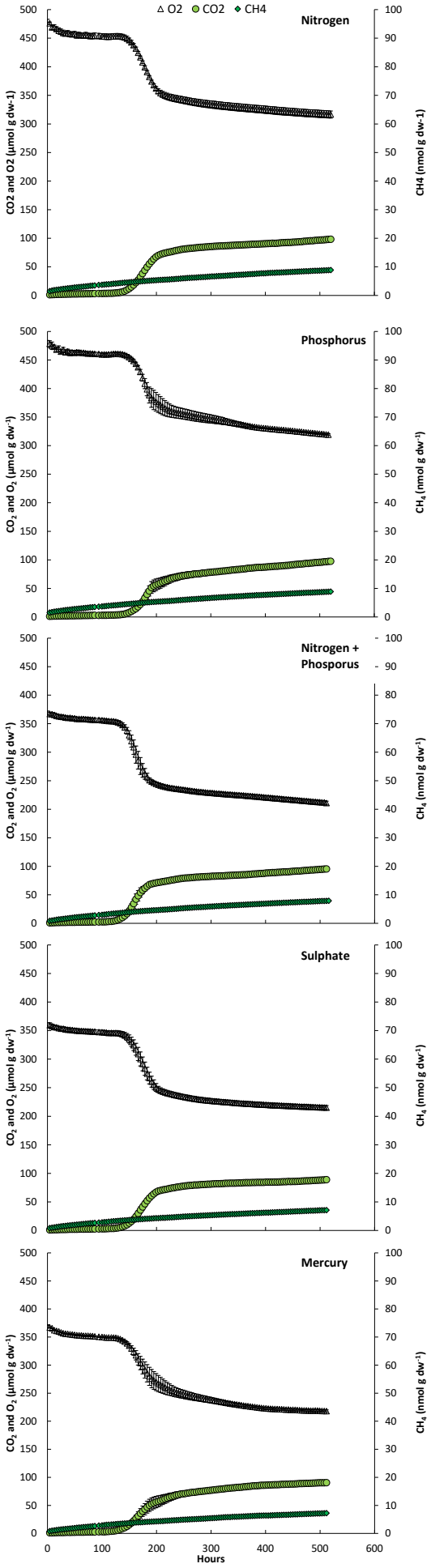

Figure A 8: DOC manipulation

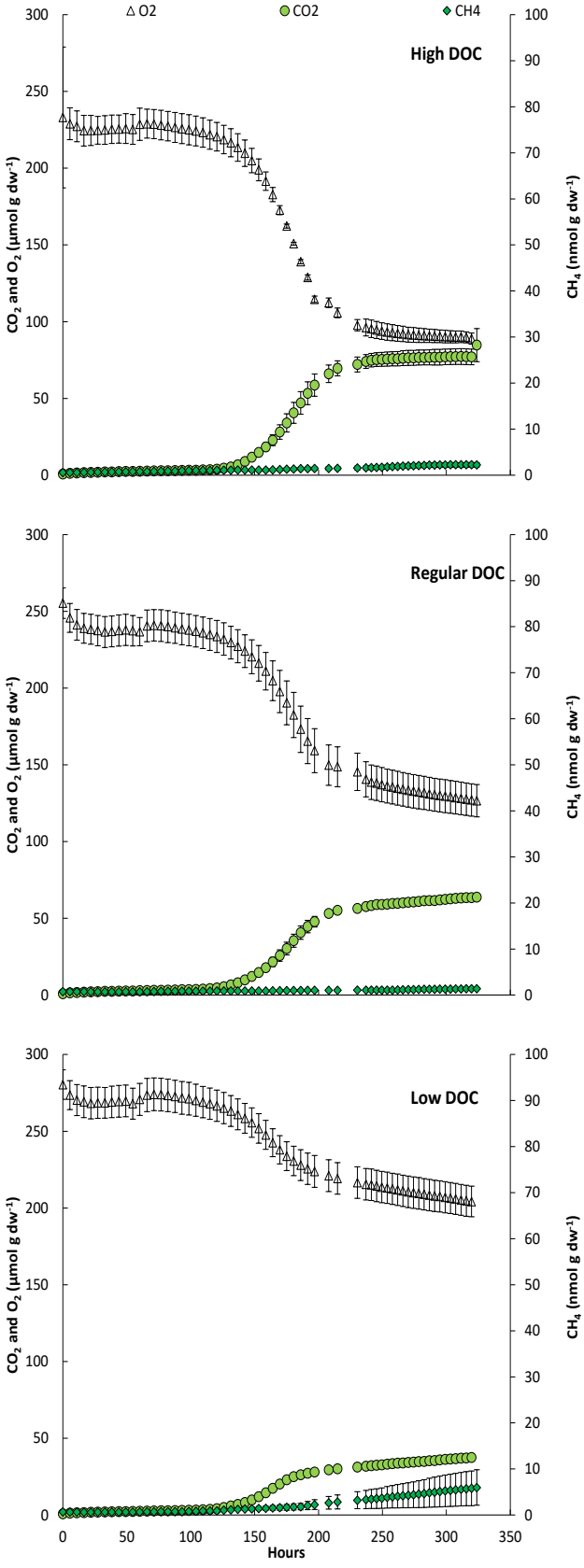

Table A 1: Concentrations of elements measured across the three peat plateaus and seven layers.

Site and depth (cm)	N mg g dw^{-1}	P mg g dw^{-1}	Al mg g dw^{-1}	Ni µg g dw^{-1}	As µg g dw^{-1}	Se µg g dw^{-1}	Cd µg g dw^{-1}	La µg g dw^{-1}	Ce µg g dw^{-1}	Pr µg g dw^{-1}	Nd µg g dw^{-1}	Sm µg g dw^{-1}	Eu µg g dw^{-1}	Gd µg g dw^{-1}	Dy µg g dw^{-1}	Ho µg g dw^{-1}	Er µg g dw^{-1}	Tm µg g dw^{-1}	Yb µg g dw^{-1}	Hg µg g dw^{-1}	Pb µg g dw^{-1}
Iškoras																					
0	9.6	0.5	0.6	2.8	0.8	0.3	0.3	0.4	0.8	0.1	0.4	0.1	0.0	0.1	0.0	0.0	0.0	0.0	0.0	0.2	8.1
25	11.7	0.3	1.8	4.5	0.1	0.3	0.0	0.0	0.0	0.0	1.8	0.3	0.1	0.3	0.3	0.1	0.2	0.0	0.1	0.0	0.4
45	15.5	0.3	2.5	7.0	0.2	0.3	0.1	4.8	7.5	1.0	4.0	0.7	0.2	0.7	0.5	0.1	0.3	0.0	0.3	0.0	0.3
60	18.0	0.4	3.2	10.0	0.7	1.3	0.1	5.5	9.0	1.4	5.5	1.1	0.3	1.0	0.9	0.2	0.5	0.1	0.4	0.0	0.4
80	22.8	0.5	4.0	14.0	0.8	1.7	0.3	10.0	17.0	2.8	11.0	2.3	0.6	2.2	1.9	0.4	0.9	0.1	0.8	0.1	0.6
106	16.4	0.5	5.1	14.0	0.5	0.9	0.0	0.0	0.0	0.0	18.0	3.3	0.8	3.2	2.5	0.5	1.4	0.2	1.1	0.0	0.3
150	16.8	0.6	9.2	31.0	1.3	0.7	1.0	22.0	50.0	6.1	24.0	4.6	1.1	4.3	3.4	0.6	1.6	0.2	1.4	0.0	1.0
Áidejávri																					
0	12.2	0.7	0.6	1.7	0.5	0.1	0.2	0.4	0.9	0.1	0.4	0.1	0.0	0.1	0.1	0.0	0.0	0.0	0.1	0.2	5.9
20	25.5	0.5	3.9	11.0	0.3	0.5	0.1	13.0	30.0	3.4	14.0	2.7	0.6	2.5	2.1	0.5	1.5	0.2	1.6	0.0	0.4
40	25.4	0.6	0.5	1.3	0.8	0.2	0.2	0.4	0.7	0.1	0.3	0.1	0.0	0.1	0.1	0.0	0.0	0.0	0.0	0.2	6.4
50	26.2	0.4	2.5	4.2	0.3	0.4	0.1	12.0	29.0	3.4	14.0	2.7	0.6	2.5	2.1	0.4	1.3	0.2	1.4	0.0	0.3
69	24.9	0.4	3.7	13.0	0.5	0.8	0.1	16.0	38.0	4.4	19.0	3.4	0.8	3.3	2.7	0.6	1.8	0.3	1.9	0.0	0.4
89	16.5	0.6	8.9	20.5	0.6	0.8	0.1	29.5	69.5	8.0	34.0	6.1	1.4	5.7	4.6	0.9	2.7	0.4	2.8	0.0	1.4
104	1.8	0.6	10.0	17.0	0.2	0.1	0.0	16.0	35.0	4.3	17.0	3.1	0.7	2.8	2.2	0.4	1.2	0.2	1.1	-	2.0
Lakselv																					
2	12.7	0.5	2.2	4.8	0.6	0.3	0.0	0.0	0.0	0.0	1.4	0.3	0.1	0.2	0.2	0.0	0.1	0.0	0.1	0.2	4.7
20	20.3	0.9	16.0	29.0	1.0	0.8	0.2	31.0	66.0	7.3	28.0	4.5	0.9	3.6	2.5	0.4	1.2	0.2	1.0	0.1	4.5
40	20.0	0.9	16.0	24.0	1.1	0.7	0.2	30.0	63.0	6.6	26.0	4.1	0.8	3.4	2.3	0.4	1.1	0.1	0.9	0.1	5.0
60	15.5	0.8	34.0	47.5	1.7	0.6	0.2	47.5	89.0	10.5	39.0	6.0	1.2	4.8	3.2	0.6	1.4	0.2	1.2	0.0	9.7
70	11.4	0.7	45.0	63.7	1.8	0.5	0.2	52.7	94.7	11.7	42.0	6.2	1.2	4.8	3.2	0.6	1.5	0.2	1.3	0.0	10.0
80	12.9	0.7	34.5	54.0	2.7	0.6	0.1	49.5	91.5	10.5	38.5	5.9	1.2	4.7	3.1	0.5	1.5	0.2	1.3	0.0	9.6
85	12.8	0.3	34.0	27.5	1.6	0.1	0.0	19.0	35.5	4.2	15.6	2.5	0.6	2.1	1.5	0.3	0.8	0.1	0.7	0.0	3.8

Table A 2: Dry weight and water content in the samples used for incubation experiments across the three peat plateaus and layers.

Treatment and layer	Iškoras		Áidejávri		Lakselv	
	Fresh soil g	Dry soil g	Fresh soil g	Dry soil g	Fresh soil g	Dry soil g
Loose oxic						
AL1	10.13	1.15	10.47	2.13	9.72	2.24
AL2	8.86	1.53	14.71	4.11	10.8	2.87
AL3	11.48	2.09	13.52	2.28	12.23	3.03
TZ	9.67	1.08	9.62	0.76	9.5	2.70
PF1	5.89	0.78	9.15	0.66	11.4	2.28
PF2	17.03	2.32	12.28	1.49	8.93	1.59
PF3	14.15	1.67	8.12	4.77	13.65	5.89
Loose anoxic						
AL1	10.62	1.20	9.3	1.89	9.4	2.17
AL2	13.52	2.34	13.29	3.72	9.6	2.55
AL3	12.16	2.21	14.34	2.42	11.12	2.75
TZ	6.77	0.76	11.42	0.91	9.6	2.73
PF1	7.09	0.94	12	0.87	11.02	2.20
PF2	12.86	1.75	11.47	1.39	10.13	1.81
PF3	11.74	1.38	10.49	6.16	14.21	6.13
Slurry anoxic						
AL1	9.05	1.03	11.56	2.36	10.39	2.40
AL2	12.18	2.10	9.78	2.73	10.35	2.75
AL3	11.64	2.11	14.91	2.52	11.68	2.89
TZ	8.73	0.98	10.23	0.81	10.86	3.08
PF1	7.37	0.98	10.32	0.75	11.73	2.35
PF2	15.62	2.12	15.29	1.86	10.34	1.85
PF3	13.15	1.55	10.19	5.98	17.82	7.69
Slurry oxic						
AL1	10.97	1.24	11.27	2.30	9.81	2.26
AL2	12.05	2.08	11.21	3.13	9.76	2.59
AL3	14.45	2.63	12.27	2.07	11.94	2.96
TZ	10.78	1.20	9.97	0.79	10.88	3.09
PF1	7.76	1.03	10.85	0.78	12.16	2.43
PF2	14.49	1.97	14.63	1.78	9.47	1.69
PF3	10.72	1.26	8.34	4.90	14.38	6.21

Table A 3: Dry weight and water content in the samples used for the nutrient experiment.

Treatment	Nutrient experiment	
	Fresh soil	Dry soil
	g	g
Control 1	14.51	1.80
Control 2	14.07	1.75
Control 3	14.7	1.83
Carbon 1	14.35	1.78
Carbon 2	14.36	1.79
Carbon 3	14.9	1.85
Nitrogen 1	14.67	1.82
Nitrogen 2	14.73	1.83
Nitrogen 3	14.38	1.79
Phosphorus 1	14.26	1.77
Phosphorus 2	14.56	1.81
Phosphorus 3	14.3	1.78
Nitrogen + phosphorus 1	14.13	1.76
Nitrogen + phosphorus 2	14.45	1.80
Nitrogen + phosphorus 3	14.23	1.77
Sulphur 1	14.61	1.82
Sulphur 2	14.22	1.77
Sulphur 3	14.75	1.83
Mercury 1	14.22	1.77
Mercury 2	14.07	1.75
Mercury 3	14.19	1.76
All 1	14.31	1.78
All 2	14.22	1.77
All 3	14.43	1.79

Table A 4: Dry weight and water content in the samples used for the DOC manipulation.

Treatment	DOC manipulation	
	Fresh soil	Dry soil
	g	g
DOC low 1	14.04	1.80
DOC low 2	13.06	1.68
DOC low 3	13.82	1.78
DOC regular 1	15.27	1.96
DOC regular 2	13.78	1.77
DOC regular 3	15.36	1.97
DOC high 1	15.43	1.98
DOC high 2	15.34	1.97
DOC high 3	14.3	1.84

Table A 5: Rates for CO_2 production determined for the three peat plateaus.

Treatment and layer	µmol CO_2 g dw^{-1} h^{-1}											
	Iškoras				Áidejávri				Lakselv			
	Instantaneous	Steepest	Stabile	Long	Instantaneous	Steepest	Stabile	Long	Instantaneous	Steepest	Stabile	Long
Loose oxic												
AL1	0.54	0.54	0.27	0.11	0.65	0.65	0.29	0.05	-	0.13	0.13	0.08
AL2	0.03	0.03	0.02	0.02	0.07	0.07	0.05	0.03	-	0.02	0.02	0.02
AL3	0.02	0.02	0.02	0.02	0.04	0.04	0.04	0.03	-	0.03	0.03	0.02
TZ	0.02	0.51	0.10	0.02	0.17	0.20	0.13	-0.81	-	0.04	0.03	0.02
PF1	0.02	0.65	0.11	0.03	0.18	0.47	0.17	0.09	0.02	0.11	0.05	0.03
PF2	0.02	0.40	0.04	0.01	0.07	0.14	0.08	0.04	0.04	0.21	0.08	0.05
PF3	0.04	0.28	0.06	0.02	0.01	0.02	0.01	0.01	0.01	0.03	0.01	0.00
Loose anoxic												
AL1	0.38	0.38	0.16	0.01	0.43	0.43	0.08	0.01	-	0.06	0.04	0.01
AL2	0.02	0.02	0.02	0.01	0.04	0.04	0.02	0.03	-	0.01	0.01	0.00
AL3	0.03	0.03	0.02	0.01	0.03	0.03	0.01	0.01	-	0.01	0.01	0.01
TZ	0.00	0.13	-	0.01	0.05	0.08	0.03	0.02	0.02	0.05	0.05	0.01
PF1	0.01	0.29	0.09	0.00	0.02	0.06	0.02	0.01	0.01	0.01	0.03	0.01
PF2	0.00	0.10	0.05	0.00	0.02	0.03	0.01	0.01	0.00	0.01	0.00	0.00
PF3	0.00	0.11	-	0.00	0.00	0.01	0.01	0.00	0.00	0.00	0.00	0.00
Slurry anoxic												
AL1	0.39	1.27	0.34	0.02	0.26	0.26	0.02	0.03	0.05	0.05	0.03	0.03
AL2	0.01	0.06	0.03	0.01	0.04	0.18	0.10	0.04	0.01	0.11	0.08	0.02
AL3	0.02	0.05	0.05	0.01	0.03	0.06	0.06	0.02	0.04	0.13	0.10	0.03
TZ	0.01	0.23	0.08	0.01	0.04	0.08	0.04	0.02	0.02	0.08	0.04	0.02
PF1	0.01	0.21	0.08	0.01	0.01	0.03	0.03	0.01	0.01	0.04	0.04	0.00
PF2	0.00	0.04	-	0.00	0.00	0.00	0.00	0.00	0.00	0.11	0.03	0.00
PF3	0.01	0.09	-	0.01	0.00	0.00	0.00	-	-	0.00	0.00	0.00
Slurry oxic												
AL1	1.04	1.33	0.30	0.01	1.06	1.06	0.07	0.02	-	0.43	0.08	0.04
AL2	0.02	0.20	0.05	0.03	0.15	0.15	0.06	0.04	0.03	0.04	0.04	0.03
AL3	0.03	0.03	0.03	0.02	0.04	0.05	0.05	0.02	0.06	0.09	0.09	0.02
TZ	0.02	1.31	0.05	0.01	0.21	0.27	0.15	0.05	-	0.09	0.05	0.02
PF1	0.05	0.83	0.06	0.01	0.31	0.69	0.09	0.04	0.06	0.11	0.06	0.01
PF2	0.02	0.45	0.06	0.00	0.15	0.29	0.03	0.01	0.04	0.19	0.09	0.03
PF3	0.04	0.30	0.08	0.01	0.01	0.01	0.00	0.00	-	-	0.00	0.00

Table A 6: Rates for CH_4 production determined for the three peat plateaus.

Treatment and layer	nmol CH_4 g dw^{-1} h^{-1}											
	Iškoras				Áidejávri				Lakselv			
	Instantaneous	Steepest	Stabile	Long	Instantaneous	Steepest	Stabile	Long	Instantaneous	Steepest	Stabile	Long
Loose oxic												
AL1	-0.05	-0.05	0.00	-	-0.01	-0.01	0.00	0.00	-	0.00	0.00	-
AL2	0.00	0.00	0.00	0.00	-0.01	-0.01	0.00	0.00	-	0.00	0.00	0.00
AL3	-0.01	-0.01	0.00	0.00	0.00	0.00	0.00	0.00	-	0.00	0.00	0.00
TZ	0.24	0.24	0.03	0.01	0.04	0.04	0.00	-0.01	-	0.00	0.00	0.00
PF1	0.20	0.20	0.03	0.01	0.06	0.08	0.00	0.00	-	0.02	0.01	0.00
PF2	0.04	0.04	0.00	0.00	0.11	0.14	0.00	0.00	-	0.04	0.03	0.00
PF3	0.05	0.05	0.00	0.00	0.02	0.02	0.00	0.00	-	0.01	0.00	0.00
Loose anoxic												
AL1	0.00	0.00	0.00	0.00	0.00	0.00	0.00	0.00	-	0.00	0.00	0.00
AL2	0.00	0.00	0.00	0.00	0.00	0.00	0.00	0.00	-	-	0.00	-
AL3	0.00	0.00	0.00	-	0.00	0.00	0.00	0.00	0.00	-	0.00	0.00
TZ	0.33	0.33	0.04	0.01	0.02	0.07	0.00	0.00	0.00	0.00	0.00	0.00
PF1	0.23	0.23	0.03	0.01	0.06	0.29	0.05	0.05	-	0.02	0.01	0.00
PF2	0.02	0.02	0.00	0.00	0.10	0.15	0.01	0.01	0.09	0.10	0.10	0.00
PF3	0.03	0.03	0.00	0.00	0.04	0.02	0.02	0.01	-	0.02	0.02	0.00
Slurry anoxic												
AL1	0.00	0.01	0.01	0.00	0.01	0.02	0.01	0.00	0.01	0.01	0.00	0.00
AL2	0.00	0.00	0.00	0.00	0.00	0.00	0.00	0.00	0.00	0.00	0.00	0.00
AL3	0.00	0.00	0.00	0.00	0.00	0.00	0.00	0.00	-	0.00	0.00	0.00
TZ	0.29	0.29	0.04	0.01	0.00	0.00	0.00	0.00	0.01	0.01	0.00	0.00
PF1	0.21	0.21	0.03	0.01	0.01	0.07	0.07	0.07	0.02	0.02	0.01	0.00
PF2	0.02	0.02	0.00	0.00	0.04	0.03	0.03	0.01	-	0.05	0.02	0.03
PF3	0.02	0.02	0.00	0.00	0.03	0.03	0.01	0.00	-	0.03	0.02	0.00
Slurry oxic												
AL1	0.00	0.00	0.00	0.00	0.00	0.01	0.01	0.00	0.00	0.01	0.01	0.00
AL2	0.00	0.00	0.00	0.00	0.00	0.00	0.00	0.00	-	0.00	0.00	0.00
AL3	0.00	0.00	0.00	0.00	0.00	0.00	0.00	0.00	-	0.00	0.00	0.00
TZ	0.33	0.33	0.03	0.01	0.02	0.02	0.00	0.00	-	0.00	0.00	0.00
PF1	0.28	0.28	0.03	0.01	0.05	0.05	0.00	0.00	-	0.02	0.01	0.00
PF2	0.04	0.04	0.00	0.00	0.06	0.06	0.01	0.00	-	0.04	0.01	0.00
PF3	0.05	0.05	0.00	0.00	0.02	0.02	0.01	0.00	-	0.03	0.02	0.00

Table A 7: pH measured in oxic or anoxic slurries after 0 and 19 days and at end of incubation across sites

Layer	pH								
	Iškoras			Áidejávri			Lakselv		
	0 days	19 days	106 days	0 days	19 days	98 days	0 days	19 days	97 days
Slurry oxic									
AL1	2.8	3.7	2.9	3.4	3.2	2.5	3.6	3.3	2.9
AL2	3.1	3.4	2.9	3.7	3.6	3.1	4.2	4.2	3.5
AL3	3.2	3.6	3.2	3.9	3.9	2.9	4.5	4.3	3.9
TZ	3.8	4.2	3.6	4.3	4.6	3.6	4.7	4.4	3.9
PF1	3.9	4.5	3.8	5.4	5.0	3.8	5.5	4.9	4.2
PF2	4.2	4.4	3.8	5.5	5.8	5.0	5.2	4.8	4.7
PF3	4.5	4.9	4.3	5.4	7.1	5.8	5.5	7.2	6.4
Slurry anoxic									
AL1	-	3.5	2.9	3.6	3.1	2.5	3.3	3.3	2.9
AL2	-	3.6	2.7	3.7	3.8	3.6	4.1	4.5	3.7
AL3	-	3.6	3.0	4.0	4.0	3.5	4.5	4.7	4.2
TZ	-	4.2	3.5	4.4	4.8	3.9	4.7	4.8	4.2
PF1	-	4.3	3.6	4.6	5.5	4.1	5.6	5.6	4.6
PF2	-	4.6	3.6	5.5	6.7	5.8	5.1	5.5	5.0
PF3	-	5.0	4.2	5.5	8.3	7.7	5.5	7.4	6.8

Norges miljø- og biovitenskapelige universitet
Noregs miljø- og biovitskapelege universitet
Norwegian University of Life Sciences

Postboks 5003
NO-1432 Ås
Norway